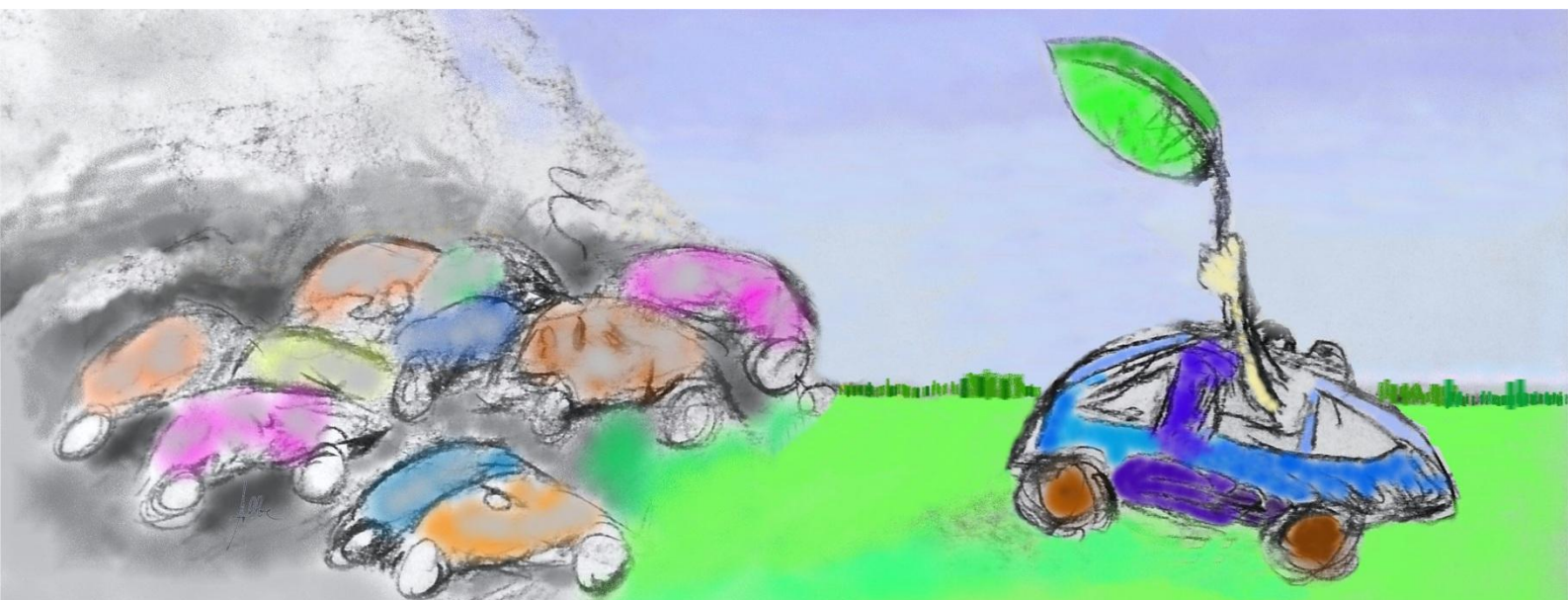# JRC SCIENCE AND POLICY REPORT

Individual mobility:

From conventional to electric cars

Alberto V. Donati
Panagiota Dilara*
Christian Thiel
Alessio Spadaro
Dimitrios Gkatzoflias
Yannis Drossinos

European Commission, Joint Research Centre,
I-21027 Ispra (VA), Italy

*Current address: European Commission, DG
GROW, B-1049 Brussels, Belgium

2015

Abstract

The aim of this report is twofold. First, to analyse individual (driver) mobility data to obtain fundamental statistical parameters of driving patterns for both conventional and electric vehicles. In doing so, the information contained in large mobility datasets is condensed into compact and concise descriptions through modelling observed (experimental) distributions of mobility variables by expected theoretical distributions. Specifically, the stretched exponential distribution is shown to model rather accurately the distribution of single-trips and their duration, and the scale-invariant power-law with exponential cut-off the daily mobility length, the distance travelled per day. We argue that the theoretical-distribution parameters depend on the road-network topology, terrain topography, traffic, points of interest, and individual activities. Data from conventional vehicles suggest three approximate daily driving patterns corresponding to weekday, Saturday and Sunday driving, the latter two being rather similar. Work trips were found to be longer than average and of longer duration. The second aim is to ascertain, via the limited electric-vehicle data available from the EU-funded Green eMotion project, whether the behaviour of drivers of conventional vehicles differs from the behaviour of drivers of electric vehicles. The data suggest that electric vehicles are driven for shorter distances and shorter duration. Data from the Green eMotion project showed that the median real-life energy consumption of a typical segment A, small-sized, electric car, for example the Mitsubishi i-MiEV and its variants, is 186 Wh/km with a spread of 55 Wh/km. The real-driving energy consumption (per km) was determined to be approximately 38% higher than the type-approved consumption. Moreover, we found considerable dependence of the energy consumed on the ambient temperature. The median winter energy consumption per kilometre was higher than the median summer consumption by approximately 40%. The data presented in this report can be fundamental for subsequent analyses of infrastructure requirements for electric vehicles and assessments of their potential contribution to energy, transport, and climate policy objectives.

Contents

1. Introduction

Road transport, a key component of economic development and human welfare, plays a growing role in world energy use and emissions of greenhouse gases. In 2010, the transport sector was responsible for approximately 23% of total energy-related carbon dioxide emissions, a potent greenhouse gas. Greenhouse gas (GHG) emissions from the transport sector have more than doubled since 1970, increasing at a faster rate than any other energy end-use sector to reach 7.0Gt carbon-dioxide equivalent in 2010. Around 80% of this increase came from road vehicles. The final energy consumption for transport reached 28% of the total end-use energy in 2010, of which around 40% was used for urban transport [1]. In the European Union, road transport contributes one-fifth of EU's total emissions of carbon dioxide. Emissions in 2012, even though they fell by 3.3%, were still 20.5% higher than in 1990. Light-duty vehicles, cars and vans, produce approximately 15% of the EU's emissions of carbon dioxide [2]. Moreover, transport in Europe is 94 % dependent on oil, 84 % of it imported, leading to a financial cost of EUR 1 billion per day and significant dependence on importing oil with the consequent threat to the EU's security of energy supply [3].

Emissions from road transport, be they gaseous like ozone and nitrogen oxides or in particulate form, for example, combustion-generated nanoparticles, influence air quality in cities. Numerous epidemiological and toxicological studies have associated urban air quality and air pollution, including particular matter, with adverse health effects [4].

Therefore, the use of fossil fuels has significant repercussions on the environment, public health, and political decisions. Burning fossil fuels leads to (i) important detrimental effects on the environment (GHG emissions and climate change); (ii) deterioration of urban air quality and associated human health effects, causing increasing environmental and human costs; and (iii) it is considered a threat to the EU security of energy supply.

The European Commission regards alternative fuels an important option to sustainable mobility in Europe. The Clean Power for Transport package, adopted in 2013, aims to foster the development of a single market for alternative fuels for transport in Europe. It contains a Communication laying out a comprehensive European alternative fuels strategy [COM(2013)17] for the long-term substitution of oil as an energy source in all modes of transport. The Directive on the deployment of alternative fuels infrastructure (2014/94/EU) requires Member States to develop national policy frameworks for the market development of alternative fuels and their infrastructure, among other elements. However, a detailed analysis of the way alternative-fuel vehicles move and consume energy is necessary to understand the needs for a European-level infrastructure.

Herein, we analyse real-life data for conventional and electric vehicles as they move in various European cities and areas. The conventional-vehicle data were collected by on-board data loggers or from specific-purpose surveys. Electric-vehicle data have become available only recently, since only in the last few years large electric-vehicle demonstration projects have been funded, as the *Zem2all* in Malaga (ES) or the Switch EV in Newcastle (UK). A brief description of both projects may be found in Ref. [5]. The data analysed in this report were obtained from the Green eMotion Project [5] that generated a wealth of data on how drivers use electric vehicles, their driving and parking patterns, and real-life energy consumption of electric vehicles in Europe.

We provide generic modelling of individual (driver) mobility, by conventional or by electric vehicles, while at the same time we analyse consumption patterns of electric vehicles. These models may be used to study the needs for infrastructure in the Member States and, thence, to support the elaboration of the national policy frameworks. The models and data summarized in this report can be used as a basis and first step to analyse the necessary electricity infrastructure investments under significant electric-vehicle deployment scenarios. For example, estimated energy consumption of observed (recorded) trips, aggregated and appropriately scaled to the population of the circulating electric vehicles, provide estimates of city-wide energy needs. Clustering techniques may be used to identify classes of driving-behaviour and related patterns that provide

insights on daily activities. Such characterization of drivers' behaviour could be used profitably to decide the optimal placement of charging stations, as well as their most cost-efficient number.

2. Datasets

Three distinct datasets, containing complementary information on urban mobility characteristics, were analysed. Two datasets, Floating-car and Survey data, were collected for conventional vehicles (powered by internal combustion engines), and one for the electric vehicles that participated in the Green eMotion (GeM) project.

The Floating-car data [6,7] were purchased from the company Octo Telematics by the JRC to analyse conventional mobility behaviour, namely to identify patterns and aspects of human mobility in urban areas under different conditions (traffic, road-network topology). The database contains a large amount of information on conventional (internal combustion engine) private and commercial vehicles: the mobility data were collected in two medium-sized Italian cities (Modena and Florence) in May 2011. The data were acquired via the Clear Box technology, whereby a GPS device (used to localize the vehicle) is connected to a remote server via GSM. As described in Ref. [7], the initial dataset contains data collected from about 52,834 (Modena) and 40,459 (Florence) conventional vehicles, a well-mixed random sample that represents 12% (Modena) and 5.9% (Florence) of the circulating fleet. As the primary interest in the analyses of the conventional-vehicle data is urban mobility, the data were filtered to eliminate vehicles driven for more than 50% of the trips outside the respective province. This filtering resulted in approximately 48 million valid sampled events arising from approximately 29 thousand vehicles. For each recorded event, the GPS device automatically acquires: timestamp (date and time), GPS position and signal strength, engine state (start, motion, stop), instantaneous speed, direction of motion, and distance travelled from the previous recorded event. The records were transmitted to the server every 2 km [6]. These Floating-car data, and the resulting travel behaviour in the two medium-size Italian cities, were extensively analysed in Refs. [7-9], albeit from a different perspective.

The Survey data [10-12] were collected by the Institute of Energy and Transport of the JRC in collaboration with TRT (Trasporti e Territorio Srl) and Ipsos Public Affairs Srl. A JRC initiative was launched in the spring of 2012 to investigate the behaviour of European car drivers, as described in detail in Refs. [11,12]. The survey data were collected through a Web-based travel diary, 24 hours per day, 7 days a week. The database contains trip diaries for six European countries (France, Germany, Italy, Poland, Spain, and UK) of about 600 individuals in each country. The sample, for each country, was chosen to guarantee the necessary statistical homogeneity and to be representative of the population in terms of age, gender, geographical area, population density, education, and occupational status. The data were collected to complement data of national surveys that, with the exception of UK and Germany, were considered insufficient to compare driving patterns across Europe. Individuals logged the information at the end of each trip, for a total of about 40,000 trips for 3,500 conventional cars; a total of about 122,000 diary entries were recorded, covering a period of about 4 months (from February to May 2012, even though for any individual vehicle the usual span was about 2 months). No information on the location of the vehicles was recorded.

The Green eMotion data [5,13] were provided to the JRC by IREC (Catalonia Institute for Energy Research) as part of a collaboration initiated at the end of 2013. The Green eMotion database contains data about the mobility of electric vehicles of various types (cars, motorcycles, and transporters), and powertrain technologies: Battery Electric Vehicle (BEV), and Plug-in Hybrid Electric Vehicle (PHEV). Most of the BEV cars were Mitsubishi i-MiEV or its versions targeted to the European market–Peugeot iOn and Citroen C-Zero - and a limited number of Think City (mainly in Spain). The vehicles were driven in 11 different Demonstration (Demo) Regions, representing various cities in six European countries (Denmark, France, Germany, Ireland, Italy, and Sweden). As the data were occasionally incomplete, we proposed appropriate guidelines for data

collection and reporting for European electro-mobility projects [14]. The database contains both static and dynamic data. Static data refer to the vehicle (type, engine technology, usage) and to the charging station (number of charging points per station, power output, location in GPS coordinates). The static information was usually updated every 6 months. The dynamic data are the start and end times of a trip, and recharging information: they were recorded by on-board loggers for the period March 2011 to December 2013. From the full database, we extracted the travel distance per trip, vehicle energy consumption, and recharge time, energy, and power. Unfortunately, vehicle location was reported (GPS location) only at the beginning and the end of a trip: no intermediate route information was available to allow us to extract instantaneous speed or acceleration. The number of electric vehicles (cars, motorcycles, and transporters) we analysed is 457, while those driven for at least one trip were 357, all of them battery-electric cars. The total number of trips analysed is 65,799.

A condensed version of this report was included in the Deliverable D1.10, "European global analysis on the electro-mobility performance" of the Green eMotion project [5].

3. Conventional vehicles

The analysis of mobility data of conventional vehicles is of importance since it allows the identification of general principles of individual (driver) mobility and the associated driving-behaviour patterns. Such information may suggest actions to be taken to allow a smooth transition from internal-combustion powered to electrically-powered vehicles.

The following list presents the variables that were analysed: some of them were subdivided by day of the week, or aggregated per working and weekend day. Distributions of some of them were also studied. The variables are:

1. Trip distance. A trip is defined as a sequence of events (GPS records) that starts with a signal of "engine on" and end with a signal "engine off";

2. Trip start time, trip duration, total time between the start and end of a trip;

3. Distance and duration of work trips, e.g. trips that can be related to a regularly performed activity that will be referred to as "work". They were defined as trips that consisted of two contiguous legs, the destination of the first coinciding with the origin of the second and vice versa, separated by a parking time between 7.5 to 9 hours;

4. Average trip speed and average motion speed, the latter being the average trip speed obtained by removing the time a vehicle was motionless from the total trip duration. The averages were calculated by dividing the total trip distance either by the trip duration (average trip speed) or by the time the vehicle was in motion (average motion speed). We also calculated segment speeds, the average speed calculated from one GPS record to the next by dividing the reported distance travelled by the time difference between the two consequently recorded events;

5. Parking duration, aggregated per week day, per working day, and per weekend day;

6. Daily mobility distance, the total distance travelled per day, and the daily number of trips;

7. Trip distance travelled before a stop of a given duration.

3.1 Floating-car data

The Floating-car data consisted of a collection of GPS signals of private and commercial (a much smaller fraction) vehicles for two medium-size Italian cities, Modena and Florence, collected in May 2011. The

monitored vehicles of the cleaned database, i.e., after removal of vehicles that travelled more than 50% of the trips outside the respective province, represented 3.7% (16,254 vehicles, Modena) ad 1.8% (12,475 vehicles, Florence) of the vehicles registered in these provinces at that time [6,7], but a slightly higher percentage with respect to the number of circulating vehicles is to be expected. The number of valid, unmerged, trips was 2,336,289 (Modena) and 1,649,871 (Florence).

We decided to aggregate further valid sequential trips if the duration of a stop was less than 10 minutes: the resulting trips, which consisted of at least two legs, are referred to as contiguous trips. For contiguous trips, the stop time is subtracted from the total trip duration, and the related stop is not added to the stop-time distribution. The 10-minute interval was chosen because it is considered to be the minimum time a driver of an electric vehicle would consider sufficient to charge the vehicle. The same time interval was also used in the survey to join two consecutive trips to a contiguous trip. We remark that the minimum distance covered as reported in the Floating-car data was 198 m (Modena) and 1,129 m (Florence), whereas the minimum reported time was 300 sec (for both cities).

Table 1 summarizes the number of valid trips (including contiguous trips) and stops, as determined by our computational procedure. The validity of a trip was determined from the quality of the signals reported; more information may be found in Ref. [6] and in the following.

Table 1: Floating-car data: Summary information.

	Number of distinct vehicles	Number of GPS records	Number of valid trips	Number of valid stops	Number of contiguous trips[1]
Modena	16,254	15,790,370	1,816,613	1,772,757	260,488
Florence	12,475	32,532,551	1,271,204	1,244,626	189,736
Total	28,729	48,322,921	3,087,817	3,017,383	450,224

According to our computational procedure valid trips and stops were determined from qualifiers associated with each recorded event. The accepted values of the qualifiers are: SG = 1 (no signal), SG=2 (weak signal) SG=3 (good signal), MS=0 (engine on), MS=1 (motion state), MS=2 (engine off). Data with (SG=1, MS=1) had already been removed before the dataset was delivered to the JRC. The conditions that specified the validity of a record were:

Anomaly conditions
1. If the time difference between two consecutive events is zero, the trip is considered anomalous (discarded).
2. If a segment has an average segment speed greater than 180 km/h or if it is less than 0, the trip is considered anomalous (discarded).
3. If a stop (motion state MS=2) is not followed by a start (MS=0), no stop time is accounted, neither a new trip is generated with the events that follow, until an event with MS=0 is found.
4. If the qualifier of the quality of the signal or motion state is not in the expected ranges, the trip is considered anomalous (discarded).

Contiguous trips: Two or more trips are merged if:
1. The time from the end of the previous trip to the beginning of the next is less than 10 minutes.
2. If the above holds, the stop time is subtracted to the total trip time, and the related stop is not added to the stop duration distribution.

Anomalous stops:
1. If the distance between a previous stop and the following start is greater than 30 m (calculated as a straight line from the GPS coordinates), the stop is considered anomalous and discarded.
2. If a MS=2 is not followed by a MS=0, the stop is discarded.

These conditions were used to clean the data and to generate the new dataset that was eventually analysed. A number of parameters in the pre-processing code can be adjusted; in particular, in the case of distributions the limits of these distributions and their binning may be adjusted. After pre-processing the data with a Java code,

---

[1] Contiguous trips are trips separated by a stop of 10 minutes or less.

they were analysed with various R scripts to visualize the distributions and to fit the data. For a brief description of the output of the processing code see Appendix B.

3.1.1 Trip Distance

The trip distance, the distance travelled between an "engine-on" event and "engine-off" event (eventually merging consecutive trips as described above), is one of the most important mobility parameters since it gives a direct indication of vehicle usage. The trip-distance distribution may be used to estimate the expected real autonomous range of electric vehicle. We found that a reasonable approximation of the probability distribution of trip distances (where the distance travelled is considered a continuous random variable x) is provided by the stretched ($\gamma < 1$) exponential probability density function (pdf)

$$p(x) = \beta \exp\left[-\left(\frac{x}{L_0}\right)^\gamma\right], \tag{1}$$

where β is the normalization constant (dependent, in general, on the limits of the distribution), γ the stretching exponent, and L_0 a characteristic length scale. Even though the range of distance travelled per trip is finite, we consider the probability distribution to be continuous with x varying from zero to infinity. Then, the normalization condition

$$\int_0^\infty dx\, p(x) = 1,$$

leads to

$$p(x) = \frac{\gamma}{L_0 \Gamma(1/\gamma)} \exp\left[-\left(\frac{x}{L_0}\right)^\gamma\right], \tag{2}$$

where the gamma function is defined by

$$\Gamma(z) = \int_0^\infty dx\, x^{z-1} \exp(-x).$$

The probability density function Eq. (2) is estimated empirically via the construction of a (frequency of occurrence) histogram that provides the empirical density function. We did not determine the probability density function, which is normalized to unity, but we analysed the overall distribution function, which is normalized to the number of events (or counts). We stress that we consider both functions to depend on a continuous random variable whose range is from zero to infinity. The procedure adopted to obtain the parameters of the theoretical distribution is follows. The observed range of the independent variable (distance travelled) is divided into equal-sized bins of length δx, each bin identified by its midpoint x_i. The number of counts $c(x_i)$ within each bin is recorded. The total number of counts (events) is then

$$C_{\text{total}} = \sum_i c(x_i).$$

The discrete distribution function $f(x_i)$ is

$$f(x_i) = \frac{c(x_i)}{\delta x} = N_\infty p(x_i) = \frac{N_\infty \gamma}{L_0 \Gamma(1/\gamma)} \exp\left[-\left(\frac{x_i}{L_0}\right)^\gamma\right],$$

where N_∞ is the total number of occurrences. The appropriate theoretical distribution function becomes

$$f(x) = N_\infty p(x) = \frac{N_\infty \gamma}{L_0 \Gamma(1/\gamma)} \exp\left[-\left(\frac{x}{L_0}\right)^\gamma\right], \qquad (3)$$

that is normalized, $x \in [0, \infty]$ and the distribution is continuous, to the total number of events

$$\int_0^\infty dx f(x) = N_\infty.$$

The three parameters of the distribution γ, L_0, N_∞ were determined numerically via the non-linear, least square fit of the Levenberg-Marquardt algorithm. The algorithm is implemented in R as the function nls.lm in the package {minpack.lm}. The numerical fit is performed by requiring that the number of counts $c(x_i)$ in bin i is approximately given by the normalized stretched exponential distribution

$$c(x_i) \sim \frac{N_\infty \gamma}{L_0 \Gamma(1/\gamma)} \exp\left[-\left(\frac{x_i}{L_0}\right)^\gamma\right] \delta x, \qquad (4)$$

where the symbol $\sim$ is interpreted (in R) as a request to fit the data $c(x_i)$ to the specified functional form. Further arguments of the *nlsLM* function specify which parameters to vary and their initial values. As a measure of the goodness of the fit we used the coefficient of determination R^2 ("R squared")

$$R^2 = 1 - \text{RSS}/\text{TSS},$$

where TSS is the total sum of squared differences from the mean

$$\text{TSS} = \sum_i (y_i - <y>)^2,$$

and RSS is the square sum of residuals

$$\text{RSS} = \sum_i [y_i - f(x_i)]^2,$$

with $f(x)$ the distribution function Eq. (3) with the three parameters determined by the non-linear regression. The closer R^2 is to 1, the better the fit describes the data.

We note that the non-linear fit was not performed on the empirical values (e.g., trip distance) but on their logarithms to ensure that the fit reproduces well the tail of the distribution (large trip distances). A fit on the values themselves would provide an accurate representation of short-distance trips since such trips are the most numerous: the fit would have placed more weight to the highly populated regions (high histogram counts per bin), which are for short distances. We opted to obtain distribution parameters that reproduce well the large-distance behaviour as such trips are important in assessing the viability and usage of electric vehicles. Therefore, the empirical data were log-transformed and the log-transformed Eq. (4) (and the histogram data)

$$\log_{10}[c(x_i)] \sim -\left(\frac{x_i}{L_0}\right)^\gamma \ln\left[\frac{N_\infty \gamma}{L_0 \Gamma(1/\gamma)} \delta x\right] / \ln(10), \qquad (5)$$

were used in the fit. The natural logarithm is denoted by ln. The expressions for TSS and RSS used to evaluate R^2 were appropriately adjusted.

The results of the fitting procedure for the trip distance distribution in Modena (left) and Florence (right) are shown in Figure 1.
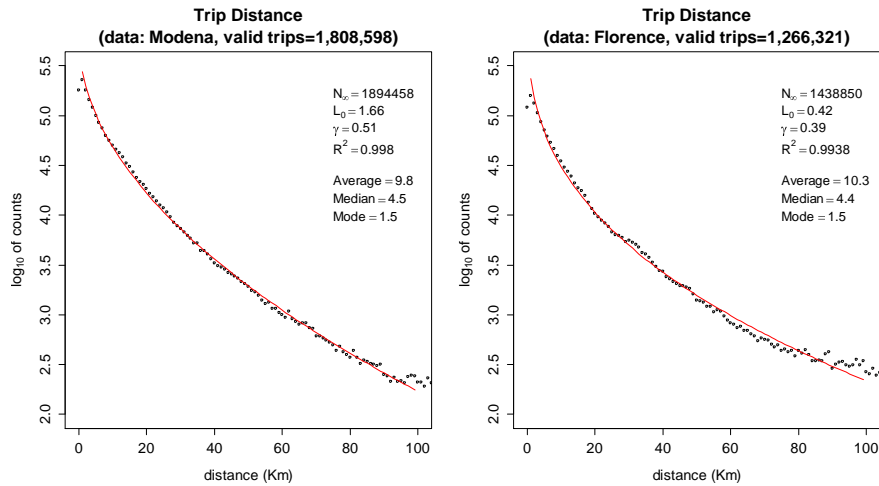
Figure 1. Trip distance distribution for Modena (left) and Florence (right), with model parameters of Eq. (3). The main statistical quantities are also shown.

Figure 2 presents the same data, but disaggregated per working day and weekend. The red line is the model (theoretical) distribution. For each distribution the average, median and mode [the value of x at the maximum of $f(x)$] are also shown in the figure. The agreement between the theoretical and experimental distributions is very good. These distributions are further compared to theoretical distributions previously proposed in the literature [15] in Figure 7.
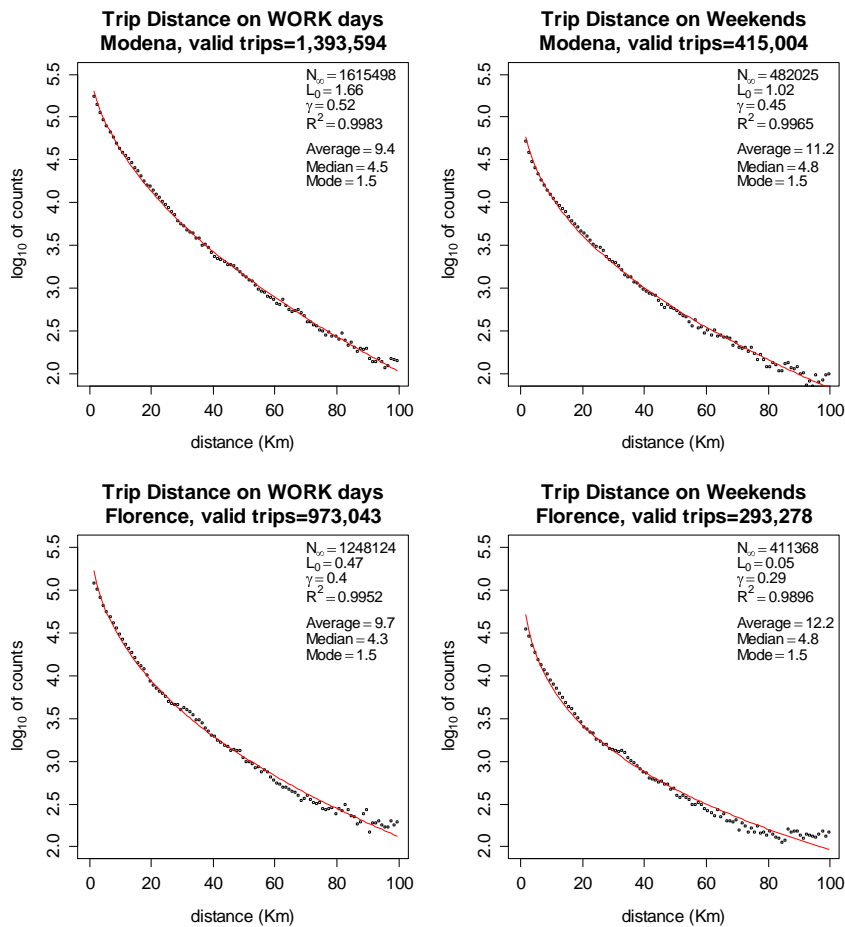

Figure 2. Trip distance distribution for Modena (top row) and Florence (bottom row) aggregated per working day (left column) and weekend day (right column).

The empirical data and the theoretical distribution, Eq. (3), are compared via quantile-quantile (Q-Q) plots in Figure 3: a quantile is a measure of the shape of a distribution, obtained by calculating the proportion of data that lie within a fixed interval. These plots provide a graphical method to compare two distributions by plotting their quantiles against each other. If the distributions to be compared are similar the plotted points lie along the $y = x$ line. The plots provide a non-parametric approach to comparing the underlying distributions. If an empirical distribution is compared to a theoretical (or expected) distribution the Q-Q plot assesses graphically whether the theoretical distribution reproduces accurately the statistical properties of the empirical distribution. Figure 3 presents Q-Q plots for week days (left column) and weekend days (right column) trip-distance distributions for Modena (top row) and Florence (bottom row). They suggest that the theoretical distribution reproduces well the quantiles of the empirical distribution: in particular, note the agreement of the two distributions in the two extremes (tails of the distribution).

We repeated the same calculations for each day of the week (Monday to Sunday). The results are shown in tabulated form in Table 2 and in Appendix A, Figs. A1 and A2. Table 2 presents the three parameters of the theoretical distribution (N_∞, γ, L_0), the coefficient of determination R^2, and the average and median distance travelled. The last two rows (for each city) present aggregated data for a typical work day and a typical weekend day. They were calculated by aggregating all the five weekdays, or the two weekend days, and then fitting the aggregate data. The three parameters of the distribution are also shown in Figure A3.
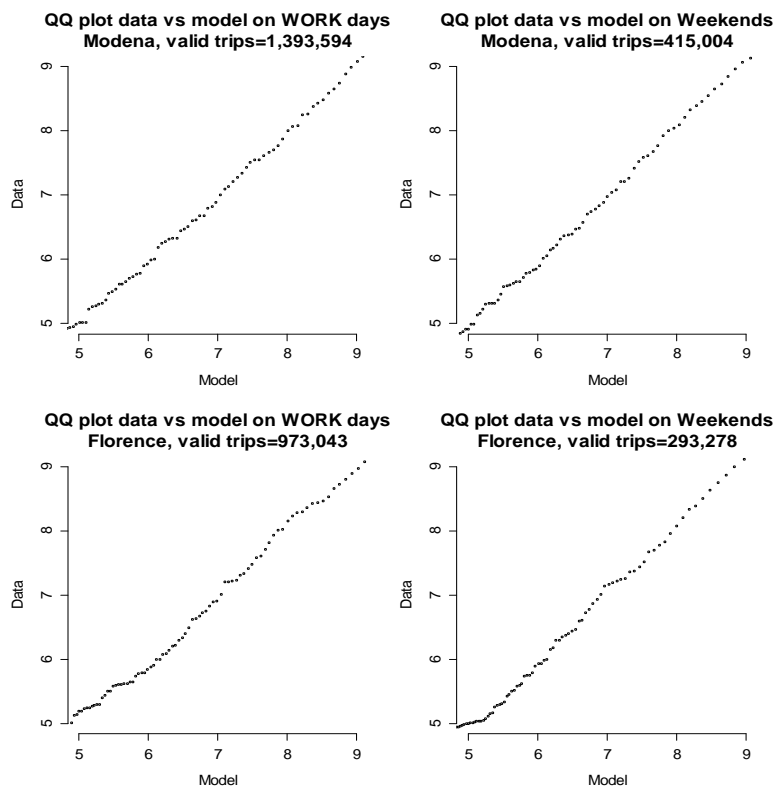

Figure 3. Quantile-quantile plots of the theoretical distribution Eq. (3) versus the empirical distribution for the distance travelled per trip. Top row Modena, bottom row Florence; left column work day, right weekend day.

The data shown in Table 2 suggest that driving behaviour during a week day is qualitatively different from driving behaviour during a weekend day. In fact, a small difference is also noted between driving on a Saturday and on a Sunday. These observation become qualitative by considering the average of the two most important parameters of the distribution, γ and L_0. Their averages, calculated from Table 2 for each working and weekend day, are reported in Table 3. In addition, Table 3 also shows the 95% confidence intervals in the

estimate of the average $\bar{x}$, expressed as $\bar{x} \pm 1.96 SE_{\bar{x}}$ where $SE_{\bar{x}} = \sigma / \sqrt{n}$ is the standard error of the mean with σ the sample standard deviation and n the number of values. The standard error of the mean is an estimate of how far the sample mean is likely to be from the population mean.

Table 2. Parameters of the theoretical distribution Eq. (7) per day, per city. Distances in km.

City	Week day	N_∞	γ	L_0	R^2	Average distance	Median distance
Modena	MON	347,926	0.54	1.89	0.9971	9.33	4.45
	TUE	372,904	0.51	1.43	0.996	9.25	4.37
	WED	292,181	0.54	1.85	0.9958	9.37	4.44
	THU	289,480	0.54	1.86	0.9973	9.44	4.51
	FRI	310,286	0.51	1.48	0.9971	9.67	4.51
	SAT	269,610	0.49	1.34	0.9961	10.16	4.55
	SUN	209,065	0.43	0.9	0.9956	12.53	5.28
	WORK days	1,615,498	0.52	1.66	0.9983	9.4	4.45
	Weekends	482,025	0.45	1.02	0.9965	11.2	4.84
Florence	MON	277,970	0.4	0.42	0.9934	9.55	4.24
	TUE	281,195	0.41	0.49	0.9949	9.59	4.31
	WED	221,617	0.42	0.59	0.9925	9.71	4.34
	THU	227,801	0.41	0.52	0.9924	9.69	4.35
	FRI	236,981	0.4	0.43	0.9922	9.98	4.36
	SAT	228,675	0.31	0.08	0.9878	10.82	4.43
	SUN	179,941	0.28	0.05	0.9889	13.87	5.44
	WORK days	1,248,124	0.4	0.47	0.9952	9.69	4.32
	Weekends	411,366	0.29	0.05	0.9896	12.21	4.85

The data reported in Table 3 show that driving dynamics during a working and a weekend day are qualitatively different since the confidence intervals for a week day and a weekend day do not overlap. It is, thus, sufficient to consider the driving behaviour during a "typical" working and a weekend day, without emphasizing the behaviour for each single week day (as is frequently done).

Table 3. Average γ and L_0 for work day (WD) and weekend day (WE) with the 95% confidence interval for Modena and Florence.

City	Working day or weekend	$\bar{\gamma} \pm \delta\gamma$	$\bar{L}_0 \pm \delta L_0$
Modena	WD	0.528 ± 0.013	1.702 ± 0.178
	WE	0.460 ± 0.042	1.120 ± 0.305
Florence	WD	0.408 ± 0.007	0.490 ± 0.055
	WE	0.295 ± 0.021	0.065 ± 0.021

3.1.2 Daily mobility distance

An equally important quantity to assess more wide spread public acceptance of electric vehicles is the daily mobility distance, the total distance (length) travelled in a day. This distance is to be compared to the reported autonomy of an electric vehicle. The daily mobility distance provides complementary information to the distance travelled per trip. All trips that start on the same day are accounted for in the calculated total daily distance (even if they terminate after midnight). Figure 4 presents relative frequencies of the daily mobility distance for the two cities. As the bin size was chosen to be 1 km, the relative frequencies may be viewed as

the corresponding histogram. The cumulative frequency distributions are also shown (in red, specifying the 80th percentile), as well as the average, mean, and mode of the empirical probability density functions. Small differences between the daily driving behaviour in the two cities are noted. In particular, the average, median, and mode distances travelled per day are slightly larger in Modena than in Florence: Modena is a smaller city close to the large city Bologna, so it is likely that some drivers commute to Bologna from Modena.
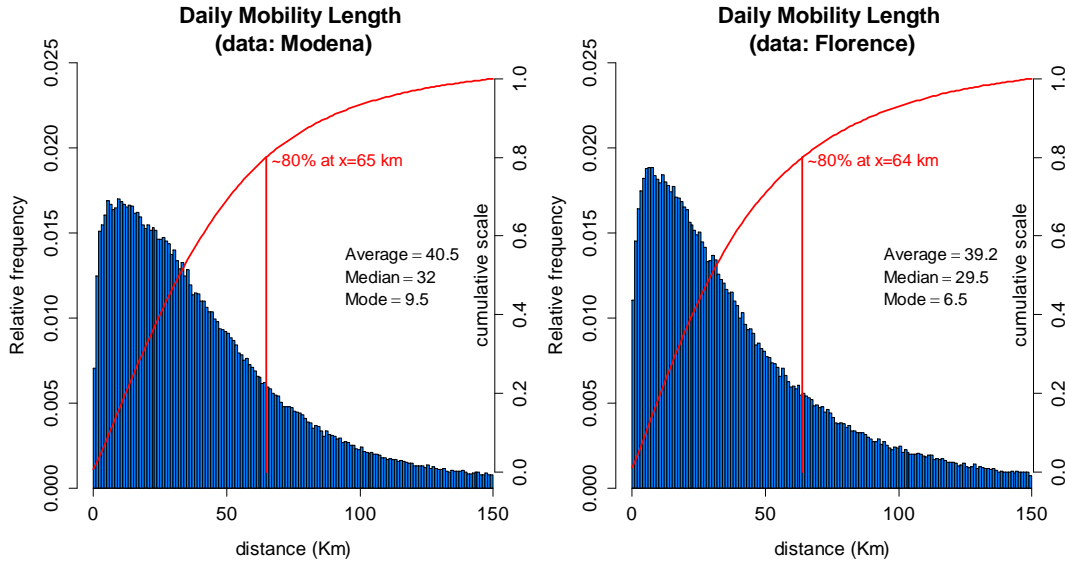

Figure 4. Relative frequency (bar) and cumulative (red, solid) distributions of daily mobility distance. Left: Modena. Right: Florence.

Note that in both cities 80% of the daily distance travelled by a vehicle is less than 65 km, well within the reported range of commercially available electric vehicles. Whereas this may suggest that a large part of the fleet could be easily replaced by electric vehicle (under the assumption that driving behaviour is independent of the vehicle powertrain), caution should be exercised in interpreting the 80th percentile. It is much more important to note that 20% of the daily distance travelled is greater than 65 km. If the choice to purchase an electric vehicle is based only on its reported autonomy, then the buyer may be more interested in the number of trips he/she would not be able to make than the numerous trips he/she could make. The buyer may place more weight on the relatively infrequent events, especially if these events are considerably more frequent than a Gaussian distribution would predict (heavy tails of the non-Gaussian distribution).

The daily mobility data are further analysed in Figure 5. As in the case of the trip-distance distribution, we modelled the data by an appropriately chosen distribution. We found that a reasonable choice is a power-law distribution with an exponential cut-off

$$y(x) = y_0 x^{\alpha} \exp\left(-\frac{x}{L_1}\right), \tag{6}$$

The empirical data and the numerical fit are presented in Figure 5 in a linear-logarithmic plot. The distribution reproduces very well the GPS-calculated distances for both cities. As before, we fitted the distribution in a logarithmic scale to ensure that long distances are accurately reproduced. An accurate estimate of the probability that a vehicle travel a long distance is important as an electric vehicle might not have enough available energy to complete the trip. In fact, drivers' anxiety about the autonomy of electric vehicles arises not from the short-frequent trips, but from the infrequent long trips, which are likely to be driven outside urban environments.
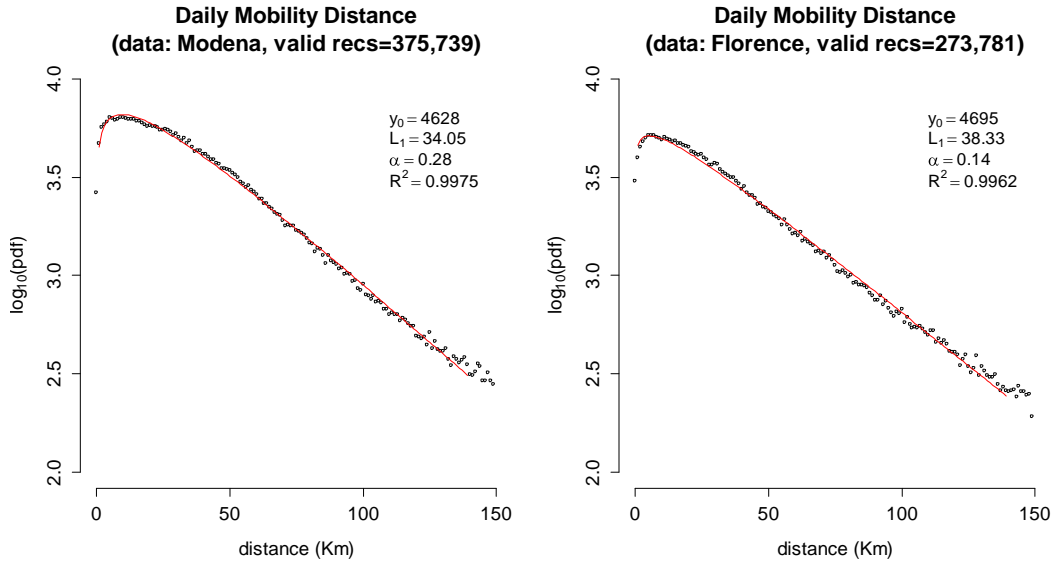
Figure 5. Daily mobility length distributions: Modena (left), Florence (right).

We remark, as in the previous section, that whereas the functional form of the distribution remains the same, data from different cities correspond to different parameters. The comparisons suggest that the exponent α and the characteristic length L_1 depend on the city. City-dependent dynamics, as determined, for example, from the road and network topology, traffic, population density, points of interest and associated activities, are reflected in the parameters of the distribution. Since the daily-mobility distance distribution is not Gaussian, the average distance travelled per day differs significantly from the median (and mode) distance. Furthermore, the change of the median distance is larger than the change of the average between the cities.

The goodness-of-fit was estimated graphically through the quantile-quantile (Q-Q) plots shown in Figure 6: the quantile-quantile comparison is reasonably good.
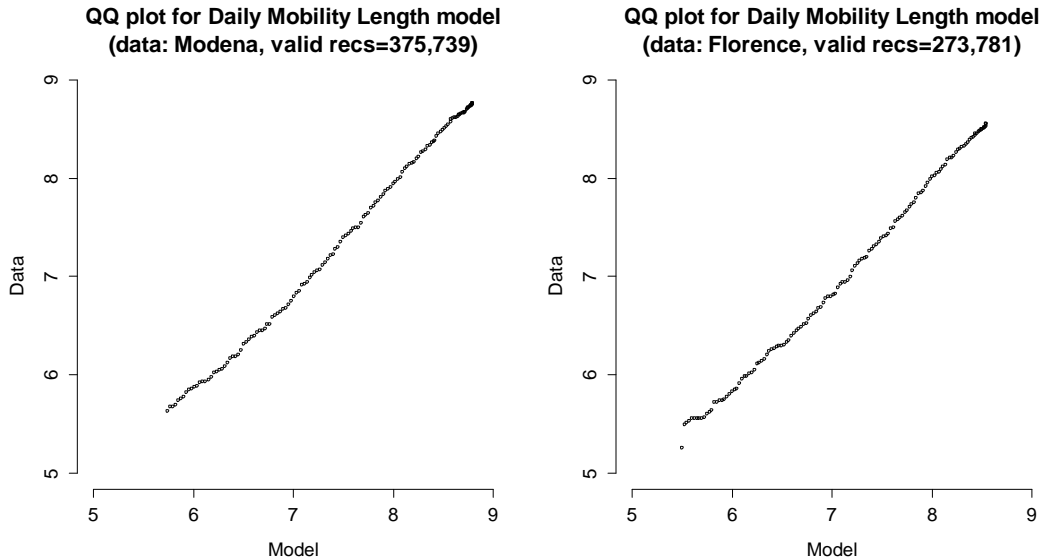

Figure 6. Quantile-quantile plots of the empirical and theoretical, Eq.(6), distributions of the daily distance travelled: Modena (left) and Florence (right).

The model distribution for the single-trip distance and the daily mobility length are compared to theoretically based distributions proposed in the literature in Figure 7. Bazzani et al. [15] used statistical-physics arguments to obtain analytical expressions for the single-trip and daily-mobility distance distributions. They suggested

12

that the single-trip distance distribution may be analytically calculated by determining the distribution of k uniformly-spread points into a segment of length L: the number of points k is the number of stops a driver makes, i.e., the number of activities associated with a trip that starts from home and returns home. They obtained

$$p_N(x) = \frac{c}{L} \sum_{k=1}^{N} (k+1) k a^k \left(1 - \frac{x}{L}\right)^{k-1} , \qquad (7)$$

where c is normalization constant and N the maximum number of daily activities. They suggested $a = 0.7, N = 18$. The comparison of the single-trip length probability distributions, Eq. (2) for Modena and Florence and Eq. (7) for Florence (Figure 7, left) is very satisfactory. The data the authors of Ref. [15] used were floating-car data, obtained from the same company as the data analysed herein, but for a different period (March 2008). Note, however, that Eq. (7) may become negative for $x \gg L$, a problem that does not arise for our proposed distribution, Eq. (2).

Bazzani et al. [15] also suggested that the daily-mobility probability distribution may be expressed as

$$p(L) = L_0 \exp\left(-\frac{L}{L_0}\right), \qquad (8)$$

where L_0 is a characteristic length scale. The normalized to unity probability distribution associated with Eq. (6) and the function to be compared to Eq. (8) is

$$h(x) = \frac{x^\alpha}{L_1^{1+\alpha} \Gamma(1+\alpha)} \exp\left(-\frac{x}{L_1}\right), \qquad (9)$$

where the two parameters are obtained from the fit to the empirical distribution, see, for example, Figure 5. The comparison of the daily-mobility distributions is not as satisfactory if the characteristic length suggested by Bazzani et al. [15], $L = 24.9$ km, is taken. Instead, better agreement is obtained by increasing the length scale to $L = 42.5$. Bazanni et al. [15] considered only trips that started within a circle of 10 km around the historical centre of Florence and remained inside that area: they were interested in selecting drivers who lived and moved within Florence. Our data, as mentioned, were filtered differently: vehicles which travelled 50% (in number of trips) outside their respective province were removed. Hence, it might be expected that if the characteristic length scale in Eq. (8) is increased the agreement would improve, an observation that is confirmed in Figure 7 (right). Nevertheless, the main difference between the two expressions is the algebraic growth factor, whose exponent is rather small: its effect is more noticeable at short distances. In fact, our proposed distribution function Eq. (9) reproduces the short-distance behaviour better than the pure exponential distribution.

Both works, this work and Ref. [15], suggest that well defined probability distribution functions, with appropriately chosen parameters, reproduce rather accurately features of driving behaviour, and in particular the single-trip and daily mobility length probability distributions. Whether the functional form of the distribution function is universal, and therefore whether it may be derived using generic arguments, via, for example, arguments based on an appropriately defined entropy or by considering the stochastic behaviour of drivers, is an issue that shall be addressed in the future. Moreover, further statistical analyses are required to ensure that the Modena and Firenze distributions are statistically different, i.e., that the two distribution do not arise from the same distribution within a given confidence.
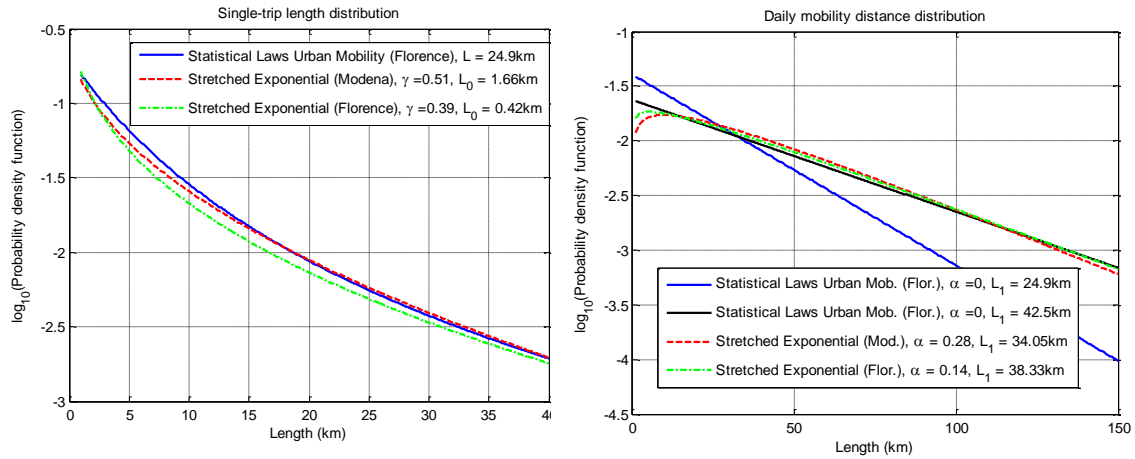
Figure 7. Theoretical probability density function (pdfs, this work) and pdfs obtained via statistical physics arguments, Bazzani et al. [15]. Left: Single-trip length distribution; Right: Daily-mobility distance distribution.

3.1.3 Number of daily trips

The number of daily trips is calculated in the same way as the daily mobility length: it is the total number of trips that started between the midnights delimiting one day. The number of trips is an important quantity because it is directly related to the number of daily activities. Figure 8 presents aggregate statistics for Modena and Florence: in both cases two maxima are noted at $n = 2$. As before, we observe similar behaviour in the two cities. The distributions of the number of daily trips per week day are presented in Appendix A, Figures A4 and A5. Note that on Sundays the second peak disappears and the remaining unique peak at n=2 becomes sharper. This is observed for both cities, suggesting, as the previous results imply, that driving behaviour on Saturdays and Sundays (and the associated activities) is qualitatively different from the behaviour during any other day. Nevertheless, we suggest that for simplicity and compactness urban mobility may be described by typical mobility during a working day and a weekend day, even though a stringer analysis would assign separate driving patterns to a working day, to Saturday, and to Sunday. Thus, three distinct week-day driving patterns may be identified, which under some conditions may be approximated to only two.
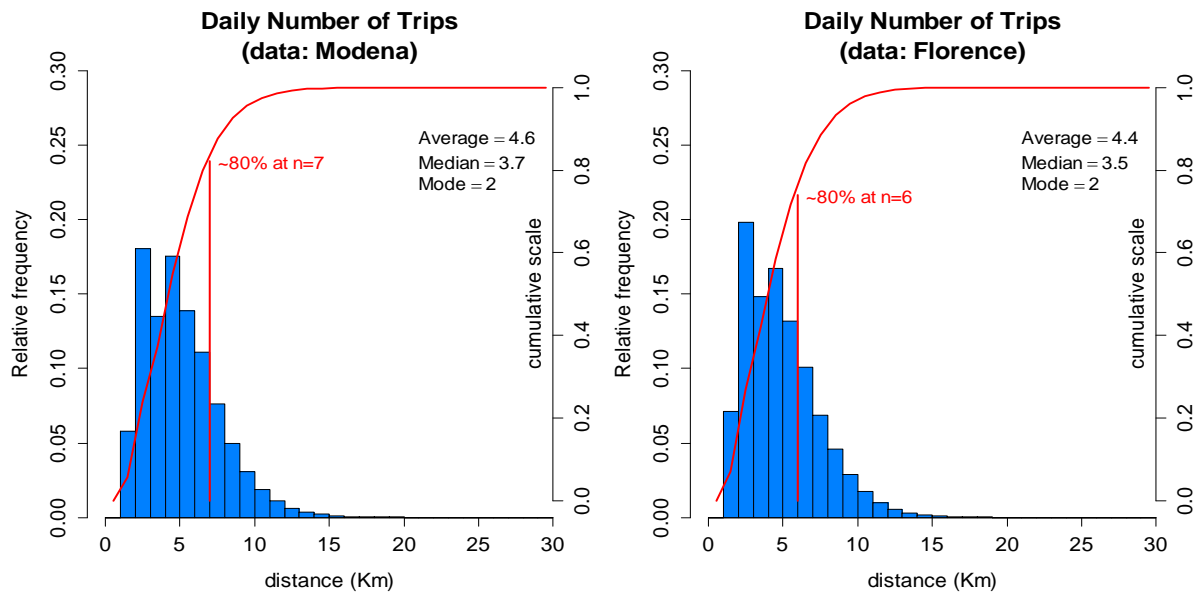

Figure 8. Daily number of trips: Modena (left), Florence (right).

14

3.1.4 Trip starting time and trip duration

The starting time of a trip is the time of the first event of the trip, namely the time the engine is turned on (MS=1). The distribution of trip-starting times, in terms of relative frequencies, is shown in Figures 9 and 10 for every week day and each city. The starting time was binned in half-hour bins. During a weekday, we note three pronounced peaks at approximately 8 h, 13 h, and 18-19 h: the first peak may be associated with a work activity, the middle with part-time work (possibly) or shopping, and the latter to return from work (office hours in Italy are usually 8:30-12:30 and 14:30-18:30). Two peaks at approximately 12-13 h and 19-20 h are noticeable during weekend days (as expected the peaks are slightly shifter to the right as people tend to sleep longer on weekend mornings).
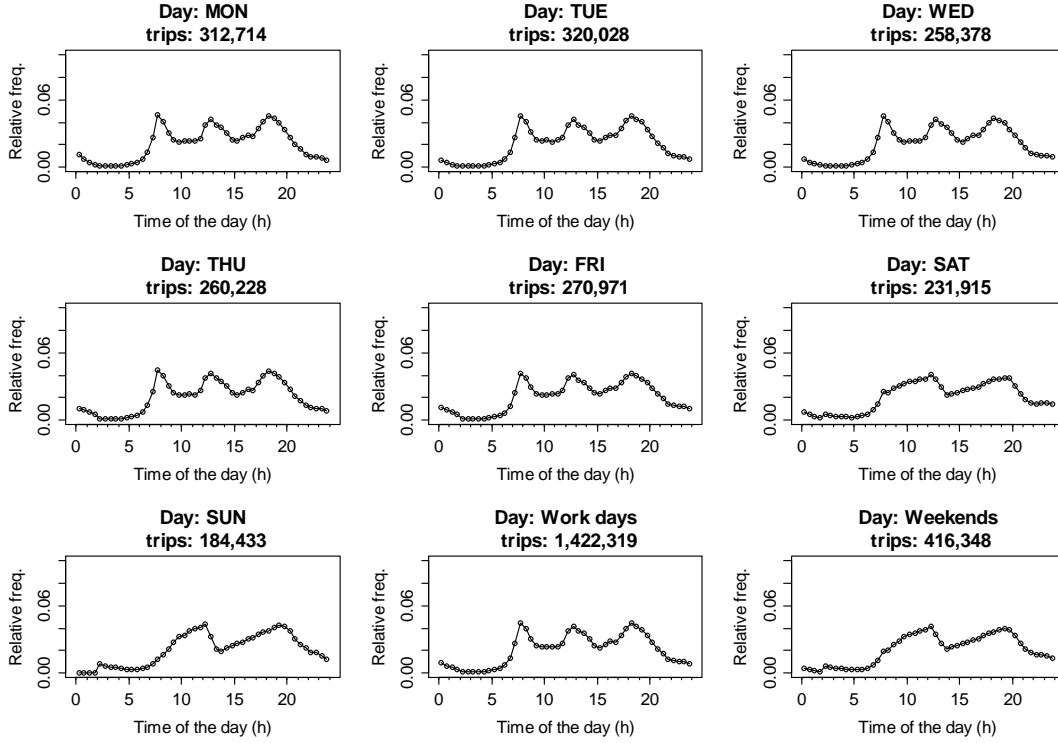

Figure 9. Distribution of trip starting time per week day and aggregated per working and weekend day (Modena).

Trip duration was calculated from the time of the first event to the time of the last event of a trip. We remind the reader that two contiguous trips were merged if the vehicle stops for less than 10 minutes. The data were fitted to the following stretched exponential distribution (normalized to the total number of trips), i.e., the same functional form as Eq. (3) but with travel time the independent variable

$$f(t) = N_\infty \frac{\gamma}{T_0} \frac{1}{\Gamma(1/\gamma)} \exp\left[-\left(\frac{t}{T_0}\right)^\gamma\right]. \tag{10}$$

As before, see discussion of the trip-distance distribution, we used non-linear regression on the logarithmic scale to obtain the three parameters of the distribution. The normalization condition ensures that the total number of trips N_∞ is reproduced. The results are shown in Figure 11, along with the model parameters and basic statistical quantities expressed in fractions of an hour.
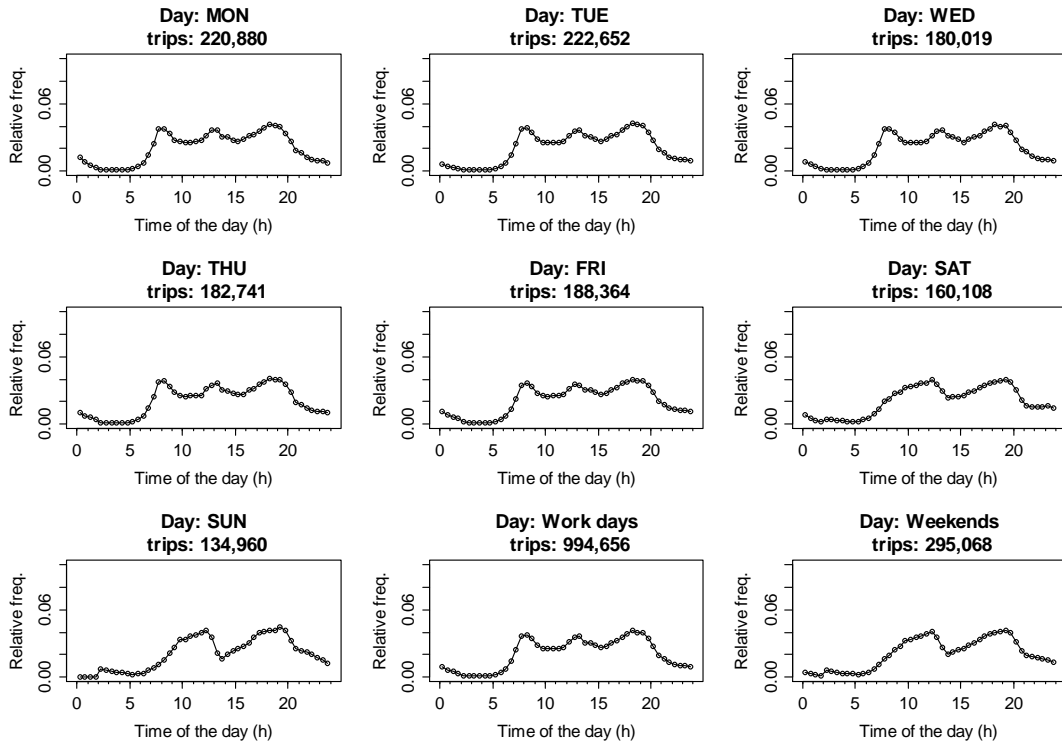
Figure 10. Distribution of trip starting time per week day and aggregated per working and weekend day (Florence).

A similar analysis was performed for each day of the week and aggregated per working day and weekend day. The results are shown in Appendix A, Figures A6 and A7. Different driving behaviour during a weekday and a weekend may be noted. In fact, as mentioned earlier, driving behaviour during the two weekend days seems qualitatively different, whereas driving behaviour during a (working) weekday appears rather similar.
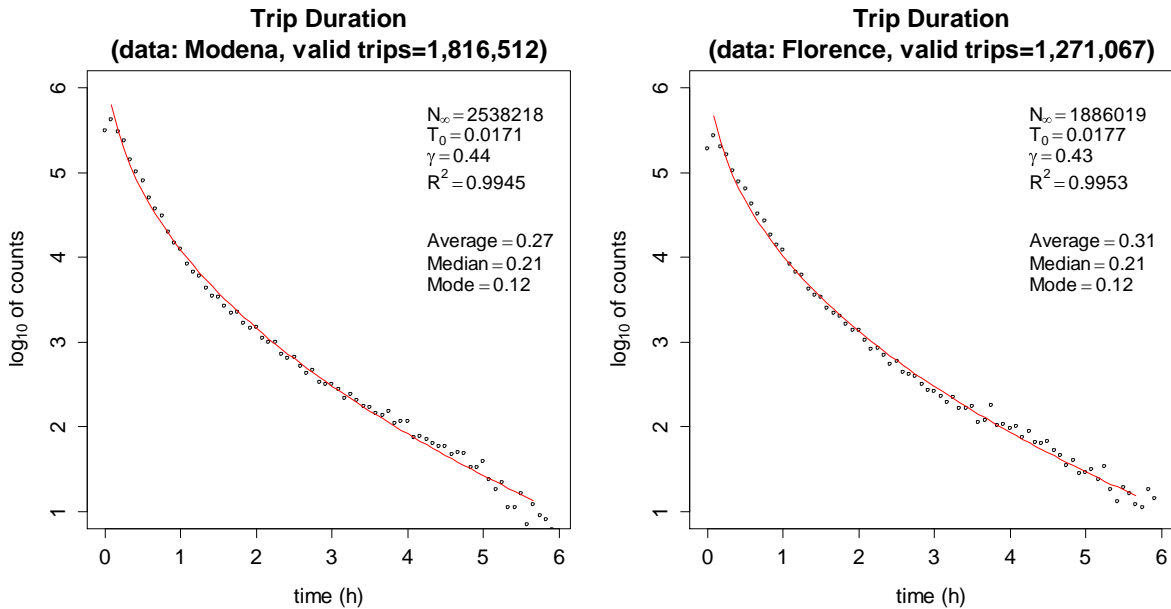

Figure 11. Trip-duration distributions, and their parameters, Eq. (18), for Modena (left) and Florence (right).

16

3.1.5 Work trips

Work trips are defined as trips that consist of two legs, the origin of the first leg being the destination of the second and vice versa, with a time difference between the two legs of 7.5 to 9 hours (typical duration of a working day). The identification of such trips, and their duration, is important in determining drivers' activities and origin/destination matrices. Trips defined as described are not necessarily trips to a working location as they could correspond to any other regularly performed activity, irrespective of whether it is remunerated or not. Origin destination locations were determined with a tolerance of 500 meters, computed from the (longitude, latitude) GPS coordinates as a straight line (Euclidean distance) between the start of the first leg and end of the returning leg.

Trip distance

The corresponding trip-distance distributions were fitted to a generic stretched exponential distribution, see, for example, Eq. (3). Results are shown in Figure 12. If these results are compared to the distribution of all the trips during a working day, Figure 2, we note that the average (and median) distance travelled increases to 12.6 km from 9.4 km (Modena) and to 13.1 km from 9.8 km (Florence). A trip to work tends to be longer than an average trip.

Similarly, we analysed the behaviour of these trips for each week day, reported in the Annex, Figures A8 and A9. The details of the distance distributions are shown there. We find that, as expected, there are considerably fewer trips during the weekend that may be characterized as work trips. The proportion of weekend generic work trips to week day work trips is approximately 25%, whereas the proportion of either week day or weekend trips to the total number of trips is approximately 3.5% (irrespective of city).
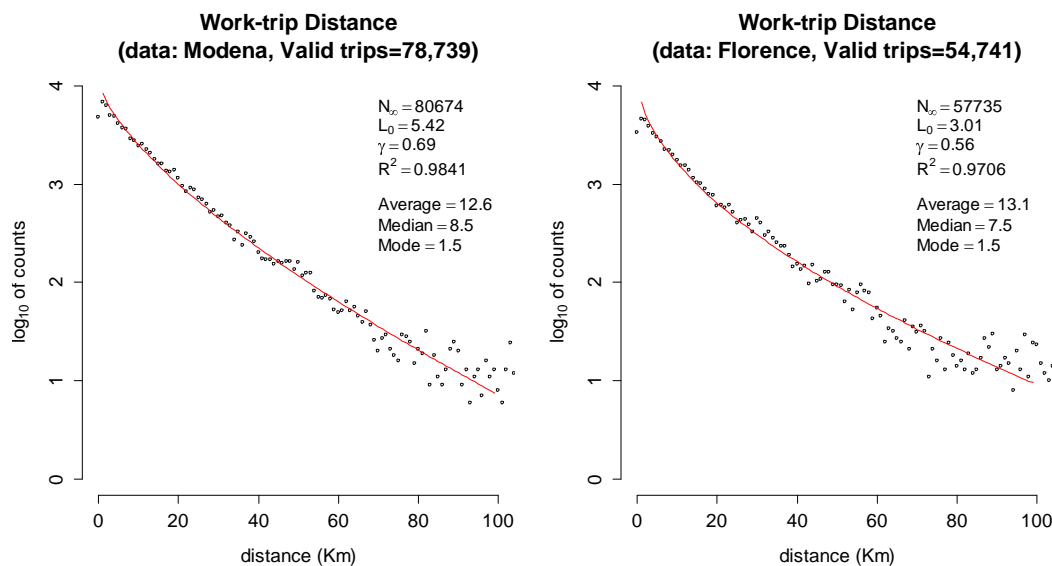

Work-trip Distance
(data: Modena, Valid trips=78,739)

$N_\infty = 80674$
$L_0 = 5.42$
$\gamma = 0.69$
$R^2 = 0.9841$

Average $= 12.6$
Median $= 8.5$
Mode $= 1.5$

Work-trip Distance
(data: Florence, Valid trips=54,741)

$N_\infty = 57735$
$L_0 = 3.01$
$\gamma = 0.56$
$R^2 = 0.9706$

Average $= 13.1$
Median $= 7.5$
Mode $= 1.5$

Figure 12. Observed and modelled, Eq. (3) distribution of work-trip distances: Modena (left), Florence (right).

Travel time

We calculated and modelled the travel time distributions for work trips. The data were fitted to a stretched exponential distribution of the form reported in Eq. (10), normalized to the total number of work trips. We decided to neglect the first reported point that represents counts between 0 and 5 min, and to neglect all trips that lasted longer than 3h: their number was deemed too low to fit. The results are shown in Figure 13. We note that the average work-trip duration is slightly longer than the average duration of all trips: surprisingly, the median, however, is slightly lower. We also generated the distributions per week day, and aggregated on working day and weekend: these calculations are presented in Appendix A, Figures A10 and A11.
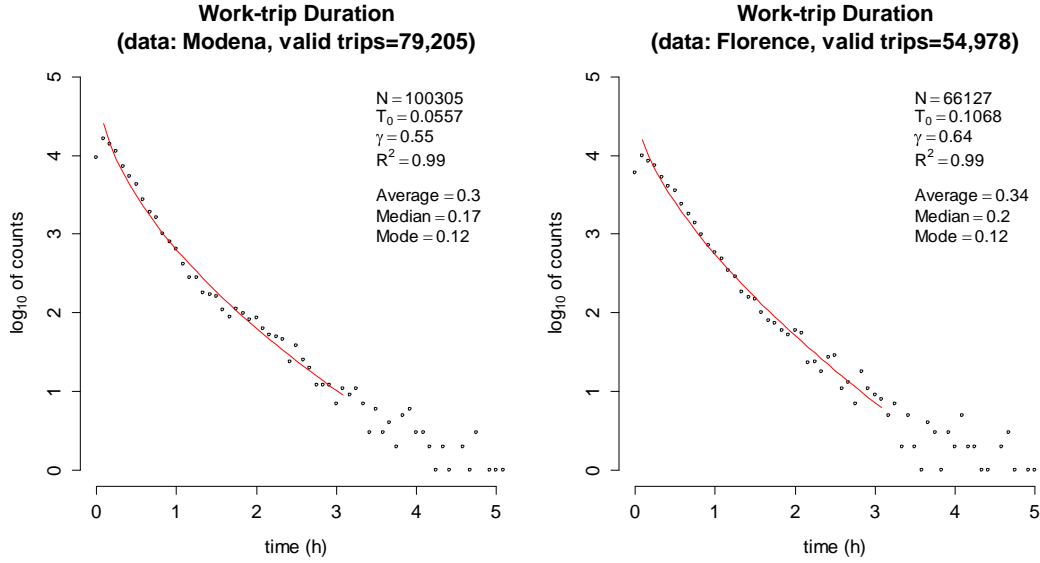
Figure 13. Distribution trip duration of work trips with fitted model parameters, Eq. (10): Modena (left), Florence (right).

3.1.6 Average trip speed, motion speed, and segment speed

The average trip speed is calculated as the total distance travelled per trip divided by the total trip time (note that the maximum intermediate stop time is 10 minutes). The average motion speed, defined as the total distance divided by the time the vehicle is moving, i.e., excluding stopping times, was also calculated. The segment speed is the speed between two GPS events obtained by dividing the distance travelled, as given in the data, by the time between the two events. Figure A12, Appendix A, presents the distributions of the average speed, the average motion speed and the segment speed for Modena and Florence. The distributions per week (and weekend) day do not present particular differences between the various days; they are not included in this document.

The data on average motion speed were fitted to two Gaussians and an exponential. We stress that the purpose of the fit is not to suggest a general functional form, as in the fits of the previous experimental distributions, but to capture their salient features. In particular, two Gaussians were chosen to identify the two peaks shown in Figure 14 (left Modena, right Florence). The chosen functional form is

$$f(\mathrm{v}) = A\exp\left[-\left(\frac{\mathrm{v}}{\mathrm{v}_0}\right)^{\gamma}\right] + B\exp\left[-C\left(\mathrm{v}-\mathrm{v}_1\right)^2\right] + D\exp\left[-B\left(\mathrm{v}-\mathrm{v}_2\right)^2\right], \qquad (11)$$

where v_1 and v_2 are the positions of the two relative maxima. These maxima can be found by a simple algorithm, but we had to adjust the first peak (Modena) by an offset (2 km/h) to improve the fit. The values are v_1 =15.5 km/h and v_2 =37.5 km/h for Modena and v_1 =9.5 km/h and v_2 =39.5 km/h for Florence. Also note that the exponent γ is less than unity, therefore the first term is a stretched exponential function.

We suspect that city topology plays a role in determining the shape of these distributions. In particular, the second visible peak for the city of Modena (Figure 14, left) could be attributed to commuting (Modena is close to the much larger city of Bologna), or, in any case, to the use of a high-speed highway. This peak is absent in the Florence data as Florence is a commuting hub, and city drivers do not commute to a larger city nor do they use on average a high speed highway during their daily routine.
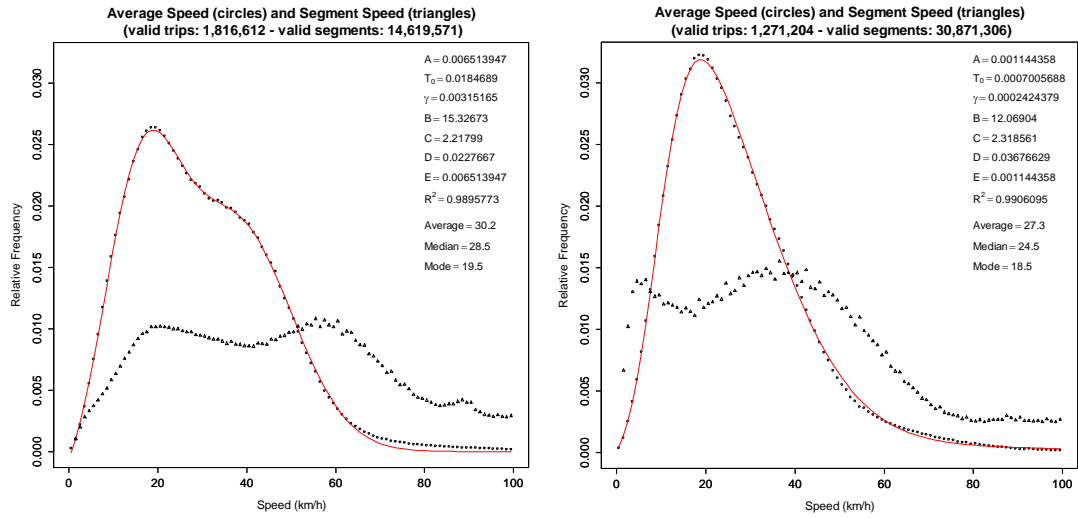
Figure 14. Average motion speed and its fit (red line), with calculated segment speed (triangles) for Modena (left) and Florence (right).

3.1.7 Parking

The vehicle parking (stopping) time and location are of great importance in the context of electro-mobility as they represent potential opportunities for recharging. For example, their geographical distribution may be analysed to suggest possible locations of future charging stations. In the Floating-car data parking times are obtained from the time difference between an engine off event (code MS=2) and the next engine on event (code MS=0). Figure 15 shows day and night parking spots for the city of Modena. It may be surmised that overnight parking is to be associated with private night parking.

Figure 15. Day (left) and night (right) parking time distribution in the city of Modena.

We also analysed the distribution of the duration of parking times. Non-linear regression was performed with a stretched exponential and four Gaussians centred at relative maxima. Regression of the stopping/parking times then follows the model

$$\ln(y) = Ax^{\gamma} + \sum_{i=1}^{4} G_i \exp\left[-g_i\left(x - x_i\right)^2\right] + C, \tag{12}$$

where A, γ, G_i, g_i, C are parameters to be determined by the non-linear regression, while x_i (for i=1,..,4) are the positions of the Gaussian peaks, determined as the relative maxima in an interval around the peak. Only the first bin (zero to 6 min stop time) is excluded by the regression. The results are shown in Figure 16.

As in the case of the average motion, the only valuable information to be obtained from the generic fit of Eq. (12) is the identification of the relative maxima (and their possible interpretation). In particular, we note that the first peak is in exactly the same position for both cities, while the others differ by little (each decimal point

19

corresponds to 6 minutes, so $\delta x_3 = 0.2$ corresponds to a 12-minute difference). A possible interpretation of these distributions is that the first peak is due to the part time jobs or other daily activities (shopping) at approximately 4 hours, the second (approximately at 9 hours) to standard-hour jobs, while the third (at 12 hours) and the fourth (at 19 hours) to night stops. The distributions were plotted in a logarithmic scale to render the four peaks visible.
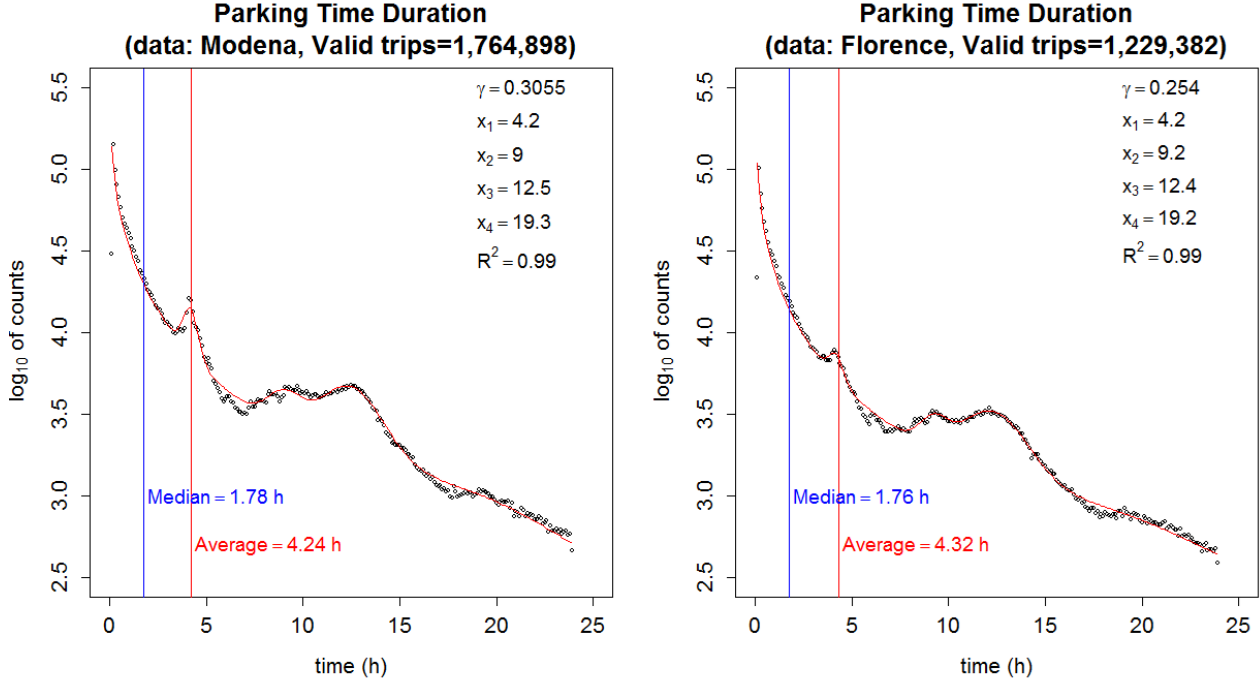

Figure 16. Parking time duration for Modena (left) and Florence (right), with the regression model and centres of the four Gaussians.

3.1.8 Discussion

We conclude this Section by mentioning previous attempts to unravel, understand, and possibly simulate individual human mobility patterns. The studies reported in Refs. [16-19] analysed large-scale human mobility patterns obtained from tracking dollar bills (via online bill-tracking websites which monitor the world-wide dispersal of large numbers of individual bank notes [16]) or from tracking anonymized mobile phone users [17,18,19]. The mobility patterns were considered to be described by three indicators: the trip distance distribution, the radius of gyration (to be defined in the next paragraph), and the number of visited locations. They suggested that long-distance human displacements may be described (on average) by the truncated power law

$$p(r) = \alpha r^{-\beta} \exp\left(-\frac{r}{\kappa}\right). \tag{13}$$

The power-law exponent β is believed to be, for different datasets, $\beta = 1.75 \pm 0.15$ (mean plus/minus standard deviation) and the cut-off values $\kappa = 400$ or 80 km, depending on the data analysed. Note that the length scale of the cut-off exponential is of the order of 100 kilometres, a distance considerably larger than the distances analysed in this report. The interesting feature of the power-law distribution Eq. (13) is that it is scale-invariant, namely it does not have a characteristic length scale associated with the observed mobility patters. The length scale associated with the exponential function is only relevant for very large distances, an effect known as "finite-size" effect in condensed matter physics. The absence of a characteristic scale implies some kind of universality, namely features of the distribution do not depend explicitly on the nature of small-

scale, local interactions. As such, the authors proposed plausible universal mechanism that would lead to a truncated power-law probability distribution, such as a continuous random walk process.

In our analyses, we did not considered the so-called radius of gyration, a concept borrowed from polymer physics that describes the mass distribution about a polymer's centre of mass. In its application to the study of human mobility, an individual's radius of gyration can be interpreted as the characteristic distance an individual travels within a time interval. The distribution of the radius of gyration revealed considerable heterogeneity, that is most individuals travel within a short radius, but others cover long distances on a regular basis [19]. This observation is implicit in the heavy tails of the theoretical distributions used to model trip distance and the daily mobility distance.

3.2 Survey data

The Survey data were collected in six European countries; the aim of the survey was to gather information about conventional-vehicle usage under conditions for which national surveys had not previously provided sufficient information. The Survey data were extensively analysed in Refs. [10-12]. Table 4 provides a summary of the main features of the data as determined by the Java processing software.

Table 4. Survey data summary.

Total number of distinct vehicles (with at least one trip)	3,489
Number of excluded vehicles	0
Regular Trips	39,955
Anomalous Trips	5
Regular Stops	39,959
Percentage of anomalous trips (with full trip removal)	0.01%
Anomalous Stops	0
Contiguous Trips found (stop<10.0 min)	833
Work Trips found	0
Records read	122,379
Computational time (s)	1.72

We, also, analysed these data with the methodology used to analyse the Floating-car data for Modena and Florence. We do not report the results of our analysis since the quality of the data is not comparable to the quality of the Floating-car data, in that there are considerably fewer data. Moreover, the analysis does not suggest any significant new features. It is perhaps worth mentioning that we noted a consistent bias in the data. It appears that reported values of distances travelled tended to be multiples of 5 or 10 kilometres. Such multiples appeared roughly 3 or 4 times more frequently than intermediate values, a possible result of the data acquisition through trip diaries. The analysis of the Survey data will focus on their comparison with the other datasets to check their compatibility with the theoretical distributions presented in the previous subsection. This analysis is presented in Section 5.

4. Electric vehicles: Green eMotion project

The data collected during the Green eMotion project (GeM) [5] provide a significant database of electric-vehicle usage. Data were collected from March 2011 to Dec. 2013 in six Demonstration Regions. The database comprises about 165,000 events (including recharging events): it represents one of the largest and more detailed databases of real-world data for electric vehicles in Europe. We identified a total of 457 electric vehicles for which sufficient information was available in the database: for example, apart from the information required for a conventional vehicle (as analysed previously) the powertrain technology is an important additional variable. The distribution of vehicles types and powertrain technologies is given in Table 5. In our analyses we used only the 357 battery electric cars for which trip information (distance and duration) was available. We refer to these cars as BEV in the following.

Table 5. Distribution of vehicles per type and technology (GeM).

Technology	cars	motorcycles	transporter
BEV	357	11	33
PHEV	56	0	0

Table 6 presents the number of trips whose length is non-zero, as well as those for which information on the energy consumed is available, parameterized by vehicle make and model. We note that the two cars with the largest number of trips are the Mitsubishi i-MiEV and the Peugeot iOn. Trips driven by these two cars constitute 85% of all trips for which the necessary information was available. These two cars are very similar: the iOn (and also the C-Zero) is the i-MiEV slightly modified for the Peugeot/Citroen brands. Both vehicles belong to segment A and they are considered "small-sized" cars. Reported technical specifications for the 2015 i-MiEV are: length 3.475 mm, width 1,475 mm, height 1,610 mm; curb weight 1085 Kg; electric motor 47 KWh, Li-ion battery of 16 kWh, range (NEDC) 160 km, electric energy consumption (NEDC) 125 Wh/km (135 Wh/km for the 2012 version), charging time approximately 8 h (regular) and approximately 30 min (80% of full charge, fast charger) [20]. Hence, the 357 BEV cars analyzed in this Section may be considered to be small variants of the Mitsubishi i-MiEVs.

Table 6. Vehicle make and model with the number of non-zero length trips and energy consumption.

Vehicle Make-Model	Type	Number of trips of non-zero length	Number of trips of non-zero length and with valid energy consumption data
no make-no model available	car	533	305
Citroen C-Zero	car	141	137
Mitsubishi i-MiEV	car	31,428	19,594
Peugeot iOn	car	25,453	24,080
THINK City	car	8,244	7,911

We analysed the Green eMotion data following the approach used to analyse the Floating-car data with minor modifications to incorporate battery charging and energy usage (battery discharge). To process the data with the same software the electric-vehicle data were pre-processed to transform them to an adequate form. The changes ensured that the correct event types were identified (by the appropriate parsers). Specifically, a charging event was classified as anomalous if the energy recharged was less or equal zero, if its duration was zero, and if the distance between the locations of the beginning of charging and its end was greater than 30 meters (Euclidean distance, if GPS coordinates are available). For every trip, which is represented as a single line in the original set, we created 3 associated events: one with an engine start index (MS=0), one in motion containing the distance travelled (MS=1), and one with an engine off (MS=2) corresponding to the end of the trip. As in our analyses of conventional vehicles, we joined two consecutive trips to a contiguous trip if the

stopping time between the two events was less than 10 min. For the charging events, we introduced new event codes, MS=100, 101, 102, indicating the start, charging, and end of charge (respectively). Thus, a charge event, which is a single line in the Green eMotion dataset, is transformed into 3 lines, each one with a time stamp, a code, and a number that may be interpreted by the previously described software.

4.1 Mobility characteristics

Figure 17 (left) presents the trip-distance distribution as a histogram, binned in 3 km bins, for the 357 BEVs (cars). We found that a 3 km binning provides a reasonable representation of the empirical distribution. The red line shows the cumulative trip distribution: it shows that 80% of the trips travelled a distance less than 10 km. The right subfigure shows the distribution of the duration of the trips, binned at 10 minutes. A predominance of short trips is noted: 80% of the trips lasted less than 22.2 min, the median trip duration was 0.06 hours (3.6 min), and the average trip duration 0.21 hours (12.6 min). For a comparison with conventional-vehicle mobility see Table 7.
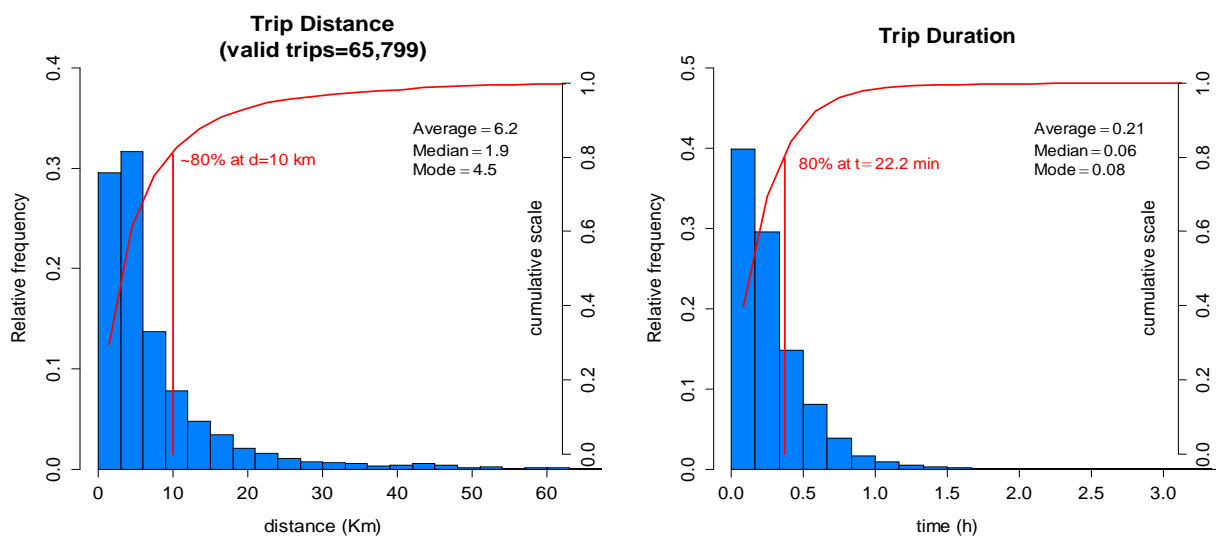

Figure 17. Left: trip distance distribution (bars) with cumulative distribution. Right: trip duration.

As in the case of the Floating-car data, the distance travelled per trip and per day of the week is of particular interest, as such distributions provide indications on different activities performed during the day. We present the data, along with average, median and mode of the corresponding distributions, in Appendix A, Figure A13.

One of the most important quantities to assess the viability of electric vehicles is the daily mobility distance, the total distance (length) travelled in a day. The daily mobility distance provides information complementary to the distance travelled per trip. This distance is to be compared to the reported autonomy of an electric vehicle. All trips initiating on the same day are accounted for in the calculated total daily distance (even if they terminate after midnight). Figure 18 presents the distribution of the daily mobility length (the sum of the length of all trips initiated on the same day), and its cumulative distribution (left), whereas the daily number of trips is shown in the right subfigure.
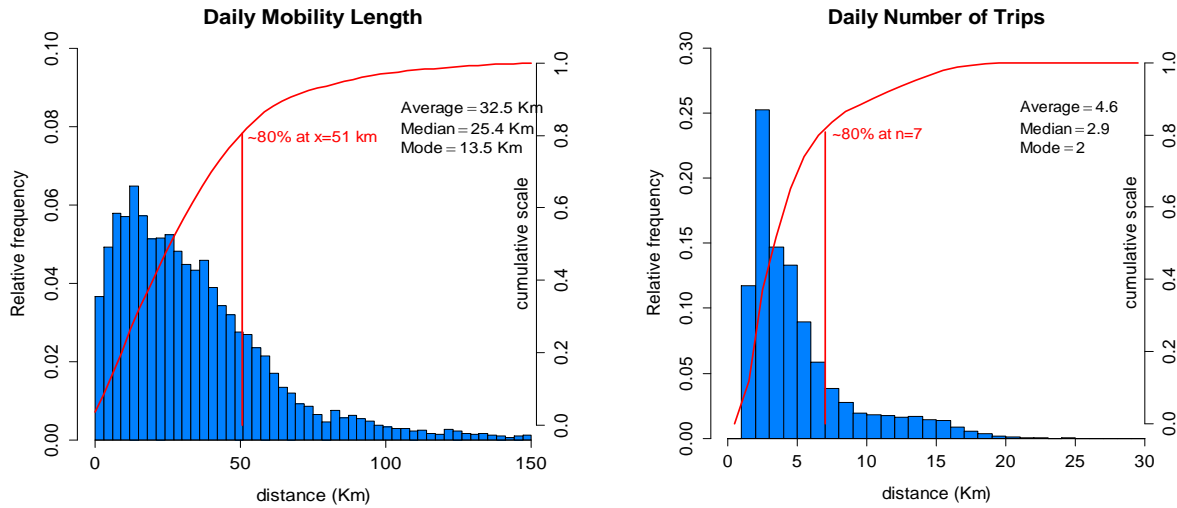
Figure 18. Left: Daily mobility distance relative frequency (bar) and cumulative (red, solid) distributions. Right: Relative frequency (bar) and cumulative distribution (red, solid) of daily number of trips.

The daily mobility distance is further compared to the daily distance covered by conventional vehicles by fitting the probability distribution function to the power-law distribution with an exponential cut off, Eq. (6). The results are shown in Figure 19. The fitting parameters were obtained using a distance range from 3 to 140km. The fit reproduces rather accurately the data, providing further support that the chosen distribution describes well the daily-mobility distance. As previously argued, specific features of the city or drivers' behaviour are reflected in the choice of the distribution parameters. The daily mobility distribution and the corresponding fit per day of the week are show in the Appendix, Figure A14.
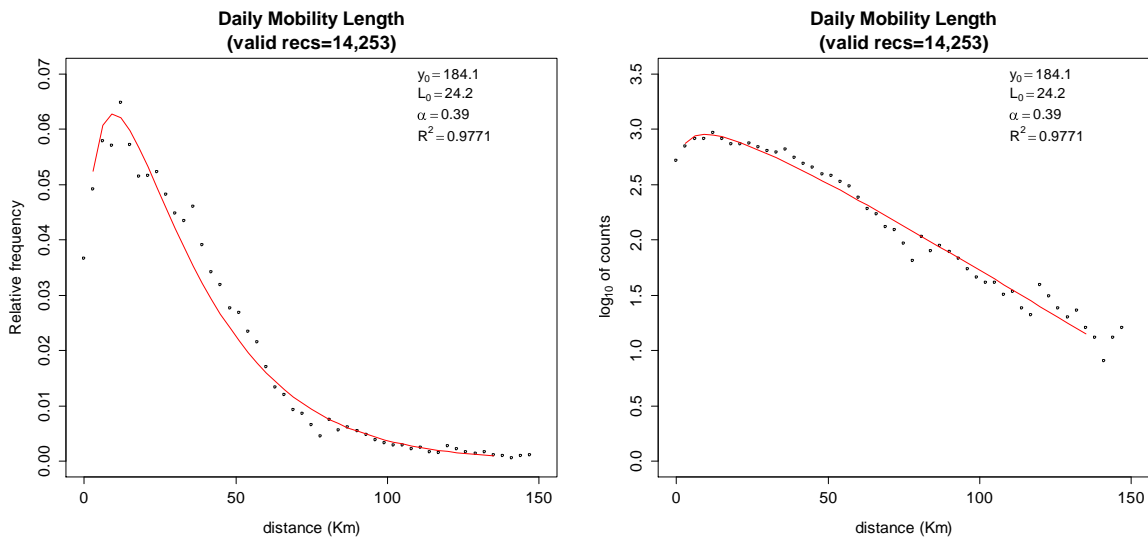

Figure 19. Daily mobility distance: data (points), fit (solid, red line); Left: linear scale. Right: logarithmic scale.

Table 7 compares aggregate statistical quantities for a number of mobility variables associated with conventional mobility (Floating- car data) and electro-mobility (GeM). The Survey data are not included. We note that the most frequently used statistical quantities (average, mean, and mean) of the trip distance, trip duration, and daily mobility distance are lower for the cars that participated in the Green eMotion than for the Floating-car vehicles. The same conclusion may be drawn by comparing the characteristic length scale L_1 of the daily-mobility distribution: it is approximately 34-38 km for the floating-car database and 24 km for the Green eMotion database. It seems that drivers of electric vehicles drive for a shorter time and fewer

kilometres per trip and per day than drivers of vehicles with internal combustion engines. This could also be a result of the car-size segment as well as the urban driving bias that dominates the GeM sample, whereas the Floating-car data covers more segments and a higher share of extra-urban driving. The same quantities for the number of trips per day are rather similar.

		Average	Median	Mode
Trip distance (km)				
	Floating-car, Modena	9.4 (wd[2]),11.2 (we[3])	4.5 (wd), 4.8 (we)	1.5
	Floating-car, Florence	9.7 (wd),12.2 (we)	4.3(wd), 4.9 (we)	1.5
	GeM	6.2	1.9	4.5
Trip duration (min)				
	Floating-car, Modena	15.6	12	7.2
	Floating-car, Florence	17.4	12	7.2
	GeM	12.6	3.6	4.8
Trips per day				
	Floating-car, Modena	4.6	3.7	2.0
	Floating-car, Florence	4.4	3.5	2.0
	GeM	4.6	2.9	2.0
Daily mobility distance (km)				
	Floating-car, Modena	40.5	32.0	9.5
	Floating-car, Florence	39.2	29.5	6.5
	GeM	32.5	25.4	13.5

The following figures summarize aspects of the driving behaviour of electric-vehicle drivers. Figure 20 presents the relative frequencies of trip starting times, the time of the day a trip starts, and the relative frequencies of parking times, the time a trip ends. Times are binned in 1h bins.
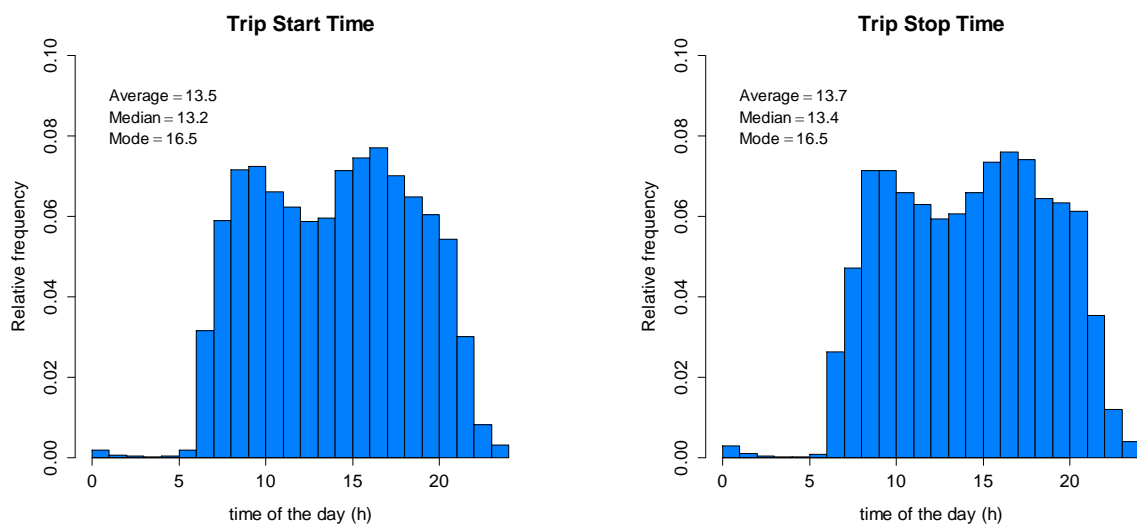

Figure 20. Trip start (left) and stop (right) time distributions as a function time of the day.

Figure 21 presents the percentage of circulating vehicles, binned per hour.
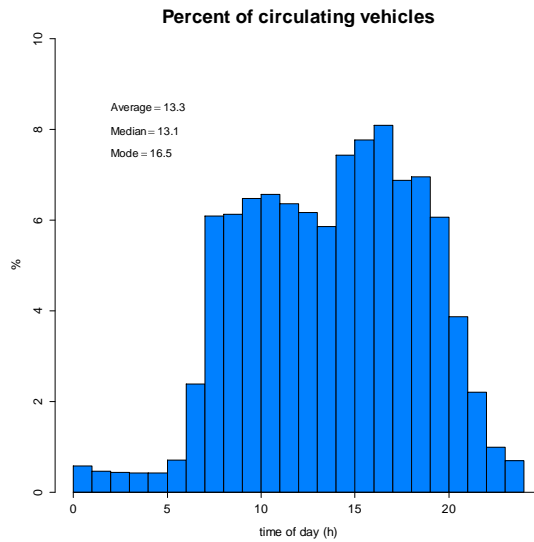
---

[2] Weekday.
[3] Weekend.

Figure 21. Percent of circulating cars during the day.

Figure 22 shows the relative frequency of the time parking starts and its duration.
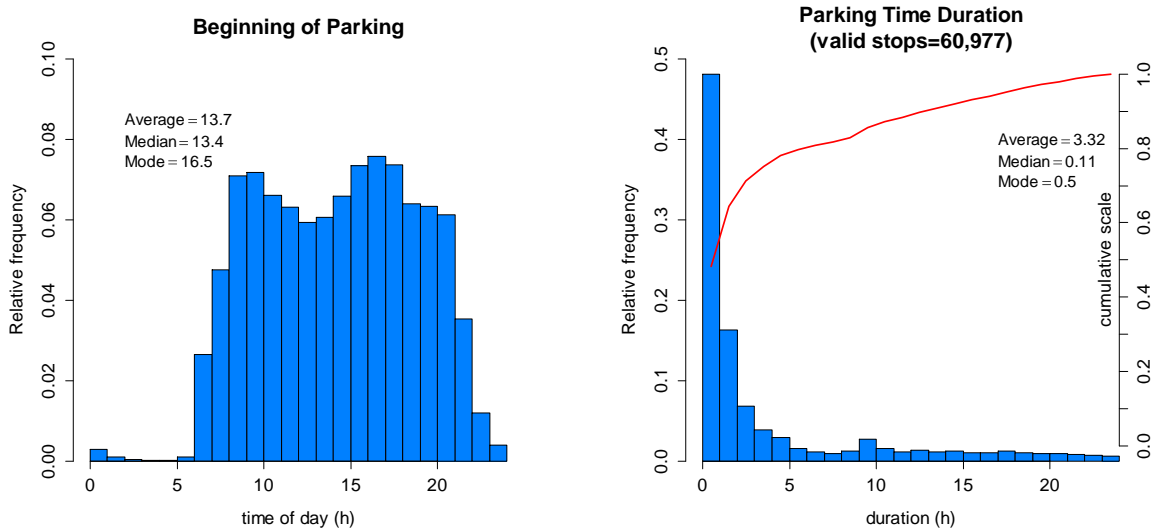

Figure 22. Beginning of parking (stop) during the day (LEFT), and parking (stop) duration, including charging times (right). Cumulative frequencies in red.

Figure 23 presents the relative frequencies of charge starting time and the percent of cars plugged to a charger during the day.
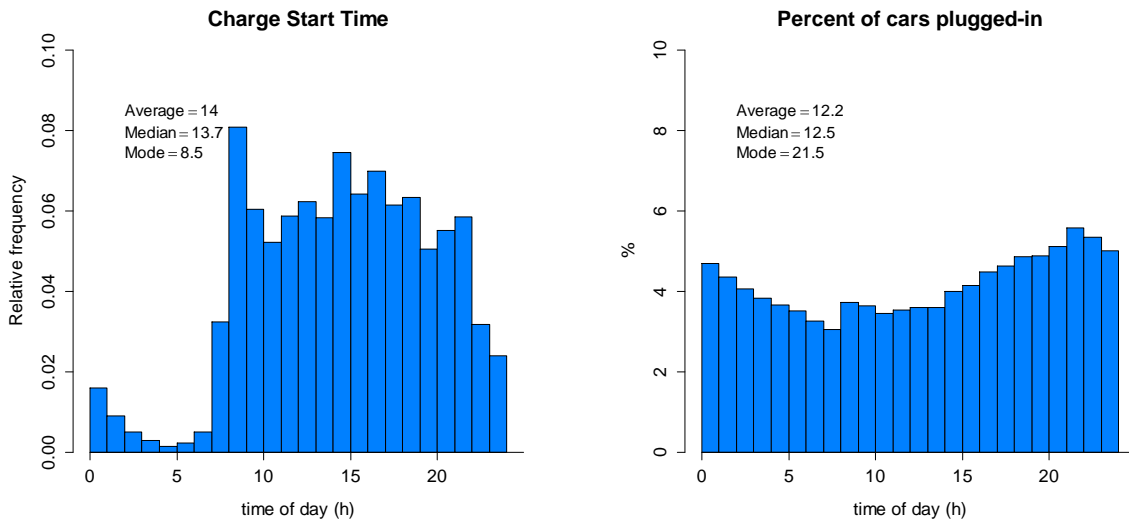
Figure 23. Charge start time distribution (left) and percentage of cars plugged-in at every hour (computed from the charge starting time and its duration), right.

Lastly, Figure 24 presents the number of charges per day along with the energy recharged, namely the amount of energy recharged in the battery, binned at 1 kWh. Note that the percentage of circulating vehicles (Figure 21) closely resembles the starting/stopping trip time distribution (Figure 20) and the beginning of parking distribution (Figure 22), suggesting that the duration of trips is relatively short.
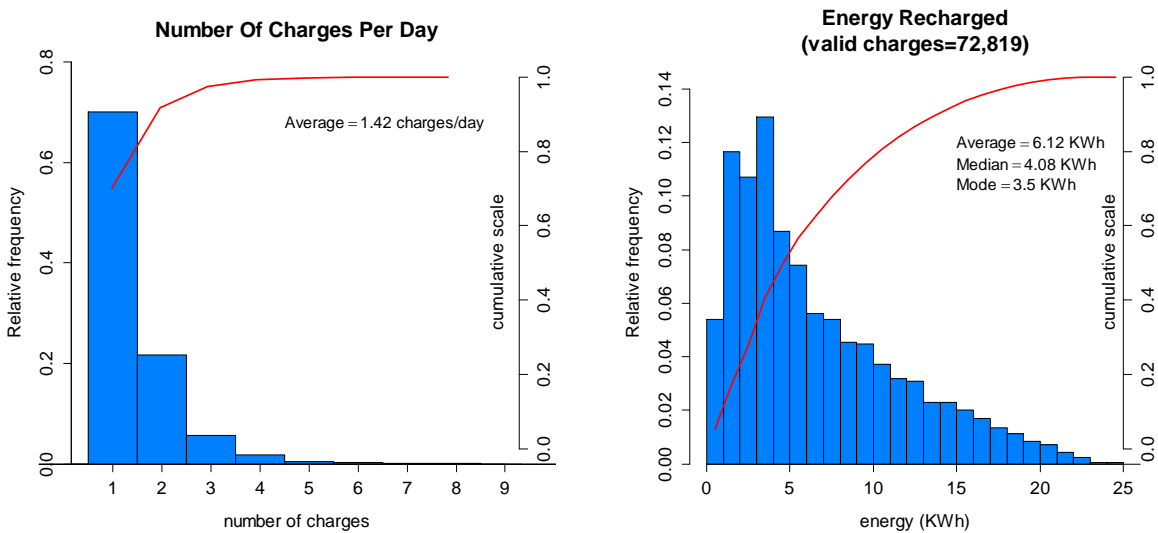

Figure 24. Number of charges during a day (left) and recharge amounts distribution (quantity of energy recharged) (right). Cumulative frequencies in red (solid lines).

4.2 Energy consumption and charging

Figure 25 presents the average energy charged per unit time (power) during the day, binned in hours. The power requested is presented in two modes: on the left, it is normalized to the number of charges performed during that hour, and, on the right, in absolute terms (not normalized) for all countries.
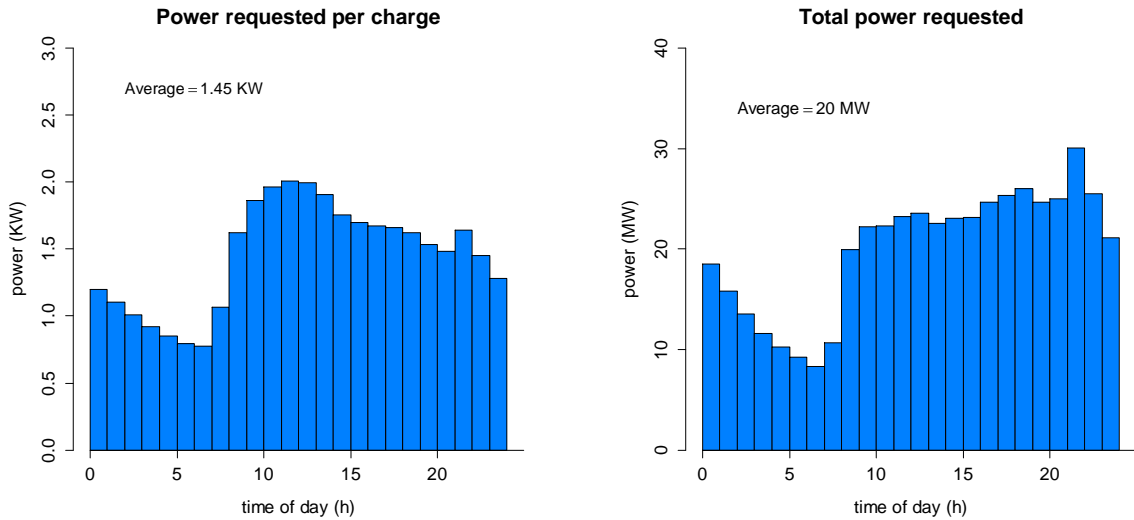
Figure 25. Energy charged during the day per charge (left), the total amount over all countries (right).

We also analysed the State-of-Charge (SoC) of the vehicle battery by considering it at the beginning and at the end of a charging operation. The relative frequencies are shown in Figure 26: in the left subfigure the battery SoC at the beginning of charging is shown, whereas the right subfigure presents it at the end of charging. The state of charge is considered as a percentage of battery charge with respect to the maximum battery capacity. Recall that the absolute value of energy recharged is shown in Figure 24 (right). The power-per-charge data show a minimum early in the morning (approximately at 06:00) and a peak at midday, decreasing slightly afterwards. The total power requested also shows a minimum early in the morning, but it remains flat for most of the day (from 10:00 to 23:00). This figure should be contrasted to Fig. 22 (left) where the time parking begins is plotted. The difference in the overall shape of the relative frequencies between power requested and beginning of parking suggests that the electric vehicles used controlled charging, and that the time parking starts does not provide sufficient information to deduce power (or energy) requested from the grid.
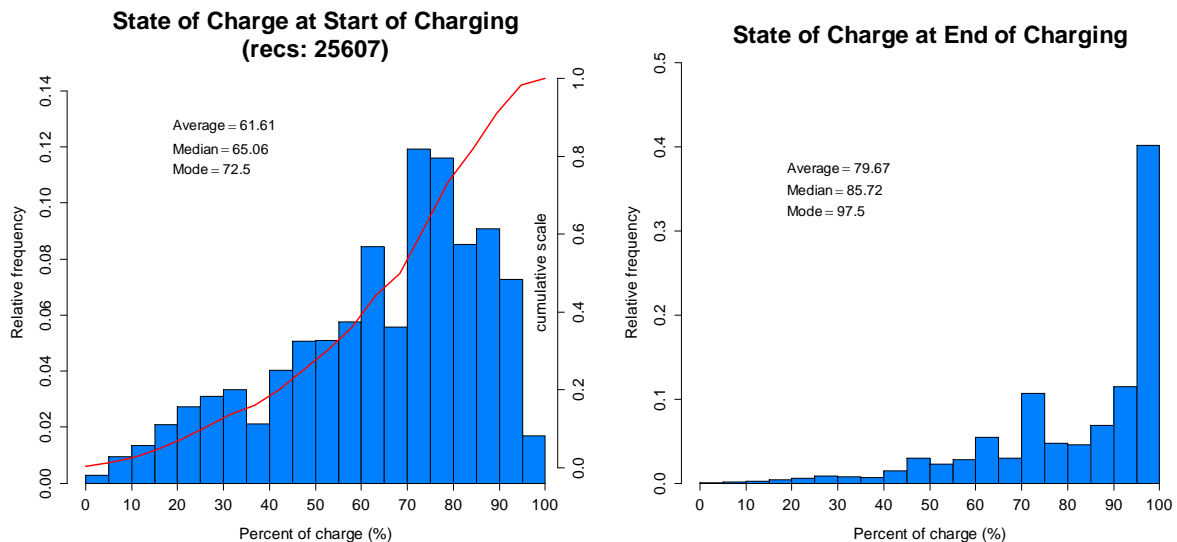

Figure 26. State of charge of the battery at the beginning and at the end of charging.

Inspection of Figure 26 shows that, contrary to what one would have expected, users tend to charge their vehicles at every opportunity they have, and not only when the state of charge is low: the relative frequencies of the SoC at the beginning of a recharge operation peak at about 70-80% charge . This is referred to as opportunity charging. The desire to charge irrespective of the state-of-charge of the battery is further confirmed by noting that more than 40% of charging operations end with a full battery, as shown in the right

graph of Figure 26. We think that the predominance of opportunity charging should be viewed with caution. The behaviour of drivers of electric vehicles may vary with time of usage: frequent charges may be more common initially and could become less frequent as the driver appreciates battery capacity and the vehicle's autonomy.

Figure 27, left, shows the percent energy variation, namely the change of battery SoC per charge, a relative measure of energy recharged. We also computed the total distance travelled between two charging operations, Figure 27, right. Its relative frequency appears to be compatible with the daily mobility length, see Figure 18, left: the 80th percentile at 45 km shows a surprising similarity to the corresponding value of the daily mobility length, 51 km. This suggests that, on average, a vehicle is charged only once per day, in agreement with Figure 24.
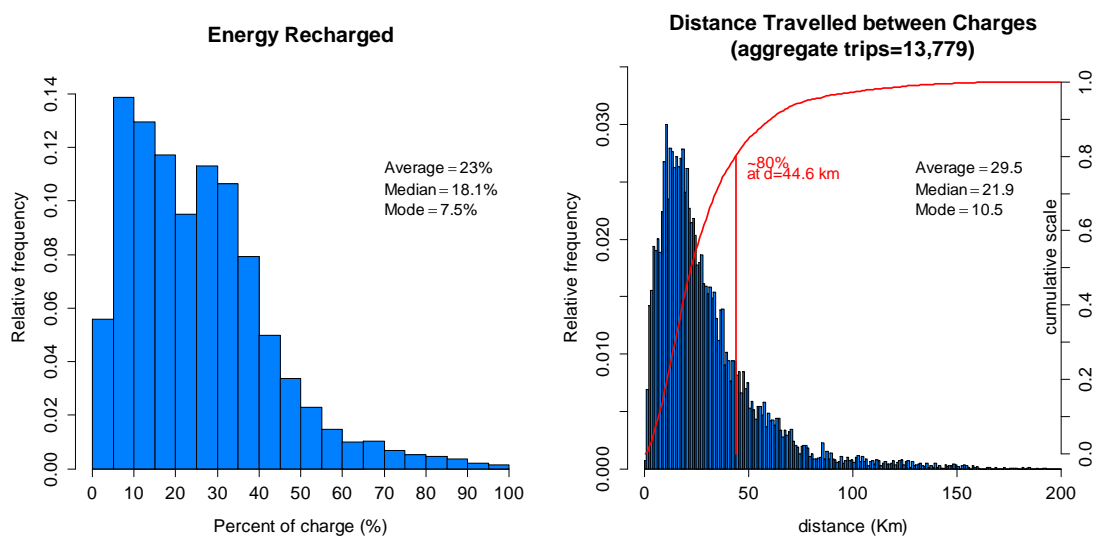

Figure 27. Percent variation of energy charged (left), total distance travelled between consecutive charges (right).

The relationship between energy charged and time to charge the battery may be parametrized by the type of vehicle, its technology, battery type, or its use. Since PHEV and BEV employ qualitatively different technologies (in the sense of a driver's strategy to recharge) a comparison between these two technologies would have provided further insights into drivers' behaviour. Unfortunately, the only available data refer to BEV vehicles.

Figure 28 shows the energy recharged as a function of recharge time parametrized by vehicle type (car, transporter, moto) and use (private or business use, renting, captive fleet). The points at the far left indicate fast charging events. Note that the points in the graph don't necessarily indicate real time charging, but the duration of the connection to the grid and the energy drawn from the grid during that period. This explains the points at the lower right end of the graphs. These events, as well as a large part of the slow charging events, can be considered as suitable for controlled charging, and hence load shifting in the electricity grid.

As BEV cars constitute an important portion of BEV vehicles, we present the same analysis only for them in Figure 29: this figure is an expanded version of the left subfigure of Figure 28. Data are presented in terms of fleet type in the four subfigures: private use, business use, rental, captive fleet.

Of particular interest of the recharge energy dataset is the information it provides on energy consumption per distance travelled, since it can be used to determine real-life vehicle autonomy. The energy consumption per kilometre is used in numerous computer codes, e.g. COPERT [21], to study fuel consumption and emissions. As argued, we have to distinguish powertrain technologies since the electric energy consumed by plug-in hybrid vehicles depends on the mix of electric-thermal energy used, and not solely on the driving pattern and the distance covered, as is the case for purely electric vehicles. Herein, we analyse only BEV cars.
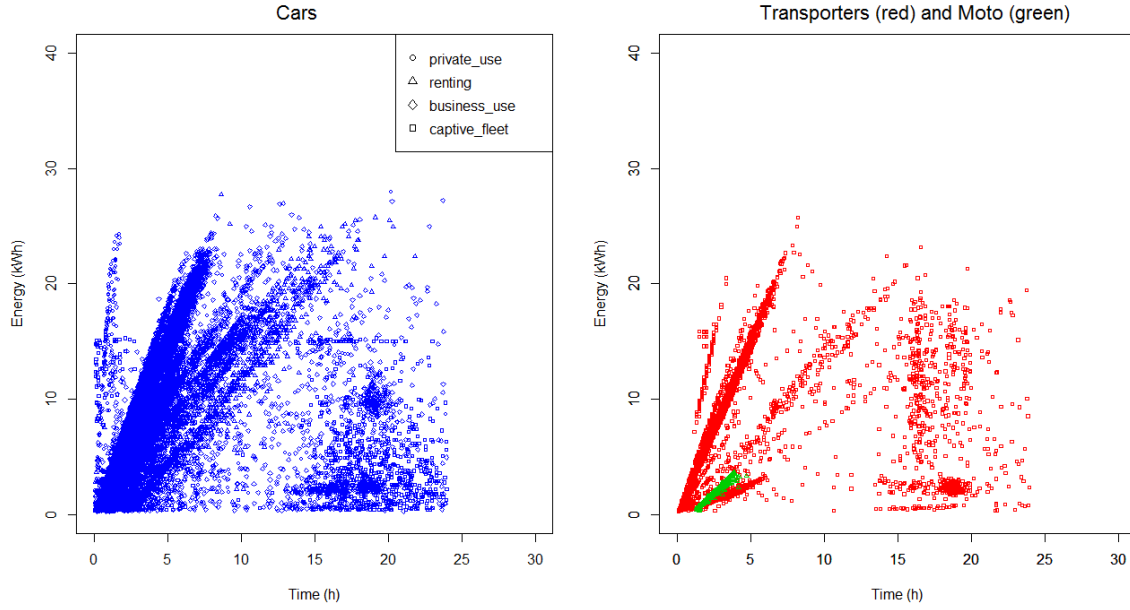
Figure 28. Recharged energy as a function of recharge time (BEV vehicles), subdivided per vehicle type. Left: cars, excluding cars with unknown usage type; Right: transporters (red) and motorcycles (green).
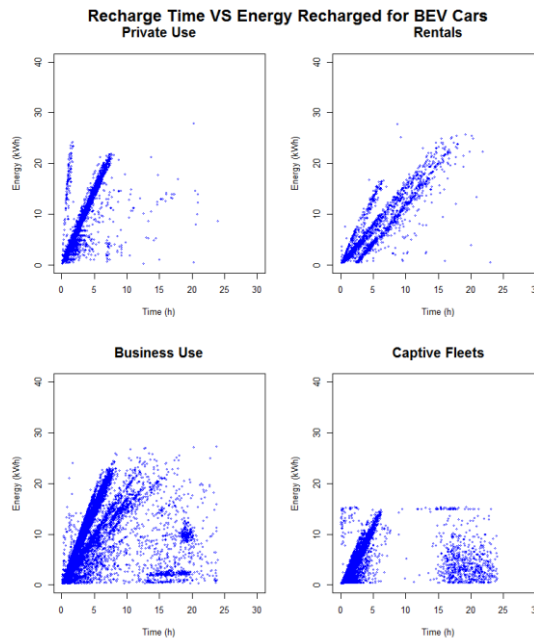

Figure 29. Recharge time versus energy recharged, BEV cars, subdivided by usage.

Figure 30 presents the energy consumed per distance in a scatter plot. The symbols denote car usage, the colour code average trip speed. We performed a linear fit to obtain an approximate indication of consumption trends. We considered only trips of length up to 50 km, which represent 99.15% of all the data, because the scatter was considerable for longer trips and their number relatively low. The linear-fit model yields (see, also the legend of Figure 30) for the energy consumed E (in Wh)

$$<E> = (182 \pm 0.3)d,$$

(14)

where the brackets denote an average and d is the distance in kilometres. The error estimate of the slope is the standard error. We note that the spread of the data about the linear fit increases asymmetrically (with respect to the linear model) as the speed increases. This asymmetric feature may be captured by a fit of the

positive and negative residuals (the two yellow lines). Figure 31 shows the energy consumed versus trip distance for vehicles classified according to fleet type or use.

Energy Consumed VS Trip Distance for BEV Cars
(trips: 52027)

Fit line:
E = (0.182±3e-04) * d

Fit of Residuals:
R+ = 0.0356 * d + 0.2124
R- = -0.0357 * d -0.0662

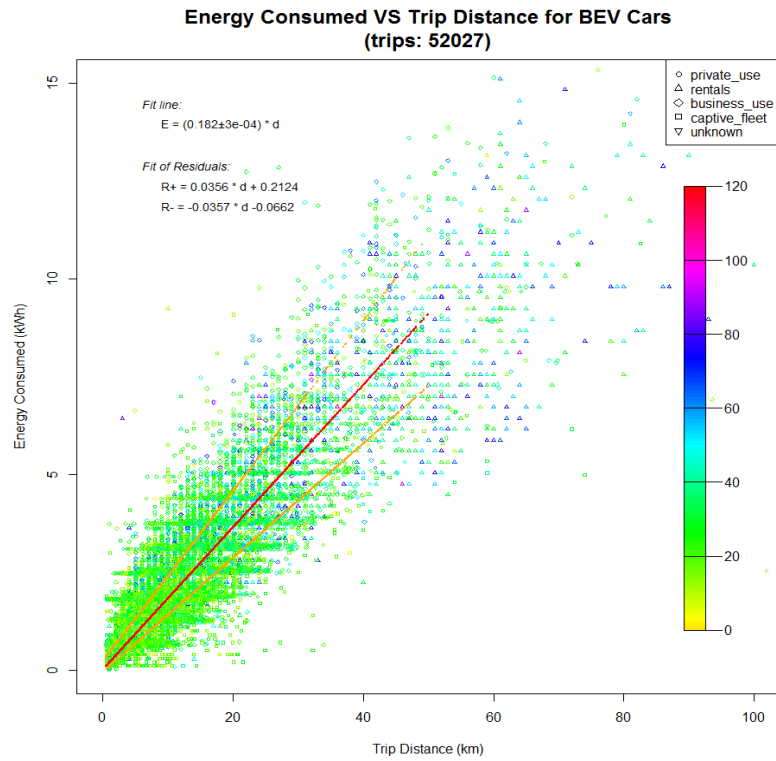**Figure 30. Energy consumption versus trip distance. The colour code denotes average trip speed (km/h).**
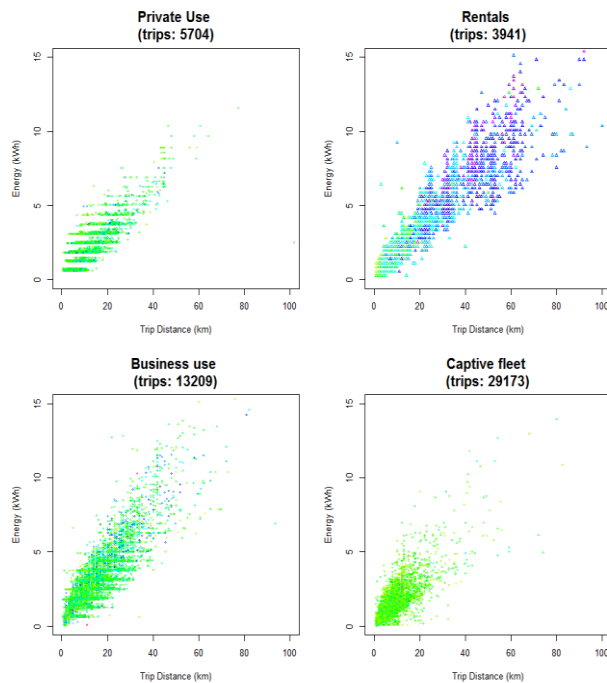

Figure 31. Energy consumption per distance subdivided by car usage, colour code as in Figure 30.

An alternative way to look at the energy consumption is the distribution of the energy consumed per unit length of trip, *E/d*. The corresponding relative frequencies are shown in Figure 32.

In agreement with Ref. [5], trips that consumed more than 1000 Wh/km were discarded, as such consumption was deemed highly unlikely. Thus, the average energy consumed per kilometre may be calculated from the relative frequency histogram via the appropriate weighted average

$$< \frac{E}{d} > = \sum_{i=1}^{N} n_i \frac{E_i}{d_i} = 208 \pm 104 \text{ Wh/km.}$$ (15)

where n_i is the number of trips in bin i, the total number of bins being N, and d_i the distance that corresponds to bin. The variation here represents the standard deviation. We note that there is an approximate 14% difference between the slope predicted by the linear model, 182 Wh/km, Eq. (14), and that predicted by the average of the *E/d* distribution, 208 Wh/km, Eq. (15). This difference is attributed to the two different averaging procedures. In particular, the result shown in Eq. (15) is a ratio estimator, i.e., it is related to the ratio of the means of two variables. It is known that such estimators are biased. We thus consider the result of Eq. (15) less representative of real-life consumption than the prediction of Eq. (14).
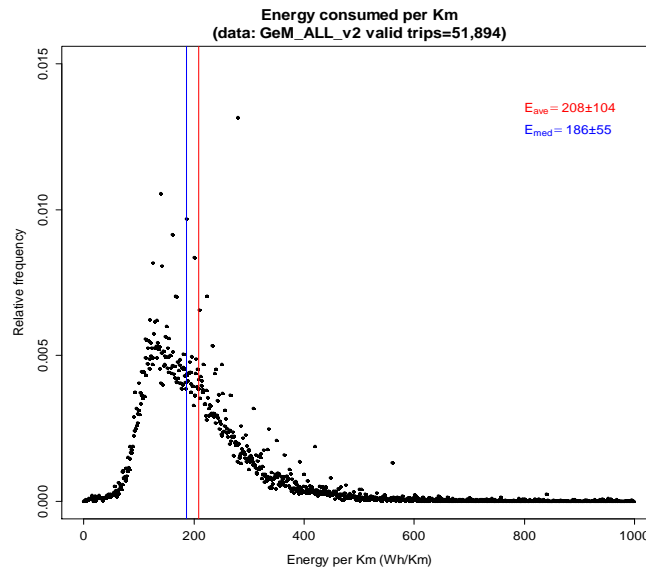

Figure 32. Relative frequencies of energy consumed by BEVs per trip length.

More importantly, inspection of the distribution, Figure 32, manifests that it is not a Gaussian distribution. Hence, a more robust estimate of the energy consumed per kilometre is provided by the *median* instead of the *average*. Equivalently, the most reliable estimator for *E/d* is the median of the distribution since ratio estimators are better described by the median of the corresponding relative frequency histograms. For the truncated distribution, energy per kilometre within 0 to 1000 Wh/km, shown in Figure 32 we found that the median is $186 \pm 55 \text{ Wh/km}$, where the spread about the median is the median absolute derivation (a generalization of the standard deviation for robust statistical analyses).

The large standard deviation of the average, Eq. (15), is another indication that energy per km is not normally distributed. We checked the dependence of the average and the median on the upper limit (1000 Wh/km). If the cut off is set to 500Wh/km (50,853 trips) the average is 199 Wh/km and the median 186 Wh/km, whereas at 2000 Wh/km (51,984 trips) the average becomes 210Wh/km, whereas the median remains 186 Wh/km. This is a further indication that the median provides a more robust description of the data than the average, since this is highly influenced by outliers. Its use is preferable to the average of the distribution of the energy consumed per kilometre. It is worthwhile to note that the median energy consumption is very close to the average slope predicted by the linear mode, Eq. (14). We remark that the estimated real-world energy consumption per kilometre refers to vehicles similar to the i-MiEV, namely small segment A cars.

The field-test derived real driving value of 186 Wh/km is 38% higher than the type-approval value of the same model-year 2012 vehicles (which is 135 Wh/km). This difference is considerably higher than the difference between real and reported (type-approved) energy consumption per km of conventional vehicles, which is estimated to be between 20 and 25% [27].

Since electric motors are much more efficient than internal combustion engines, heating and cooling the vehicle interior and the battery play an important role in real-life energy consumption. We calculated, and show in Figure 33, the consumption (energy per distance) per month for four Demonstation regions to identify changes in the energy consumption during the year. Results show, as expected, that energy consumption is ambient-temperature dependent, reaching highest values during cold seasons/locations. Figure 33 shows calculated average (circles) and median (squares) energy consumption per kilometre for Denmark (DK), Ireland (IE), Spain (ES) and Sweden (SE). No data were available for Germany, France, and Italy. Note that the relative change of the energy consumption per kilometer is much large for the two cold northern states (Denmark, Sweden) than the change in a southern state (Spain). The relative change in Ireland is inbetween. Results are summarized in Table 8.
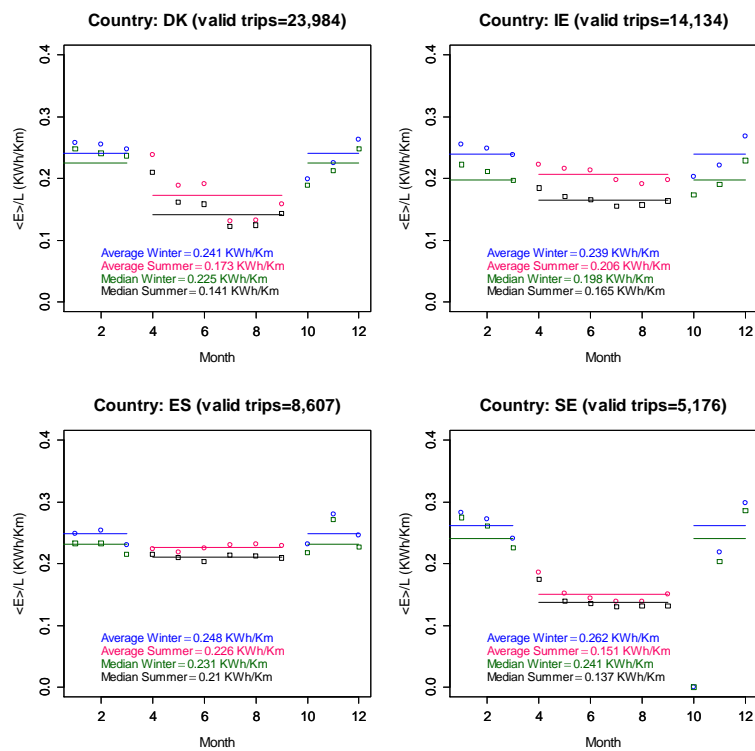

Figure 33. Monthly average (circles) and median (squares) energy consumption per kilometre. Averages and median for the winter months and summer months are also shown.

Note that the October data for Sweden are missing: this month was excluded from the calculation of the winter average. Figure 34 presents aggregated data for all countries. Note that, on average, the median winter energy consumption is higher than the summer consumption by approximately 40%. We also calculated the complete distribution of the energy consumption per trip length per month for the four countries. Results are shown in a series of figures in Appendix A: Figure A15 for Denmark, Figure A16 for Ireland, Figure A17 for Spain, and Figure A18 for Sweden.

The dependence of electric energy consumption on location and month may become more qualitative by considering its dependence on the ambient (external) temperature. For each trip that originated in a particular region (or city, with the code extracted by the vehicle ID), we associated the date of the trip with the average

temperature of that day at that location (where the trip originated). Historical temperatures were taken from the Underground Weather web site, Ref. [22].
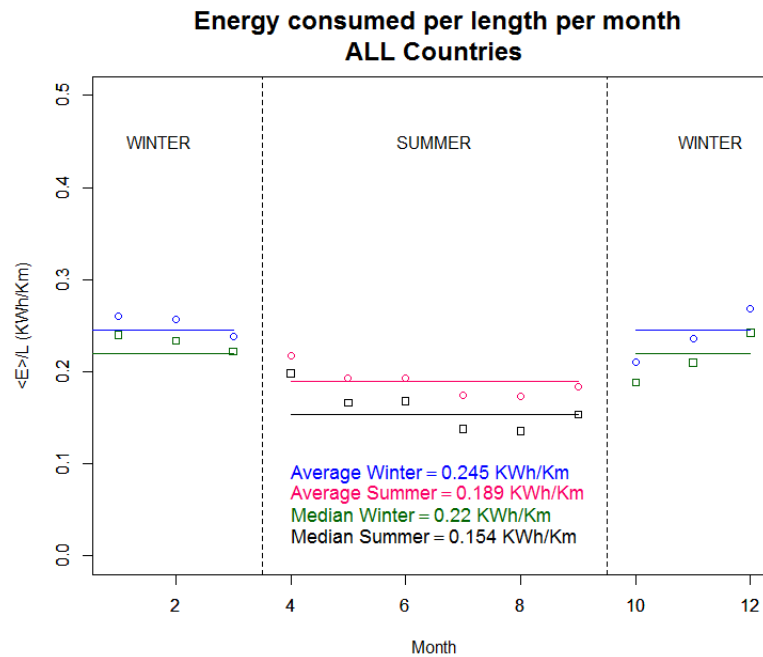

Figure 34. Monthly energy consumption per kilometre, subdivided in winter and summer. Average (circle) and median (squares) are shown.

The results, expressed in terms of average energy consumption and presented in Figure 35, show that in cold and hot weather energy consumption increases, most probably due to the use of on board equipment (heating or cooling). The blue error bars denote one standard deviation, the red the standard error in the evaluation of the mean. For the case of Barcelona/Malaga, it was not possible to distinguish which trips were in Malaga and which were in Barcelona: this leads to the noisiness of the data (we used the Barcelona temperature as a reference). These trips were not added to the aggregate result shown in Figure 34. Similarly, for Region ES2 that included Madrid and Guipúzcoa, a province in the North of Spain (Basque Country), no location information was available, so we used Madrid temperatures for all cars. The data show a remarkable trend: a gradual decrease of energy consumption as the ambient temperature increases from negative/zero degrees to approximately 12^0-13^0C, whereupon consumption stabilizes till the ambient temperature reaches 20^0C. As the temperature increases beyond 20^0C consumption increases rapidly. The observed temperature trend, and specifically the range of temperatures, should be viewed with caution as the high ambient temperature (greater than 20^0) data all come from Madrid/ Guipúzcoa (Demo region ES2).

Table 8. Average energy consumption for four regions correlated to mean winter and summer ambient temperatures.

Country	Average T winter (°C)	Average T summer (°C)	Energy per km Winter average/median (Wh/km)	Energy per km Summer average/median (Wh/km)	Relative median consuption change (%)
DK2 (Copenhagen)	3.5	14.0	241/225	173/141	60
SE1 (Malmö)	-0.11	12.8	262/241	151/137	76
IE1 (Dublin)	6.3	12.2	239/198	206/165	20
ES2 (Madrid, Guipúzcoa)	9.2	20.7	248/231	226/210	10

The estimated average/median energy consumption per kilometre may be used to assess real-range of electric vehicles under the condition of the Green eMotion project. Such calculations are summarized in Section 4.3. We should mention that our analysis of the energy consumed by electric vehicles does not take explicitly into account elevation changes, a factor that influences significantly energy consumption.
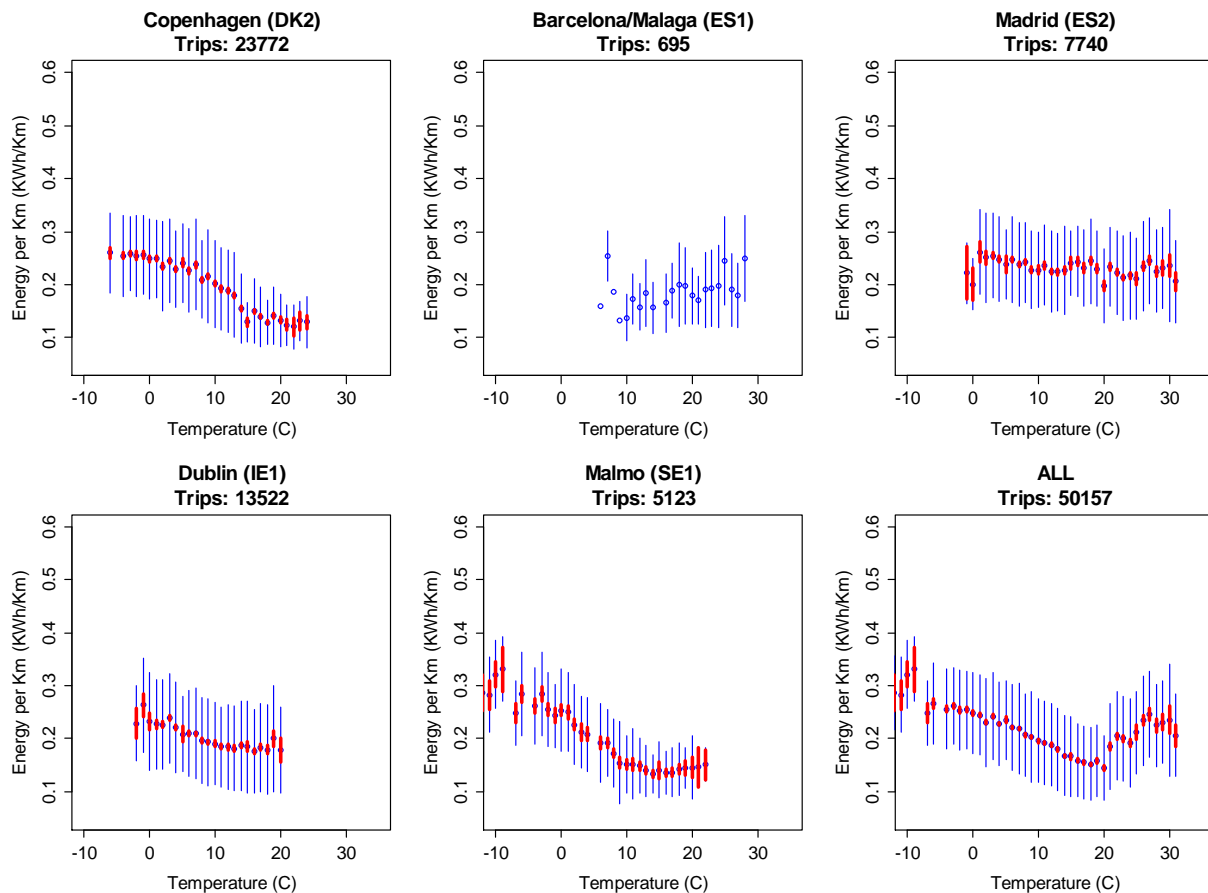

Figure 35. Average energy consumption per kilometre versus external temperature

We conclude the analysis of the energy consumption of BEVs by comparing it to a characteristic estimate of consumption of conventional cars (internal combustion engines using gasoline or diesel). Similarly-sized conventional cars, optimised for energy efficiency, use between 407 Wh/km (diesel-propelled car) and 440 Wh/km (gasoline-propelled car)[4].

4.3 Driving range

As argued, electric vehicles consume different amounts of energy depending on the external temperature due to the use of air conditioning or heating. Furthermore, under extreme ambient temperatures the battery may need pre-conditioning (e.g., heating/cooling) before driving. Other factors that affect energy consumption include traffic characteristics and topography, with a hilly terrain leading to a higher consumption than a flat terrain.

A reasonable estimate of the real range of electric vehicles (their autonomy) is a determining factor in deciding where appropriate infrastructure should be located. Currently, the decision where charging stations will be placed is based on the requirement that no electric vehicle remain without charge on the road. Two cases should be considered: placement on a city level (urban road network) and placement on regional/national level (rural network and highways), as conditions and required input differ. Whereas infrastructure placement

---

[4] Calculated from type-approval values of Volkswagen Polo Blue Motion variants and the addition of an assumed 20% difference between real-world and type-approval fuel consumption values.

in urban settings depends on, among other variables, points of interest [23, 24] (shopping centres, museums, schools, places of work), population density, parking availability, etc., infrastructure placement in highways is primarily determined by the expected real driving range as well as availability of parking bays. Infrastructure placement in urban settings may, thus, be viewed as a much more complex problem.

Herein, we consider the placement of charging stations along highways (inter-city transport). For a detailed GIS analysis of infrastructure placement the reader may refer to Refs. [8,9,23]. We follow the methodology proposed in Refs. [25,26], with some modifications. We define the minimum real range R_{min}^{real} as the product of the declared range R_{decl} times a weather factor WF and a traffic factor TF

$$R_{min}^{real} = R_{decl} \times WF \times TF. \tag{16}$$

The weather factor incorporates use of air conditioning or heating and the effect of weather on battery performance, whereas the traffic factor incorporates driving-profile effects. As such the traffic factor depends on the average vehicle speed, traffic condition, road network topology, and terrain topography. It is frequently assumed that the real minimum distance between recharging events D_{min} should include a safety margin SM to render it

$$D_{min} = R_{min}^{real} \times (1 - SM). \tag{17}$$

A safety margin is introduced to ensure that even vehicles that are not fully charged can reach the next charging station with reasonable certainty. A typical value is about 10%.

The Weather Factor is the ratio of the minimum to the maximum energy consumption per km. As shown in the previous section (for the vehicles that participated in the Green eMotion project) the maximum energy consumption, either average or median, occurs in the winter. We consider the average energy consumption (preferable to the median for this calculation, as it is higher and our estimate is conservative) in two countries in Europe: Sweden in Northern Europe and Spain in Southern Europe. A small electric vehicle in Sweden in the summer ($T_{mean} = 13^o$ C) consumes on average the least energy (of the four Demonstration regions), 151 Wh/km (Table 8, SE1) since neither heating nor air-conditioning is used. This GeM-derived estimate is to be compared to the declared energy consumption of 125 Wh/km for the vehicles sampled in Sweden (mostly i-MiEVs) [20]. The declared consumption refers to the 2015 i-MiEV: it is 135 Wh/km for the 2012 version. Since the same vehicle in Sweden in the winter consumes (on average) 262 Wh/km, the increase of energy consumption in the winter is roughly 60%, the WF being approximately 0.58.
In Spain, energy consumption ranges between 226 Wh/km in the summer (with air-conditioning on) to 248 Wh/km in the winter (with heating), Table 8, ES2. The previous calculation gives a weather factor of 0.91, as there is a relatively small variation of energy consumption during the year, see, also, Figure 35. We prefer, however, to provide a more conservative estimate of real-driving consumption by estimating the minimum energy consumption. All the cars in Spain (region ES2) were Think City whose declared consumption is 150 Wh/km. We modify the summer consumption by the same factor that modified the declared (summer) energy consumption in Sweden to obtain the minimum energy, namely by 151/125=1.21. Thus, the estimated minimum energy consumption in Spain is 150x1.21=182 Wh/km. The corresponding (estimated) weather factor for Spain becomes 182/248=0.74. These calculations are summarized in Table 9.

Table 9. Declared and GeM average energy consumption per kilometre in Sweden and Spain.

	Vehicle	Declared Consumption (Wh/km)	Minimum Consumption (Wh/km)	Summer Consumption (Wh/km)	Winter Consumption (Wh/km)	WF=Min/Winter
Sweden	i-MiEV	125	151 (real)	151	262	0.58 (real)
Spain	Think City	150	182 (estimated)	226	248	0.73 (estimated)

The traffic factor can be estimated from similar studies for conventional vehicles because it reflects the extra energy consumed at high velocities (around 25% for driving at 120 km/h) and/or aggressive driving (around 5%). The total TF is usually estimated to be 0.7.

Therefore, to create the minimum infrastructure in Spain, one has to consider that a vehicle with the minimum declared range (in this case the C-zero, declared range 150 km) can find a recharging station at least every 81 km, while in Sweden every 61 km, Table 10.

Table 10. Minimum range in Sweden and Spain, Eq. (16).

Vehicle	Declared Range in km	Min. Real (Spain)	Min. Real (Sweden)
Nissan Leaf	199	102	81
C-zero	150	77	61

In addition, if we consider the safety margin, Eq. (17), the minimum distance between charging stations reduces to about 55 km in Sweden and 69 in Spain. Indeed in Ref. [25] a distance of 60 km was set for installation of infrastructure in highways in Estonia, a Northern European country.

Table 11. Minimum calculated distance for re-charging stations, Eqs. (16) and (17).

	Declared Range km	Minimum Real Range (km)	Minimum Distance for recharging stations (km)
Spain	150	77	69
Sweden	150	61	55

5. Comparison and discussion

The data previously analysed are compared graphically in this Section. We opted to compare trip distances (Figure 36), daily mobility length (Figure 37, left), daily number of trips (Figure 37, right), and parking duration (Figure 38).

Figure 36 shows the trip-distance data (symbols) and the corresponding theoretical distribution functions (and their parameters). As mentioned earlier, we had to bin all data into 5 km bins as the survey data were registered at such accuracy: thence, the limited number of points. We also show the 80th percentile of the cumulative distribution function (vertical lines): for example, the Survey data suggest that 80% of the vehicles travelled less than 24 km per trip (calculated on the initial data, binned at 1 km). As argued the corresponding value for Green eMotion vehicles is smaller, 10 km. We note that the trends are similar, but, as the previous detailed analyses showed, the corresponding theoretical distribution functions, even though they have the same functional form, have different parameters. We argued that these parameters reflect particular features of the sampling, network topology, driving habits, traffic, road topography. It seems that the Floating-car data and the Green eMotion distributions are in relatively close agreement, differing slightly from the Survey data.
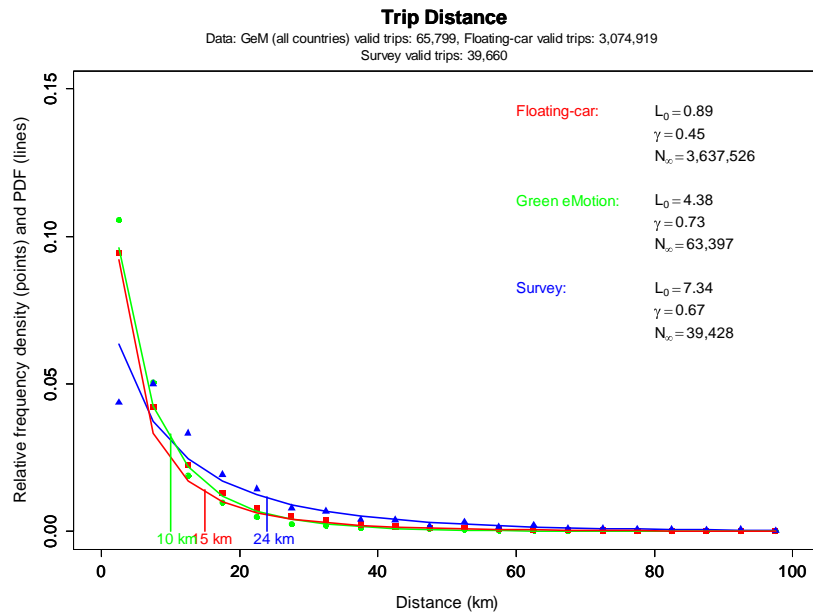
Figure 36. Comparison of single-trip distance distributions. Vertical lines represent the value of 80% of the cumulative distribution.

The left subfigure of Figure 37 presents the daily mobility distance relative frequencies. Note the jagged feature of the Survey data, a consequence of the drivers' tendency to report distances travelled that are multiples of five kilometres. The right subfigure shows the daily number of trips: again the Survey data seem to suggest two-trips per day were much more frequent than the other two datasets would suggest.
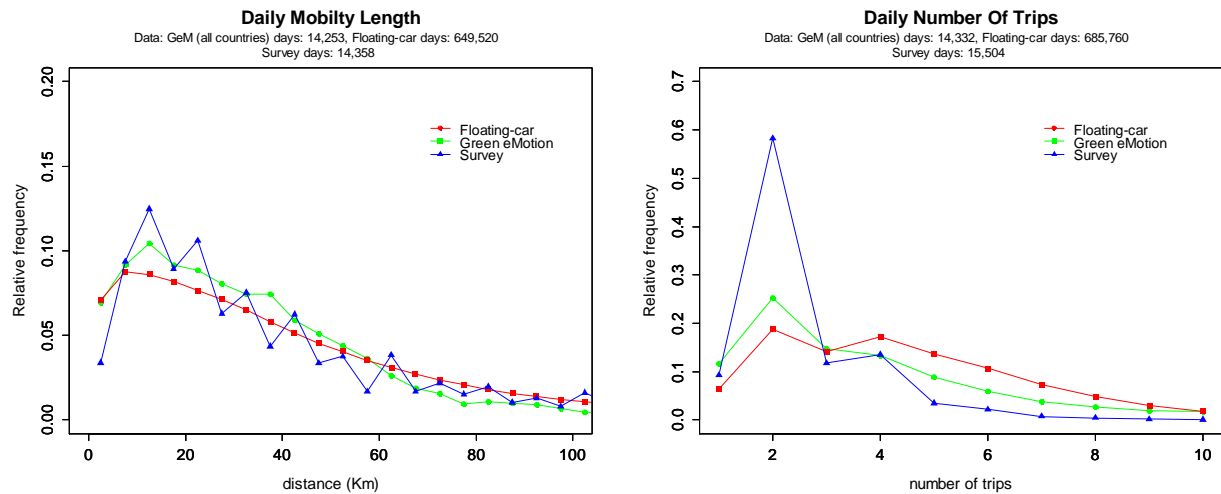

Figure 37. Daily mobility length binned at 5 km (left) and daily number of trips (right).

Figure 38 presents the relative frequency of parking duration (both in a linear and a logarithmic scale). The three distributions have some common features, even though the relative frequencies differ and not all three exhibit the same relative peaks. Specifically, the Green eMotion and Survey data show a pronounced peak in the interval 9-10h and 8-9h, respectively, while the same peak in the Floating-car data is smoother, the interval extending from 8 to 12 h. The Survey data also show a second peak in the interval 14-15h.
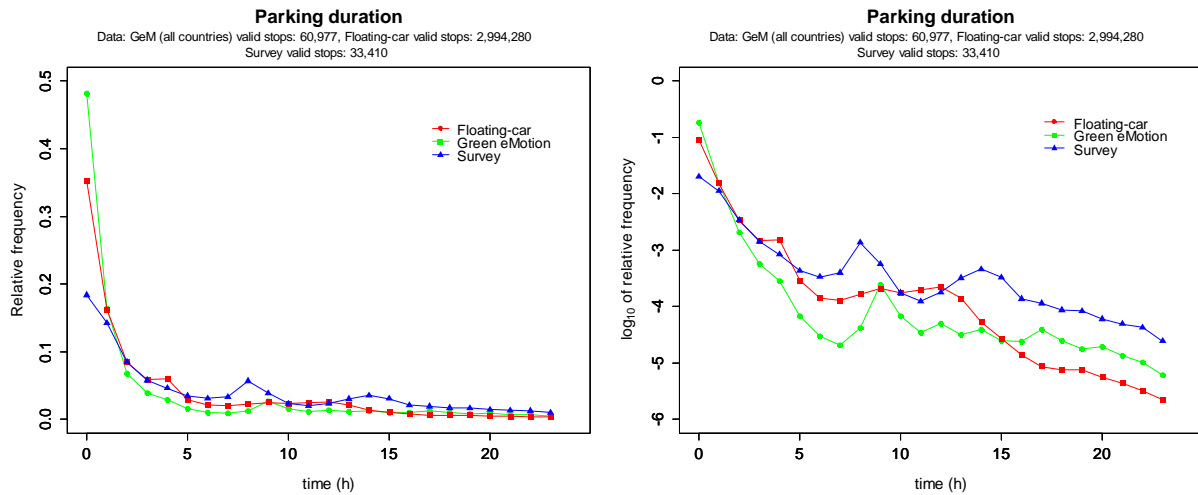
Figure 38. Parking duration of the three datasets. Left: linear scale; Right: logarithmic scale.

We would be remiss in our analysis if we did not compare our results to previous analyses of the data presented in this report. The same Floating-car data were extensively analysed in Ref. [7]. The primary difference between this report and Ref. [7] is our attempt to use the data to obtain theoretical distributions that reproduce compactly and efficiently meaningful information. We suggest that relatively simple formal expressions could reproduce the distribution of single-trips, daily mobility distance, and trip duration. We also suggest that daily driving behaviour of conventional vehicles may be grouped into three, or even two groups: a characteristic driving pattern for a working day, for Saturday, and for Sunday. The latter two being rather similar may be aggregated to define a driving pattern for a typical weekend day.

The overall results and conclusions, though comparable, are not identical. Table 11 compares mean and median values of a few quantities with those calculated in Ref. [7], subdivided by city. We compare to the algebraic averages reported in Ref. [7], their Table A3. We note that our analysis gives larger trip distances and duration, and larger parking duration. We believe the differences arise primarily from our definition of contiguous trips that represent approximately 15% of all valid trips. The inclusion of contiguous trips, by joining some sequential trips and thereby eliminating some brief stops, lowers the number of daily trips, and it increases the average single-trip distance, the daily mobility length, and the parking duration.

Table 11. Comparison of the estimation of various quantities with literature.

	Mean/median trip distance (km)	Mean/median trip duration (min)	Mean/median Parking duration (h)	Mean/median daily mobility length (Km)	Mean/median speed (km/h)	Mean/median number of trips per day
Refs. [2,3] **Modena**	7.82/3.26	11.70/7.55	3.98/0.77		29.03/26.70	6.64/6
This work **Modena**	9.8/4.5	16.2/12.6	4.24/1.78	40.5/32 (80% at 65)	30.2/28.5	4.6/3.7
Refs. [2,3] **Florence**	8.01/3.19	13.18/8.28	4.25/0.73		26.24/23.51	6.4/5.0
This work **Florence**	10.3/4.4	18.6/12.6	4.32/1.76	39.2/29.5 (80% at 64)	27.3/24.5	4.4/3.5

We merged sequential trips with an intermediate stop of less than 10 minutes, the argument being that at least 10 minutes are required to consider charging an electric vehicle with a fast charger. We believe this

merging is appropriate if one is interested in a driver's decision whether to charge or not (with a fast charger, if available). It is not, however, appropriate if one wants to determine the activities that provide destinations to explain drivers' behaviour and the ensuing traffic patterns. Hence, the two approaches are, in a sense, complementary.

Lastly, Refs. [8,9] consider the *average* energy consumed by a small vehicle to be 185 Wh/km. Our estimate of 186 Wh/km of the *median* derived from field data implies that the efficiency is the same, with a difference of less than 1%. Note, however, that the GeM estimated average energy consumption is 208 Wh/km, leading to a difference of approximately 12%. The authors of Refs. [8,9] considered that a medium-sized car consumes 210 Wh/km, or 205 Wh/km if highly efficient.

The Green eMotion data were extensively analysed in Ref. [5], where parts of the current analyses were also presented. Only minor differences between the two analyses may be noted. In particular, the authors of Ref. [9] suggest that shorter trips (less than 5 km) have higher average trip consumption (220 Wh/km) than trips of length greater than 40 km, which have a consumption of 170 Wh/km. Moreover, shorter trips are also slower, their average speed being 23 km/h whereas the average speed of longer trips is 66 km/h. Thus, according to Ref. [9] shorter-slower trips consume on average 23% more energy per kilometre than longer-faster trips. They also considered energy consumption of two different battery types: Lithium-ion (i-MiEV, C-Zero, iOn) and zebra (molten-salt battery, Think City used in GeM, Spain, region ES2). They found that for short trips (distance travelled less than 5 km) the average energy consumption of lithium-ion EV batteries was 220 Wh/km, whereas vehicles with molten salt batteries consumed more, 290 Wh/km. No difference in energy consumption was noted for longer trips (more than 40 km), the average energy consumption being approximately 170 Wh/km.

A project related to the Green eMotion project is SwitchEV, Newcastle (UK) that collected EV data from 44 vehicles in the North East of England between 2010 and 2013 [28,29]. The vehicles used were Leaf (Nissan) and iOn (Peugeot). The number of EV journeys recorded was 85,000, and over 19,000 recharging events were recorded minute-by-minute at more than 650 public and 260 private charging points. Herein, we do not present a detailed comparison of our results with those of Ref. [28], but we note that during the SwitchEV project the average daily mileage of EV drivers was 38.9 km, to be compared to the calculated GeM average of 32.5 km. Moreover, they determined that 50% of all charging events started at a battery SoC greater than 53%, the corresponding GeM median is 65%. The authors of Ref. [28] emphasized that SoC of the EV batteries before it is recharged depends crucially on the driving profile, i.e., driving behaviour and driving conditions.

6. Conclusions

We presented the analyses of three datasets that describe the behaviour of drivers (individual mobility data) of conventional (internal-combustion engine) and (pure) battery electric vehicles (segment A, small-sized cars, the Mitsubishi i-MiEV and its European versions the Peugeot iOn and the Citroen C-Zero , and a few Think City). The conventional-vehicle datasets were obtained from on-board data loggers (Floating-car data, approximately three million valid trips) and from a JRC-sponsored survey in six EU countries (600 participants per country). The electric-vehicle data were obtained from the EU-funded Green eMotion (GeM) project (approximately 165,000 records, including charging events, approximately 52,000 valid trips). We developed a common and generalized Java/R software framework to pre-process the data in a highly efficient, unified, and coherent manner. The data were at first described by simple statistical variables (average, median, mode) of the most relevant variables, e.g. single-trip distances and their duration, daily distance travelled (daily mobility), parking duration, parking start and end time, number of daily trips. Specific variables for electric vehicles included electric energy consumed, number of daily recharges and energy delivered, battery state-of-charge at the beginning and end of charging, power requested from the electric grid.

We then identified functional forms of expected (theoretical) distributions that are compatible with the empirical distributions for some variables. We found that a stretched exponential distribution provides a reasonable fit of the single-trip distribution and its duration, whereas a power-law distribution with an exponential cut-off provides a reasonable approximation of the daily mobility distance. These mappings allow the description of aspects of drivers' behaviour by few parameters. In this sense the theoretical distributions provide a meaningful and concise method to present complex information inherent in large datasets.

The Floating car data (conventional mobility) showed that a driver's daily pattern may be divided into three groups corresponding to driving on a weekday, on a Saturday, and on a Sunday. For simplicity the last two may be group to a weekend driving pattern.

We found significant similarities between the three datasets, in particular in the distributions of the distance travelled per trip and duration of parking. However, some differences between battery electric vehicles (GeM data) and conventional vehicles (Floating-car data) were noted. The average and median daily distances travelled by BEVs (cars) were approximately 20% less than the distances travelled by conventional vehicles (in Modena and Florence, the two cities studied via floating-car data), whereas the mode was larger. The analysis of the electric vehicles showed that 80% of the trips covered a distance less than 10 km, 80% of the trips lasted less than 22 min, and 80% of the daily mobility of a car is less than 51 km, so well within the real range for most BEVs currently available on the EU market. The corresponding values for conventional mobility (Floating-car data) are 80th percentile of single-trip distance is 15 km and approximately 65 km for the daily mobility. We remarked that a buyer's choice to purchase an electric vehicle might not depend on the large number of daily trips that are within the reported autonomy range of the vehicle, but on the more than expected (from a Gaussian distribution) number of trips that are beyond the reported range.

We estimated the electric energy consumed per kilometre by the BEV cars that participated in the GeM project. We found that the *median* energy consumed was 186 Wh/km with a relatively large spread of 55 Wh/km. A linear regression model (applied only to trips that covered a maximum of 50 km) also predicted an electric energy consumption of 182 Wh/km with a spread of 0.3 Wh/km. A naïve *average* of the distribution of the energy consumed per kilometre gave a consumption of 208 Wh/km, a manifestation that its distribution is non-Gaussian. We suggested that the median, being a robust estimator, is a preferable choice. The energy consumption was determined to depend on the ambient temperature, the minimum consumption occurring when the external temperature was in the range 10^{0}C to 20^{0}C. This dependence was attributed to the use of on-board heating/cooling systems. Median energy consumption in winter months was found to increase by 10% (Spain) to 75% (Sweden) with respect to summer consumption. We used the estimated real-driving consumption to argue that highway placement of charging stations could be approximately every 55 km.

The model distributions presented in this report seem to describe drivers' behaviour under different conditions with a limited number of parameters, suggesting the applicability of the proposed expected distributions to mobility data beyond those tested. Nevertheless, further studies are required to explore this possibility and to confirm the identified difference in the driving dynamics (driver behaviour) of conventional and electric vehicles.

In our analyses of the data we found that there is a clear need to harmonize the way individual (driver) mobility data are collected and treated to increase their quality and usefulness [14]. As more data are expected to be gathered from on-going and future demonstration projects, we remark that a permanent repository would be very useful. We note, however, that one has to be aware that there are personal data protections issues associated with mobility data that need to be treated appropriately.

The data elaborations summarized in this Report form an important building block for subsequent analyses on infrastructure requirements for electric vehicles as well as their potential contribution to wider energy, transport, and climate policy targets. Both will become important for the elaboration of national policy

frameworks in the context of the implementation of the Directive on the deployment of alternative fuels infrastructure (Directive 2014/94/EU).

7. Acknowledgments

8. References

[1] Sims R., R. Schaeffer, F. Creutzig, X. Cruz-Núñez, M. D'Agosto, D. Dimitriu, M. J. Figueroa Meza, L. Fulton, S. Kobayashi, O. Lah, A. McKinnon, P. Newman, M. Ouyang, J. J. Schauer, D. Sperling, and G. Tiwari, "Climate Change 2014: Mitigation of Climate Change", Contribution of Working Group III to the Fifth Assessment Report of the Intergovernmental Panel on Climate Change, Cambridge University Press, Cambridge, United Kingdom and New York, NY, USA (2014), ISBN: 9781107654815

[2] http://ec.europa.eu/clima/policies/transport/vehicles/index_en.htm

[3] Clean transport, urban transport, http://ec.europa.eu/transport/themes/urban/cpt/index_en.htm

[4] B. Giechaskiel, B. Alföldy, and Y. Drossinos, "A metric for health effects studies of diesel exhaust particles", *Journal of Aerosol Science* 40, 639 – 651 (2009).

[5] C. Corchero, S., González Villafranca, M. Cruz, M. Sanmartí, P. Dilara, A.V. Donati, Y. Drossinos, D. Gkatzoflias, A. Spadaro, D. Shingo Usami, G. Giustiniani, C. Contu, L. Guala, and M. Piu, "European global analysis on the electro-mobility performance", Deliverable D1.10, Green eMotion Project, March 2015.

[6] Octo Telematics: "Fornitura di dati di attivita' di veicoli leggeri: specifica tecnica", 25 Nov. 2011.

[7] M. De Gennaro, E. Paffumi, G. Martini, and H. Scholz, "A pilot study to address the travel behaviour and the usability of electric vehicles in two Italian provinces", *Case Studies on Transport Policy* 2 , 116-141 (2014).

[8] E. Paffumi, M. De Gennaro, G. Martini, and H. Scholz, "Assessment of the potential of electric vehicles and charging strategies to meet urban mobility requirements", *Transportmetrica A,* 11, 22-60 (2014).

[9] M. De Gennaro, E. Paffumi, H. Scholz, and G. Martini, "GIS-Driven analysis of e-mobility in urban areas: an evaluation of the impact on the electric energy grid", *Applied Energy* 124, 94-116 (2014).

[10] G. Pasaoglu, D. Fiorello, A. Martino, L. Zani, A. Zubaryeva, and C. Thiel, "Driving and parking patterns of European car drivers – a mobility survey", *JRC Scientific and Policy Report*, EUR 25627 EN (2012).

[11] G. Pasaoglu, A. Zubaryeva, D. Fiorello, and C. Thiel, "Analysis of European mobility surveys and their potential to support studies on the impact of electric vehicles on energy and infrastructure needs in Europe", *Technol. Forecast. Soc. Change* 87, 41-50 (2014).

[12] G. Pasaoglu, D. Fiorello, A. Martino, L. Zani, A. Zubaryeva, and C. Thiel, "Travel patterns and the potential use of electric cars – Results from a direct survey in six European countries", *Technol. Forecast. Soc. Change* 87, 51-59 (2014).

[13] C. Corchero, R. Gumara, and A. Romero, "Green eMotion Demo Regions Reporting Guidelines", IREC, Dep. Power Electronics and Electrical Grids, *Technical Report*, October 2011.

 [14] C. Corchero, R. Gumara, M. Cruz-Zambrano, M. Sanmartí, D. Gkatzoflias, P. Dilara, Y. Drossinos, and A.V. Donati, "Data Collection and Reporting Guidelines for European electro-mobility projects." *JRC Scientific and Policy Report*, EUR 26969 EN (2014)

[15] A. Bazzani, B. Giorgini, S. Rambaldi, R. Gallotti, and L. Giovannini, "Statistical laws in urban mobility from microscopic GPS data in the area of Florence", *J. Statistical Mechanics: Theory and Experiment*, P05001 (2010).

[16] D. Brockmann, L. Hufnagel, and T. Geisel, "The scaling laws of human travel", *Nature* 439. 462-465 (2006).

[17] M.C. González, C.A. Hidalgo, and A.L. Barabási, "Understanding individual human mobility patterns", *Nature* 453, 779-782 (2008).

[18] C. Song, T. Koren, P. Wang, and A.-L. Barabási, "Modelling the scaling properties of human mobility", *Nature Physics* 6, 818-823 (2010).

[19] C.M. Schneider, V. Belik, T. Couronné, Z. Smoreda, and M.C. González, "Unravelling daily human mobility motifs*", J. R. Soc. Interface* 10: 20130246 (2013).

[20] http://www.mitsubishi-motors.com/en/showroom/i-miev/specifications/

 [21] Ntziachristos, L., Gkatzoflias, D., Kouridis, C., and Samaras, Z. "COPERT: A European Road Transport Emission Inventory Model Information Technologies in Environmental Engineering", in Athanasiadis, I.N., Rizzoli, A.E., Mitkas, P.A., Gómez, J.M. (Eds.), Springer, Berlin Heidelberg, pp. 491–504 (2009).

[22] Underground Weather: http://www.wunderground.com/history/

[23] D. Gkatzoflias, Y. Drossinos, P. Dilara, and C. Thiel, "Optimal allocation of electric vehicle charging infrastructure for city and regional/national level", JRC Science and Technical Report, EUR (to be published) (2015).

[24] M. De Gennaro, E. Paffumi, and G. Martini, "Customer-driven design of the recharge infrastructure and Vehicle-to-Grid in urban areas: A large-scale application for electric vehicles*", Energy* 82, 294-311 (2015).

[25] A. Colmenar-Santos, C. de Palacio, D. Borge-Diez, O. Monzon-Alejandro, "Planning minimum interurban fast charging infrastructure for electric vehicles: Methodology and Application to Spain", *Energies* 7, 1207-1229 (2014).

[26] L. Lindblad, "Deployment methods for electric vehicle infrastructure", Master Thesis, Uppsala Univeristy (2012).

[27] G. Fontaras and P. Dilara, "The evolution of European passenger car characteristics 2000 – 2010 and its effect on real-world CO_2 emissions and CO_2 reduction policy", *Energy Policy* 49, 719-730 (2012).

[28] M. Neaimeh, G.A. Hill, Y. Hübner, and P.T. Blythe, "Routing systems to extend the driving range of electric vehicles", *IET Intel. Transport Syst.* 7, 327-336 (2013).

[29] M. Neaimeh, R. Wardle, A.M. Jenkins, J. Yi, G. Hill, P.F. Lyons, Y. Hübner, P.T. Blythe, and P.C. Taylos, "A probabilistic approach to combining smart meter and electric vehicle charging data to investigate distribution network impacts", *Applied Energy* (in press), dx.doi.org/10.1016/j.apenergy.2015.01.144 (2015).
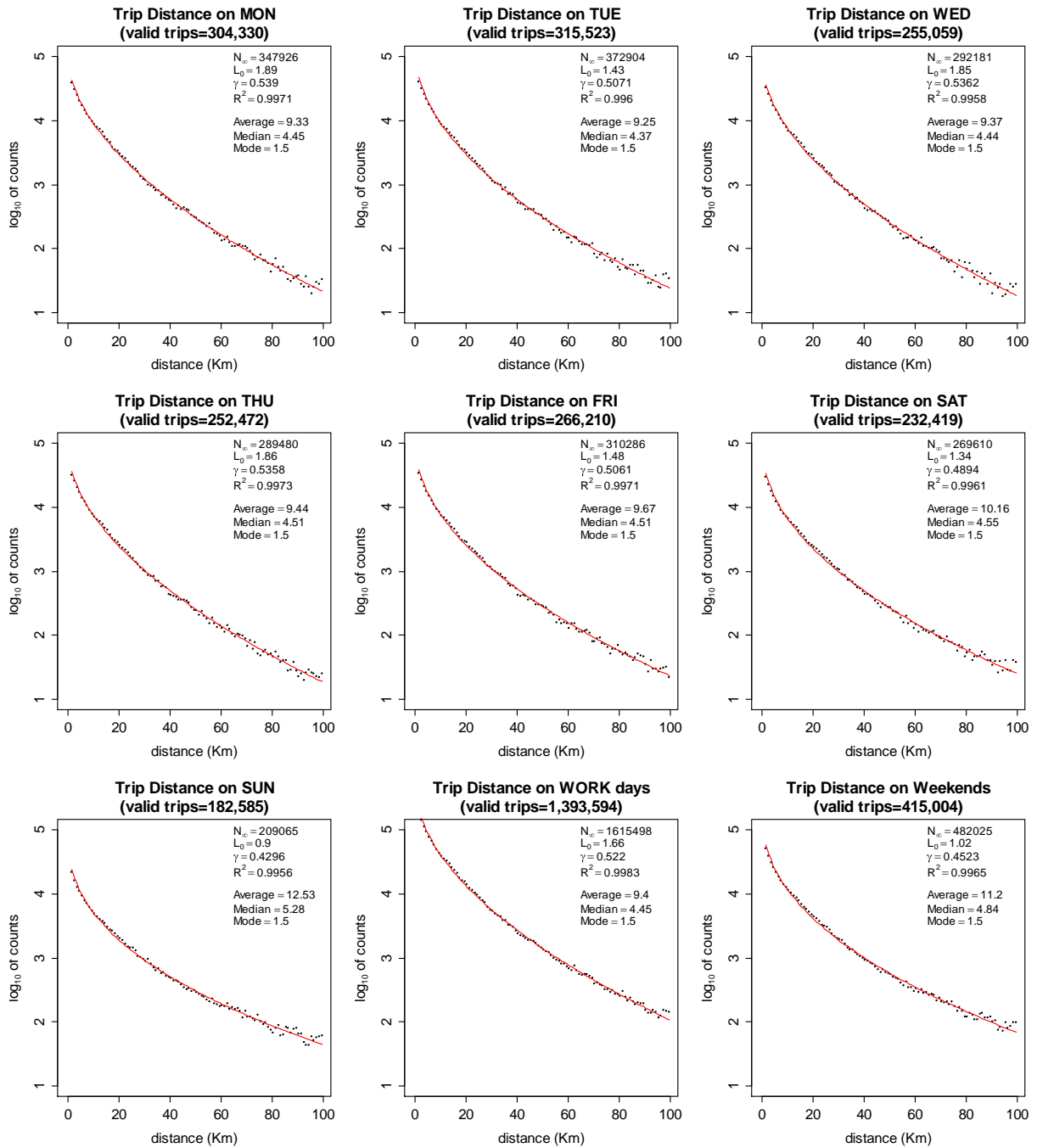
Appendix A

Figure A1. Modena (Floating-car data). Distribution of single-trip distances per day of the week and aggregated per working and weekend day (symbols). Fitted distribution, Eq. (3) (red solid line).
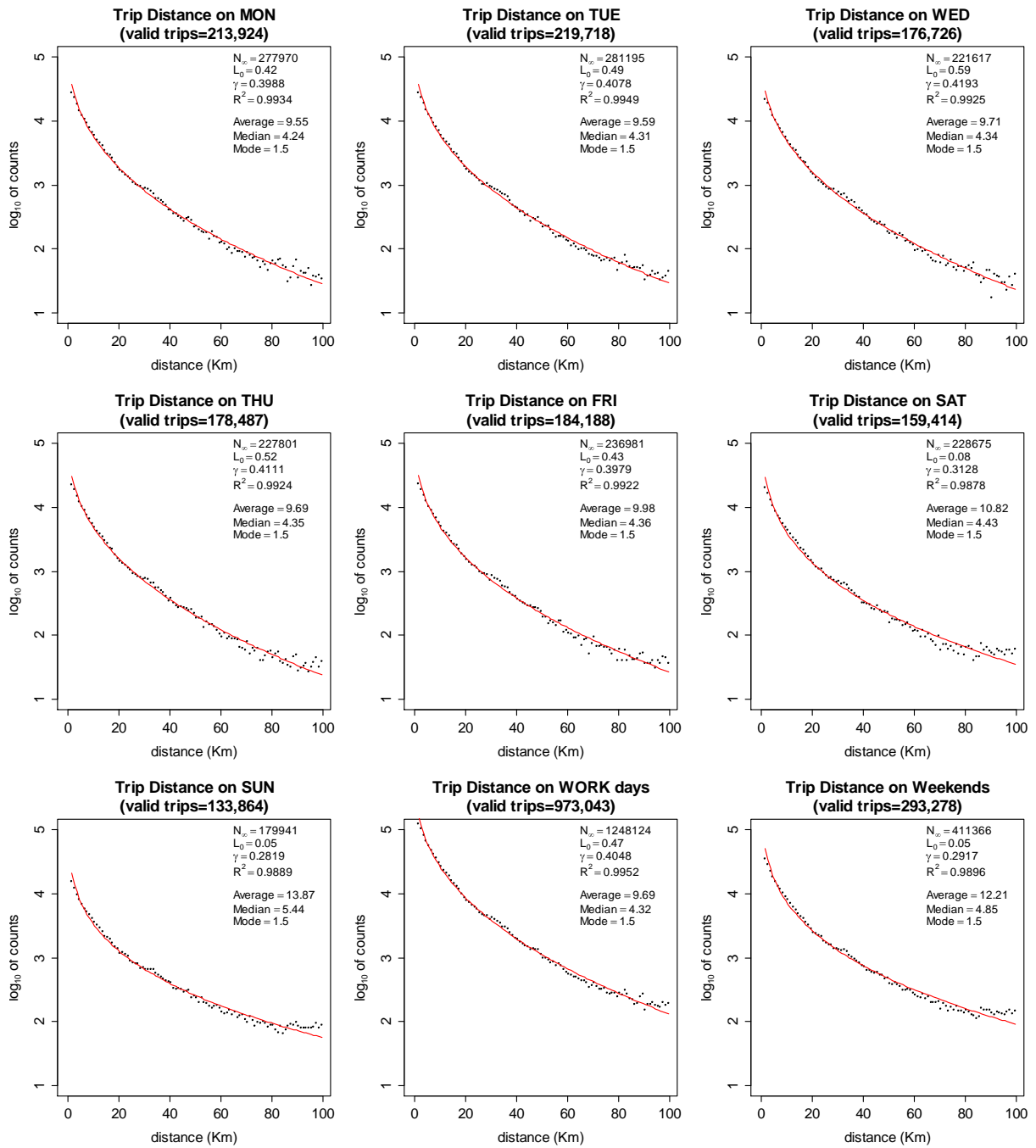
Figure A2. Florence (Floating-car data). Distribution of single-trip distances per day of the week and aggregated per working and weekend day (symbols). Fitted distribution, Eq. (3) (red solid line).

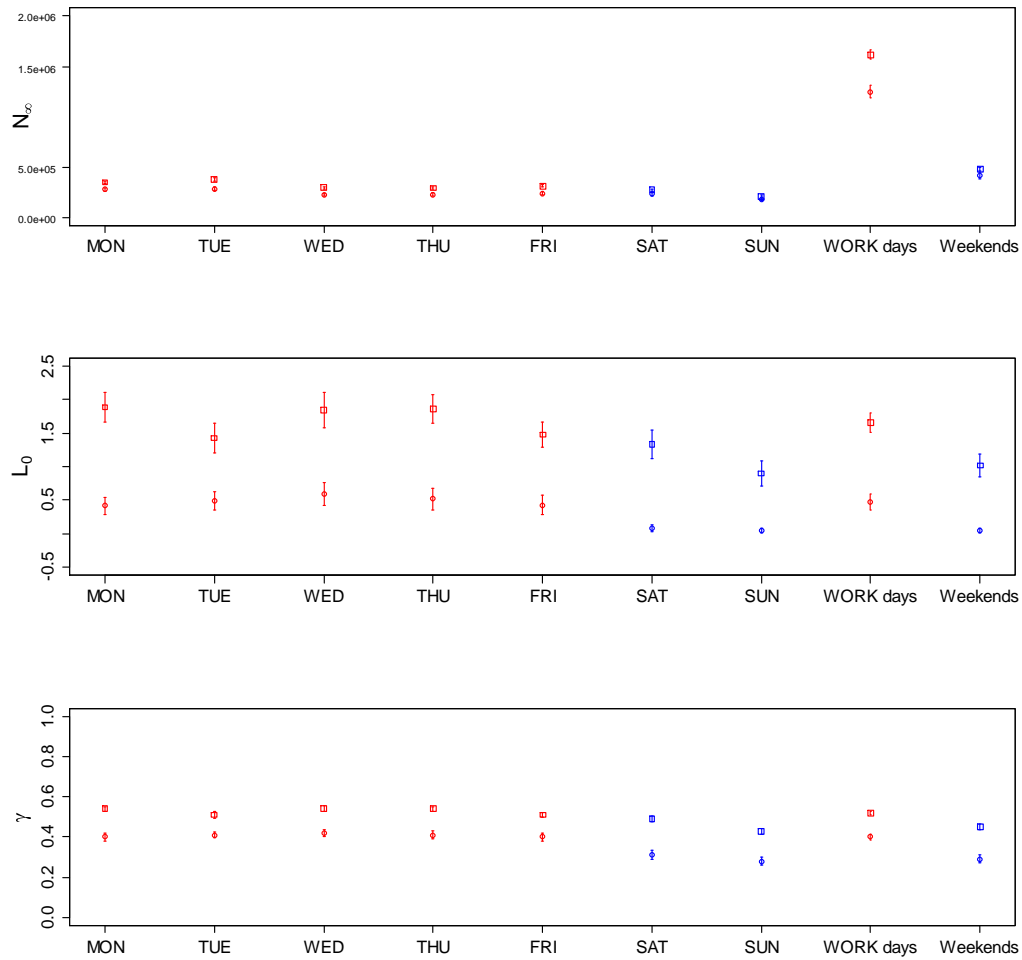**Figure A3. Floating-car data: Parameters of the fitted, single-trip distribution, Eq. (3). Modena (squares), Florence (circles). Red color denotes work days and their aggregate, blue weekend days and their aggregate. Vertical bars represent the standard error in the parameters estimate.**
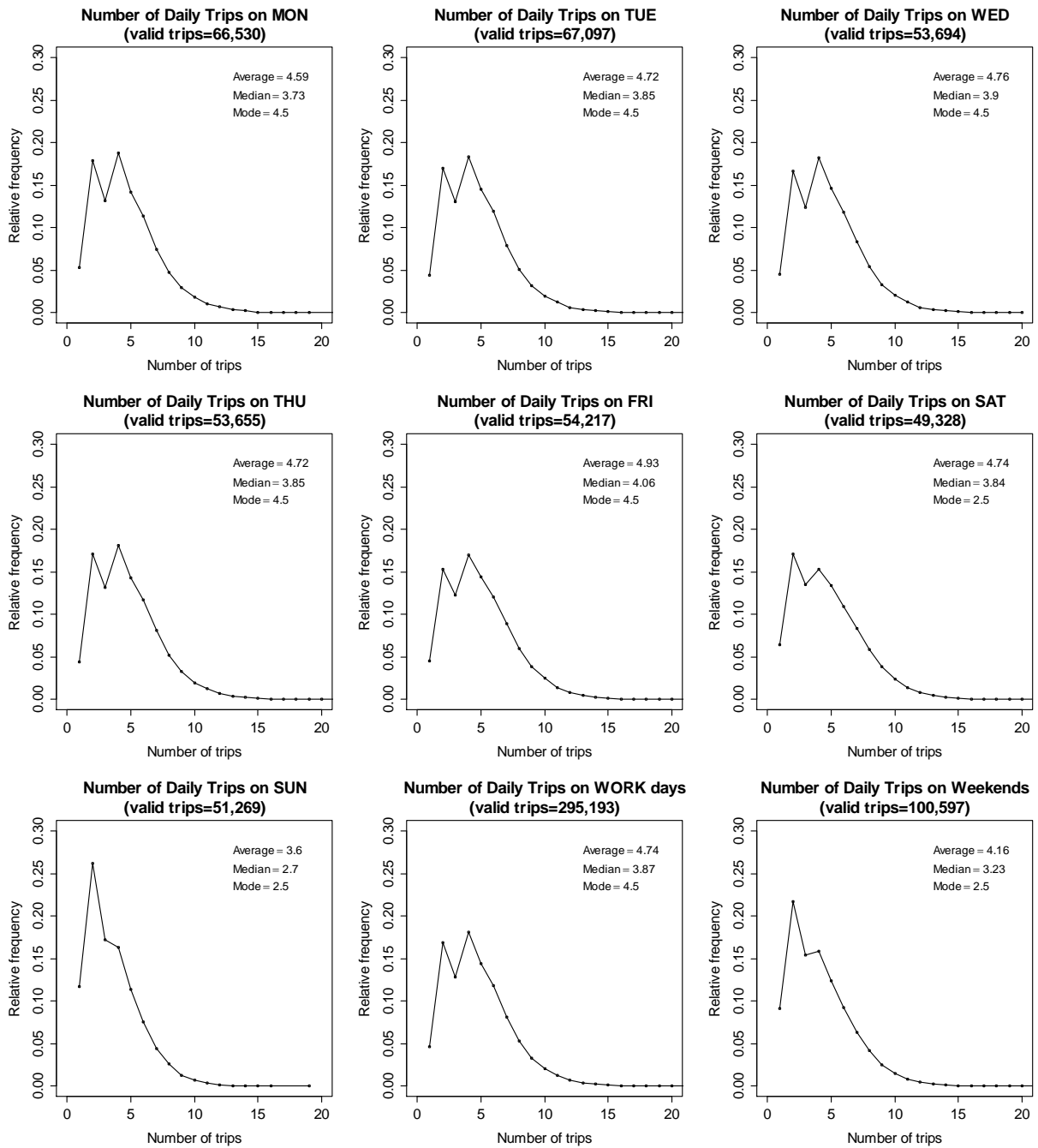
Figure A4. Modena (Floating-car data): Number of daily trips per week day. Relative maxima occur usually at n=2 and n=4.
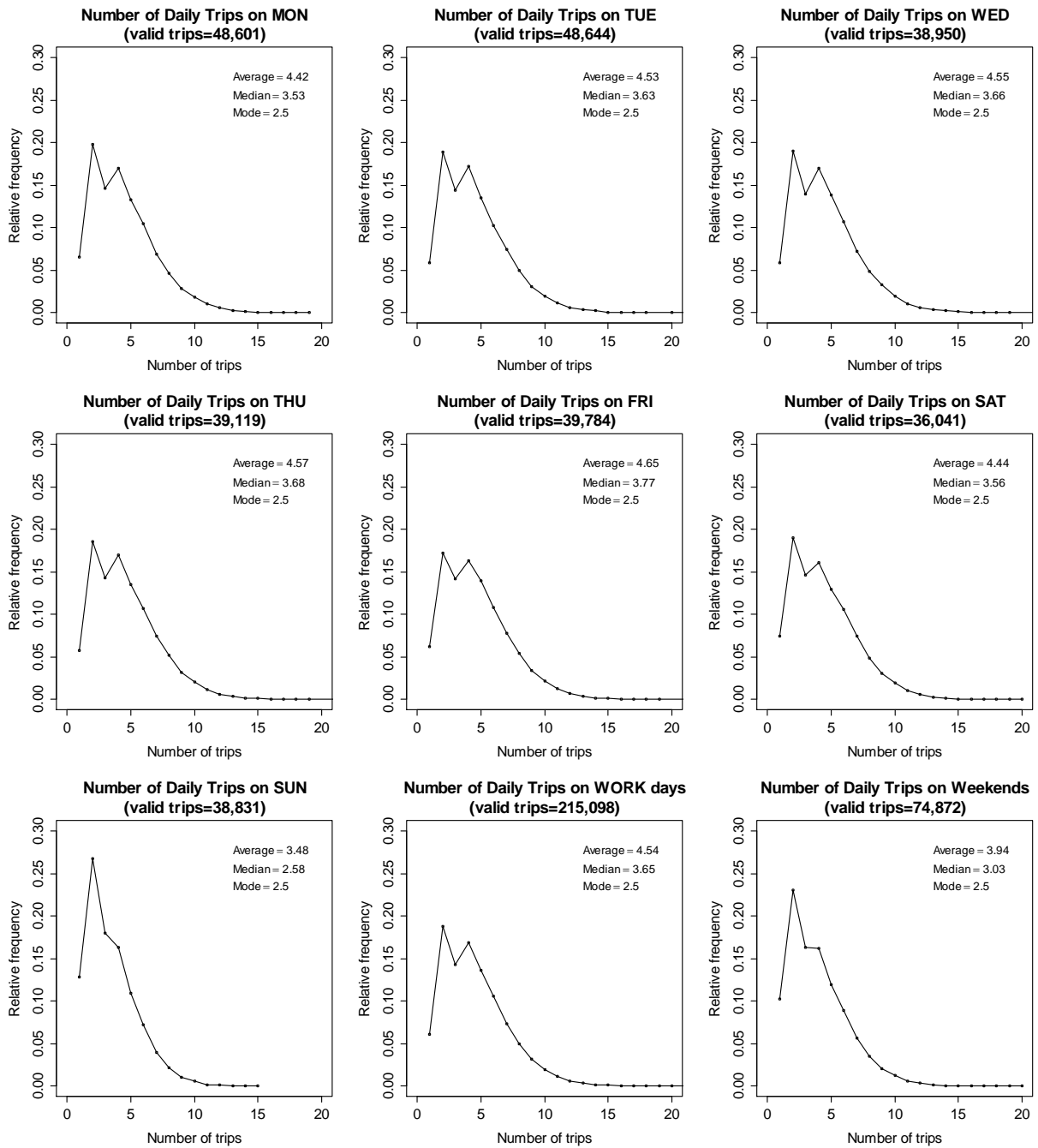
Figure A5. Florence (Floating-car data): Number of daily trips per week day. Relative maxima occur usually at n=2 and n=4.

Trip Duration on MON
(valid trips=305,335)

$N_\infty = 596362$
$T_0 = 0.0036$
$\gamma = 0.36$
$R^2 = 0.9895$

Average = 0.26
Median = 0.21
Arg Max = 0.12

log$_{10}$ of counts

time (h)

Trip Duration on TUE
(valid trips=316,428)

$N_\infty = 638442$
$T_0 = 0.0029$
$\gamma = 0.35$
$R^2 = 0.986$

Average = 0.26
Median = 0.21
Arg Max = 0.12

log$_{10}$ of counts

time (h)

Trip Duration on WED
(valid trips=255,781)

$N_\infty = 403639$
$T_0 = 0.0097$
$\gamma = 0.41$
$R^2 = 0.9839$

Average = 0.26
Median = 0.21
Arg Max = 0.12

log$_{10}$ of counts

time (h)

Trip Duration on THU
(valid trips=253,255)

$N_\infty = 461692$
$T_0 = 0.0048$
$\gamma = 0.37$
$R^2 = 0.9855$

Average = 0.26
Median = 0.21
Arg Max = 0.12

log$_{10}$ of counts

time (h)

Trip Duration on FRI
(valid trips=267,344)

$N_\infty = 387432$
$T_0 = 0.0131$
$\gamma = 0.42$
$R^2 = 0.9853$

Average = 0.27
Median = 0.21
Arg Max = 0.12

log$_{10}$ of counts

time (h)

Trip Duration on SAT
(valid trips=233,625)

$N_\infty = 295806$
$T_0 = 0.0497$
$\gamma = 0.54$
$R^2 = 0.9881$

Average = 0.27
Median = 0.21
Arg Max = 0.12

log$_{10}$ of counts

time (h)

Trip Duration on SUN
(valid trips=184,744)

$N_\infty = 167781$
$T_0 = 0.1565$
$\gamma = 0.68$
$R^2 = 0.9859$

Average = 0.31
Median = 0.21
Arg Max = 0.12

log$_{10}$ of counts

time (h)

Trip Duration on WORK days
(valid trips=1,398,143)

$N_\infty = 2421075$
$T_0 = 0.0059$
$\gamma = 0.38$
$R^2 = 0.992$

Average = 0.26
Median = 0.21
Arg Max = 0.12

log$_{10}$ of counts

time (h)

Trip Duration on Weekends
(valid trips=418,369)

$N_\infty = 394528$
$T_0 = 0.1276$
$\gamma = 0.66$
$R^2 = 0.9921$

Average = 0.28
Median = 0.21
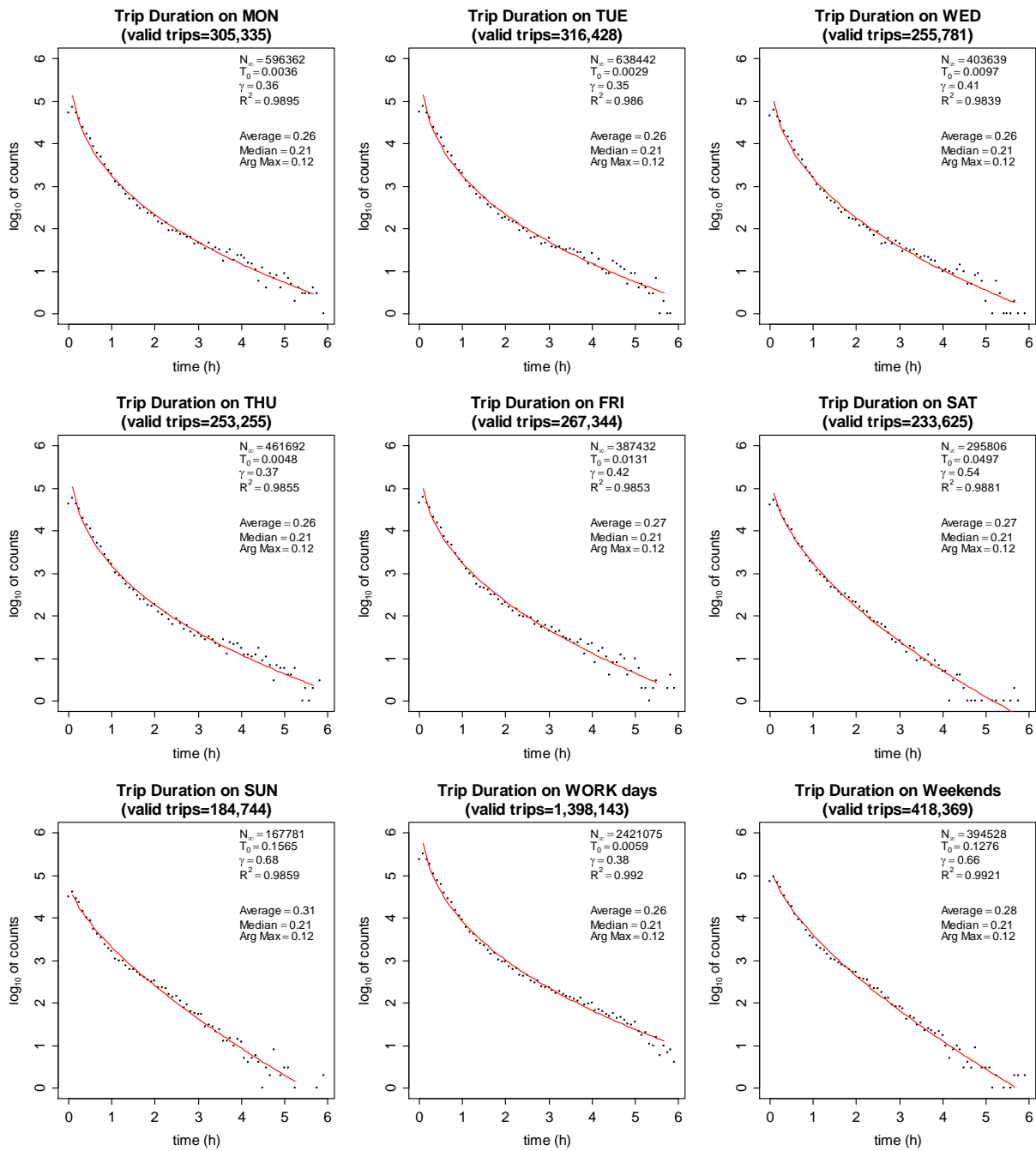Arg Max = 0.12

log$_{10}$ of counts

time (h)

Figure A6. Modena (Floating-car data). Trip duration per week day and aggregated per working and weekend day (symbols). Fitted distribution, Eq. (10) (red solid line).
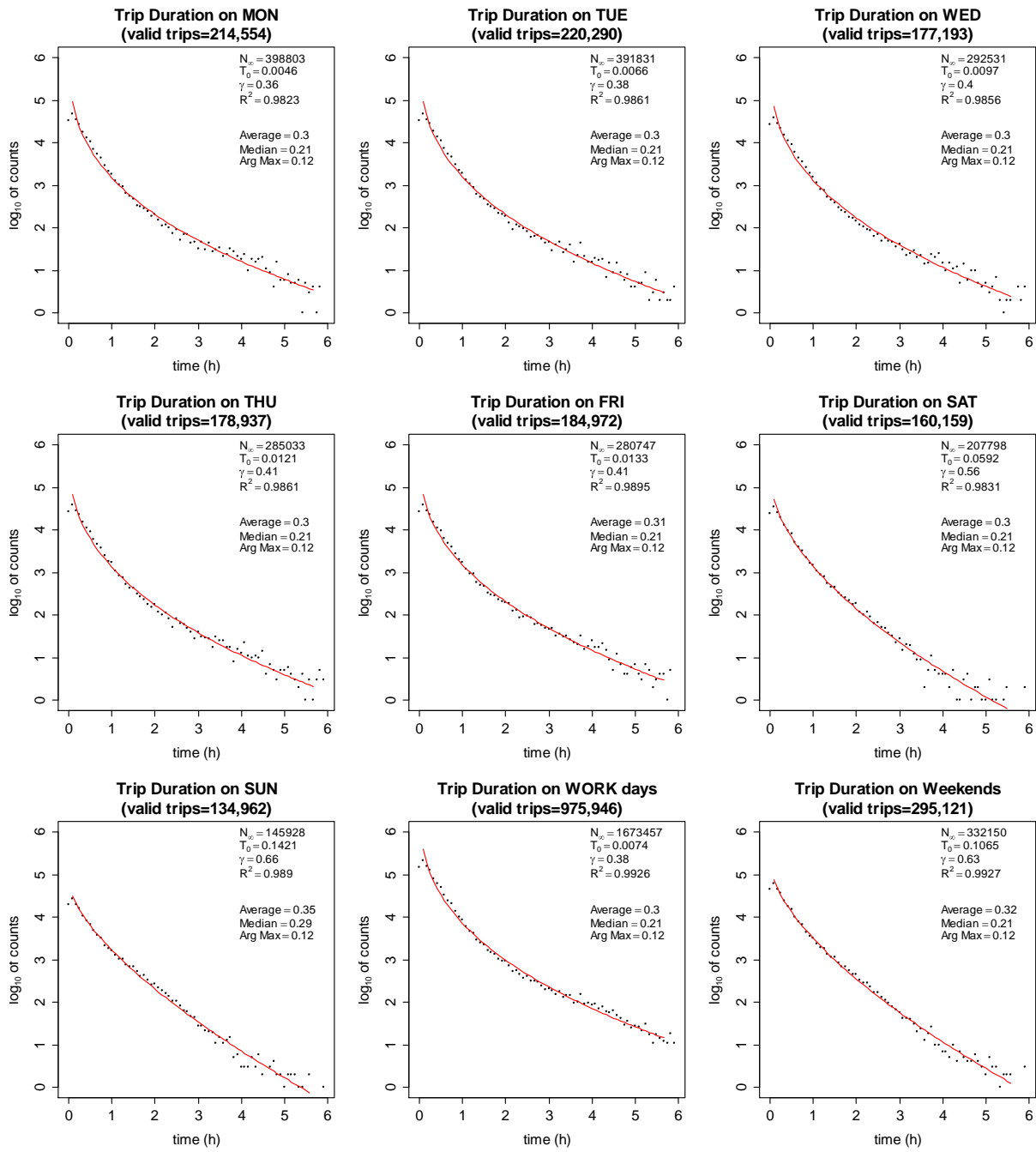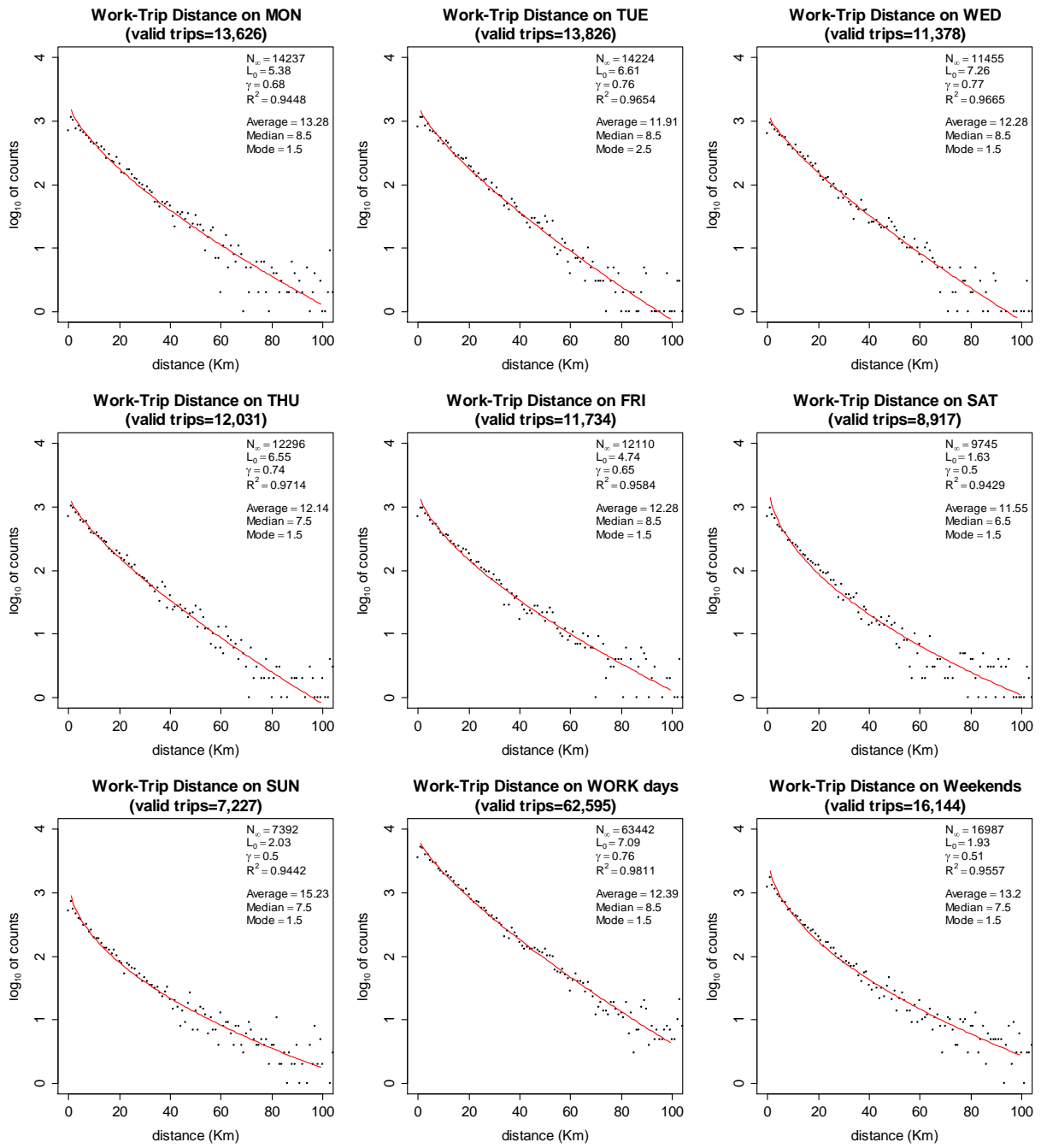
Trip Duration on MON
(valid trips=214,554)

$N_\infty = 398803$
$T_0 = 0.0046$
$\gamma = 0.36$
$R^2 = 0.9823$

Average = 0.3
Median = 0.21
Arg Max = 0.12

log$_{10}$ of counts

time (h)

Trip Duration on TUE
(valid trips=220,290)

$N_\infty = 391831$
$T_0 = 0.0066$
$\gamma = 0.38$
$R^2 = 0.9861$

Average = 0.3
Median = 0.21
Arg Max = 0.12

log$_{10}$ of counts

time (h)

Trip Duration on WED
(valid trips=177,193)

$N_\infty = 292531$
$T_0 = 0.0097$
$\gamma = 0.4$
$R^2 = 0.9856$

Average = 0.3
Median = 0.21
Arg Max = 0.12

log$_{10}$ of counts

time (h)

Trip Duration on THU
(valid trips=178,937)

$N_\infty = 285033$
$T_0 = 0.0121$
$\gamma = 0.41$
$R^2 = 0.9861$

Average = 0.3
Median = 0.21
Arg Max = 0.12

log$_{10}$ of counts

time (h)

Trip Duration on FRI
(valid trips=184,972)

$N_\infty = 280747$
$T_0 = 0.0133$
$\gamma = 0.41$
$R^2 = 0.9895$

Average = 0.31
Median = 0.21
Arg Max = 0.12

log$_{10}$ of counts

time (h)

Trip Duration on SAT
(valid trips=160,159)

$N_\infty = 207798$
$T_0 = 0.0592$
$\gamma = 0.56$
$R^2 = 0.9831$

Average = 0.3
Median = 0.21
Arg Max = 0.12

log$_{10}$ of counts

time (h)

Trip Duration on SUN
(valid trips=134,962)

$N_\infty = 145928$
$T_0 = 0.1421$
$\gamma = 0.66$
$R^2 = 0.989$

Average = 0.35
Median = 0.29
Arg Max = 0.12

log$_{10}$ of counts

time (h)

Trip Duration on WORK days
(valid trips=975,946)

$N_\infty = 1673457$
$T_0 = 0.0074$
$\gamma = 0.38$
$R^2 = 0.9926$

Average = 0.3
Median = 0.21
Arg Max = 0.12

log$_{10}$ of counts

time (h)

Trip Duration on Weekends
(valid trips=295,121)

$N_\infty = 332150$
$T_0 = 0.1065$
$\gamma = 0.63$
$R^2 = 0.9927$

Average = 0.32
Median = 0.21
Arg Max = 0.12

log$_{10}$ of counts

time (h)

Figure A7. Florence (Floating-car data). Trip duration per week day and aggregated per working and weekend day (symbols). Fitted distribution, Eq. (10) (red solid line).

52

Figure A8. Modena (Floating-car data). Observed (symbols) and modelled (red solid line, Eq. (3)) work-trip distance distribution per week day and aggregated per work and weekend day.

Figure A9. Florence (Floating-car data). Observed (symbols) and modelled (red solid line, Eq. (3)), work-trip distance distribution per week day and aggregated per work and weekend day.
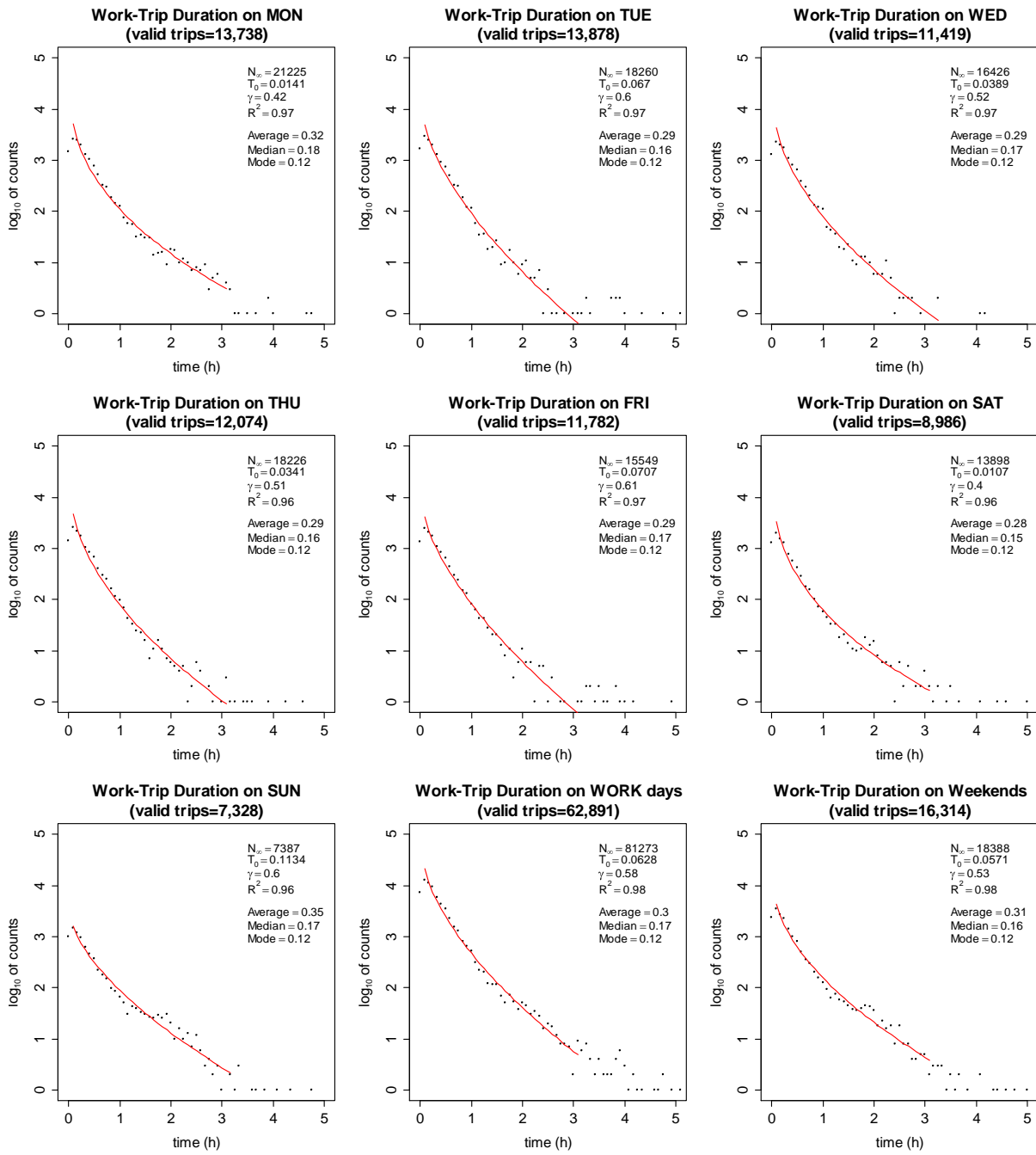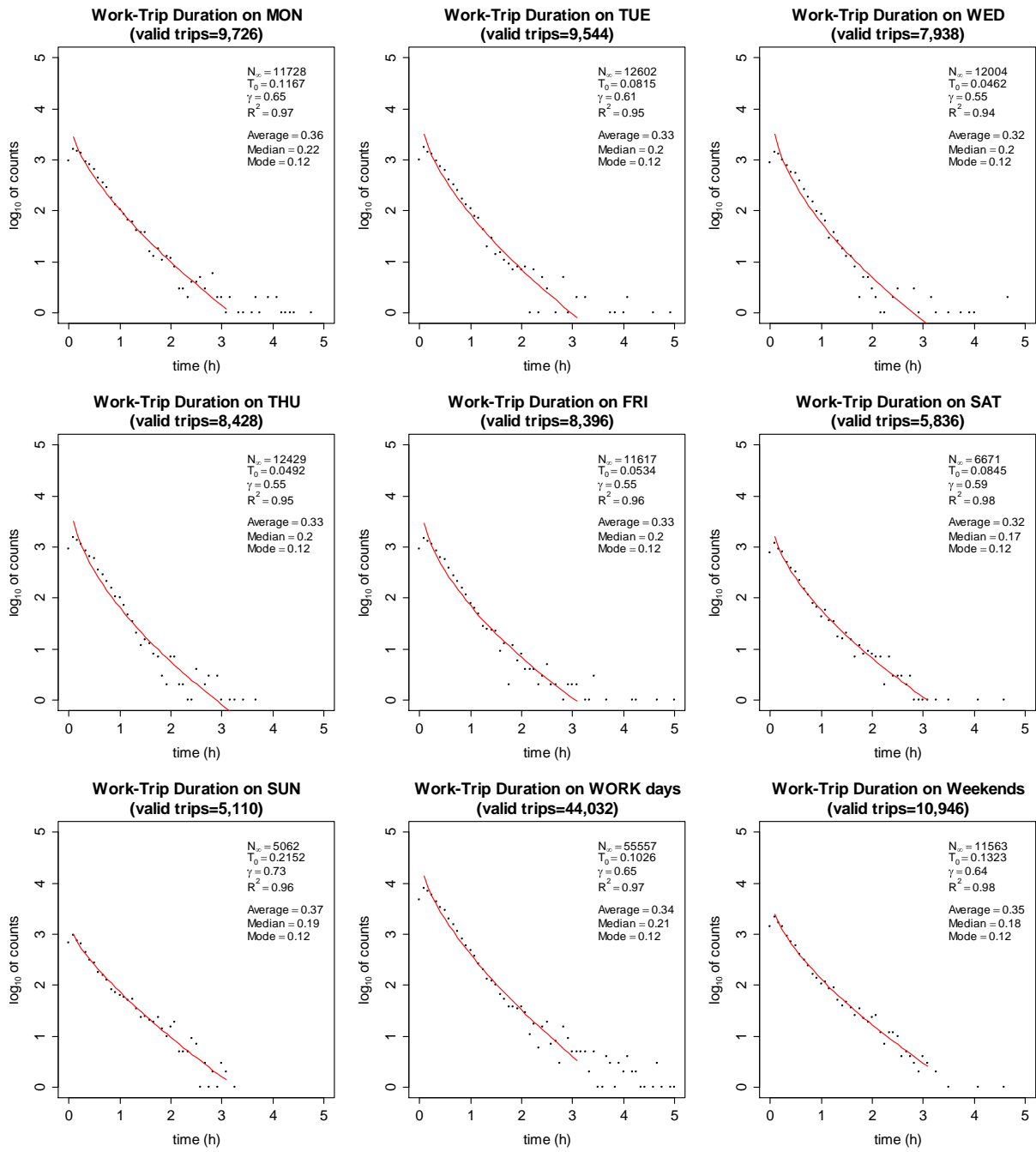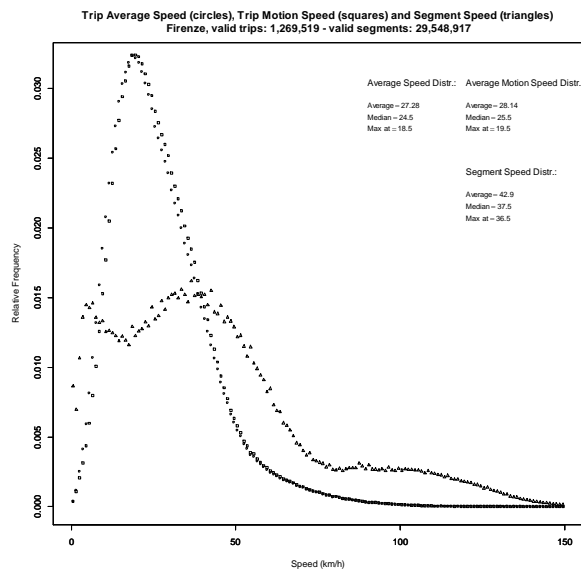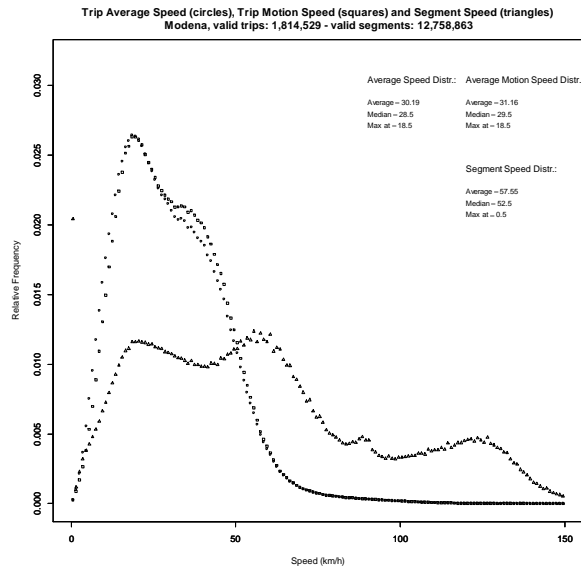
Figure A10. Modena (Floating-car data). Trip duration of work trips per day and aggregate per working and weekend day (symbols). Red solid line fitted distribution, Eq. (10).

Figure A11. Florence (Floating-car data). Trip duration of work trips per day and aggregate per working and weekend day (symbols). Red solid line fitted distribution, Eq. (10).

Figure A12. Modena (top) and Florence (bottom) (Floating car data). Distribution of travel speeds: average speed, motion speed (obtained by removing intermediate stops), and the segment speed.
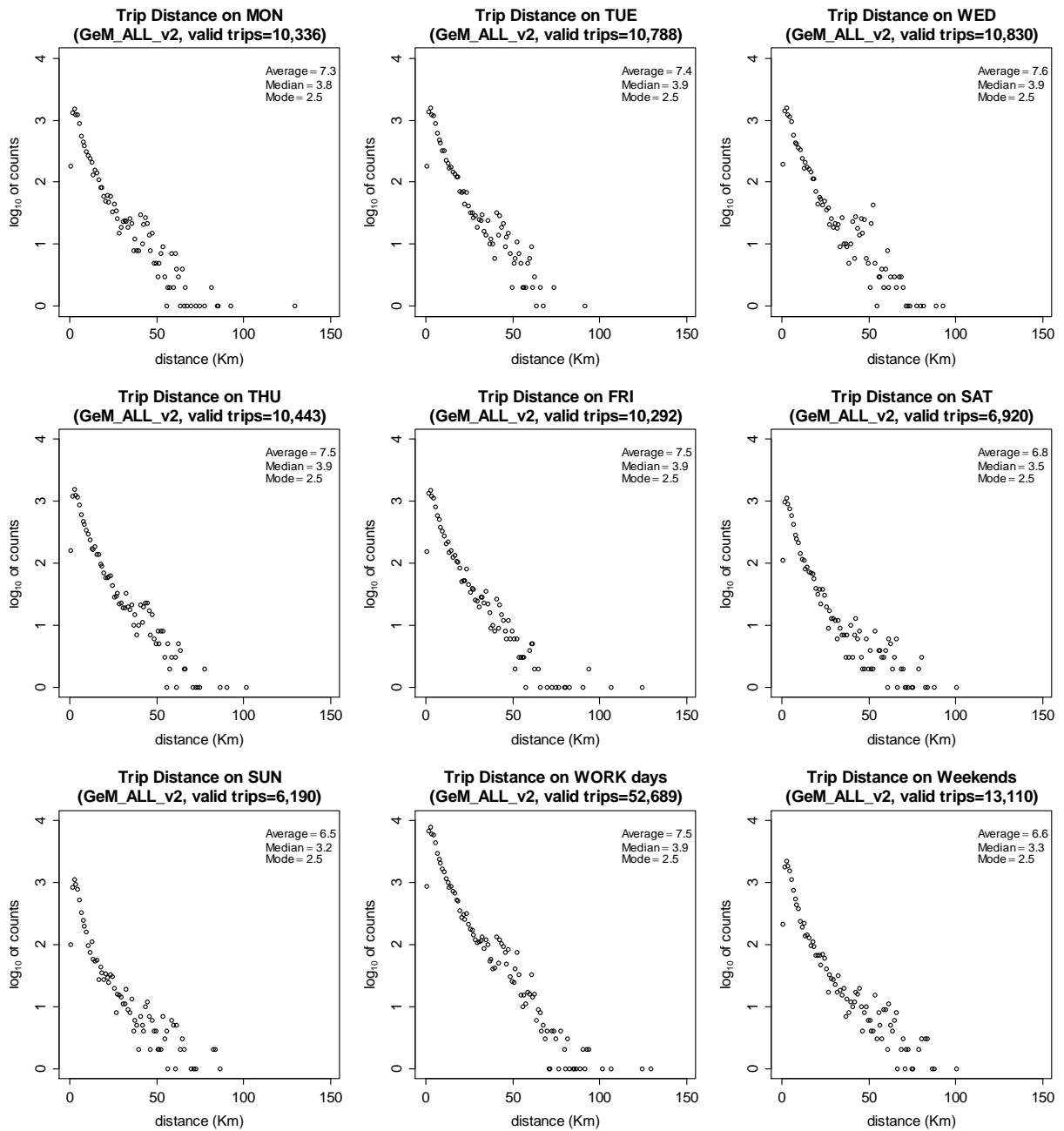
Figure A13. Green eMotion data: Trip distance per week day and aggregated per working and weekend day.
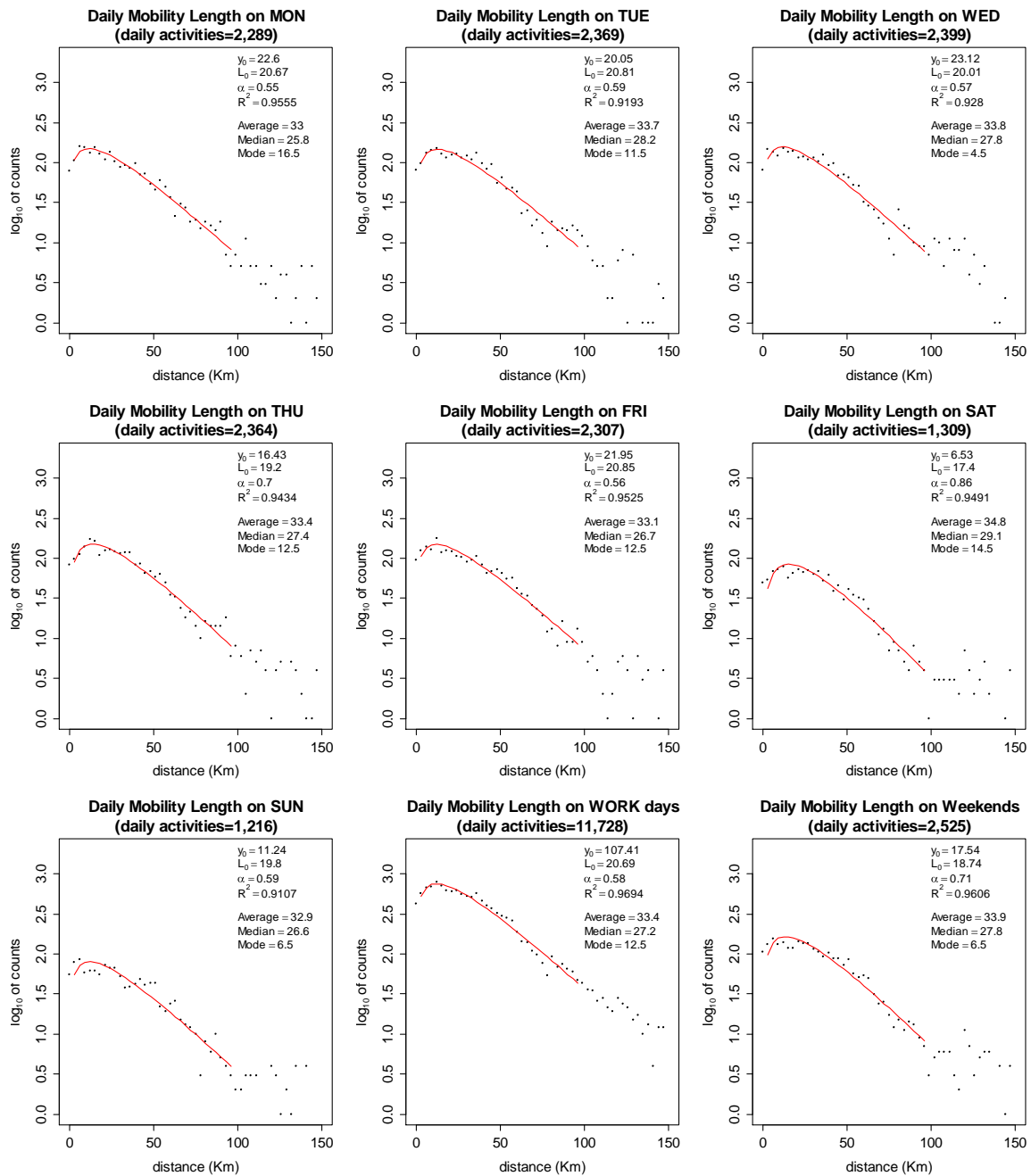
Figure A14. Green eMotion data: Observed daily mobility length distribution and fitted distribution, Eq. (6), per week day.
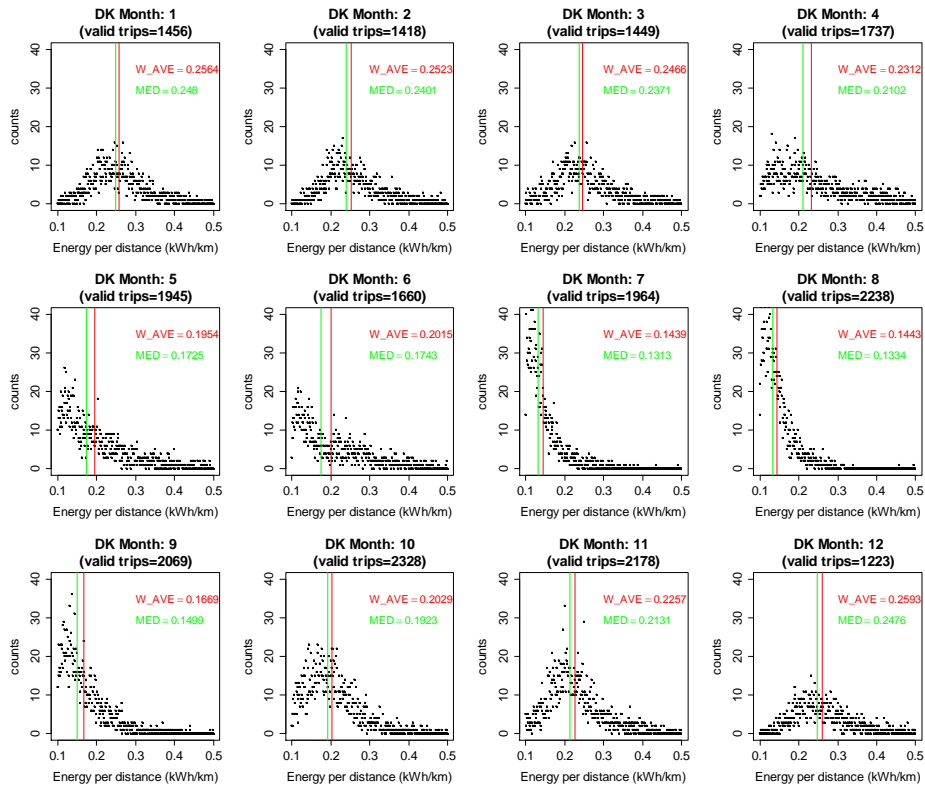
Figure A15. Electric energy consumption per km (Denmark) during the year: 1=Jan to 12=Dec.
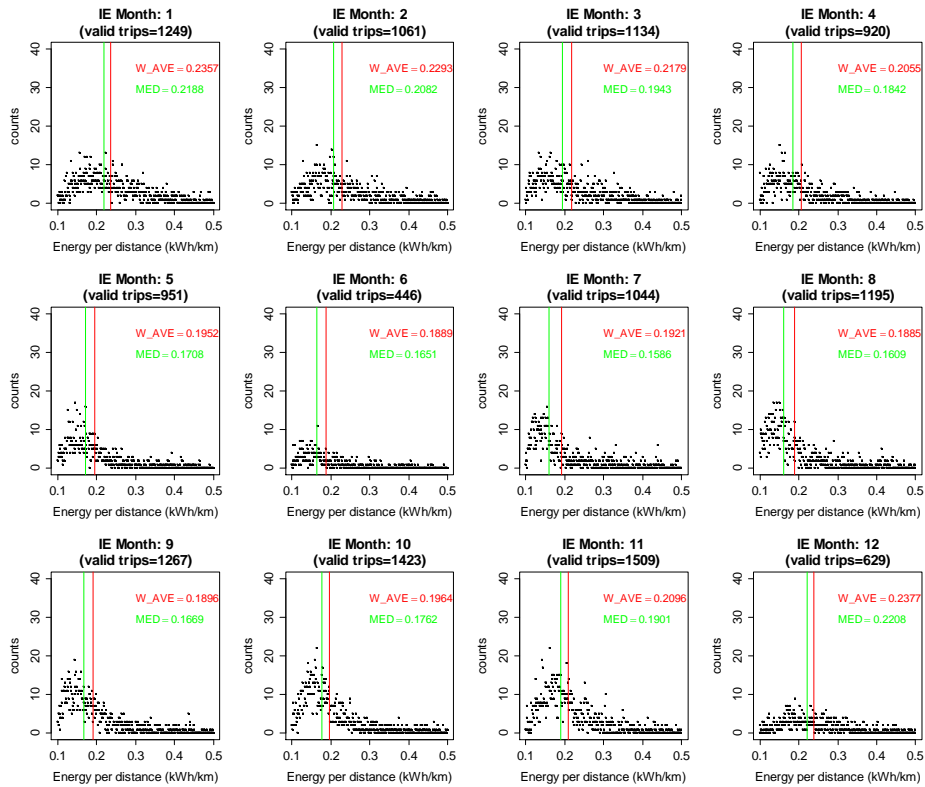
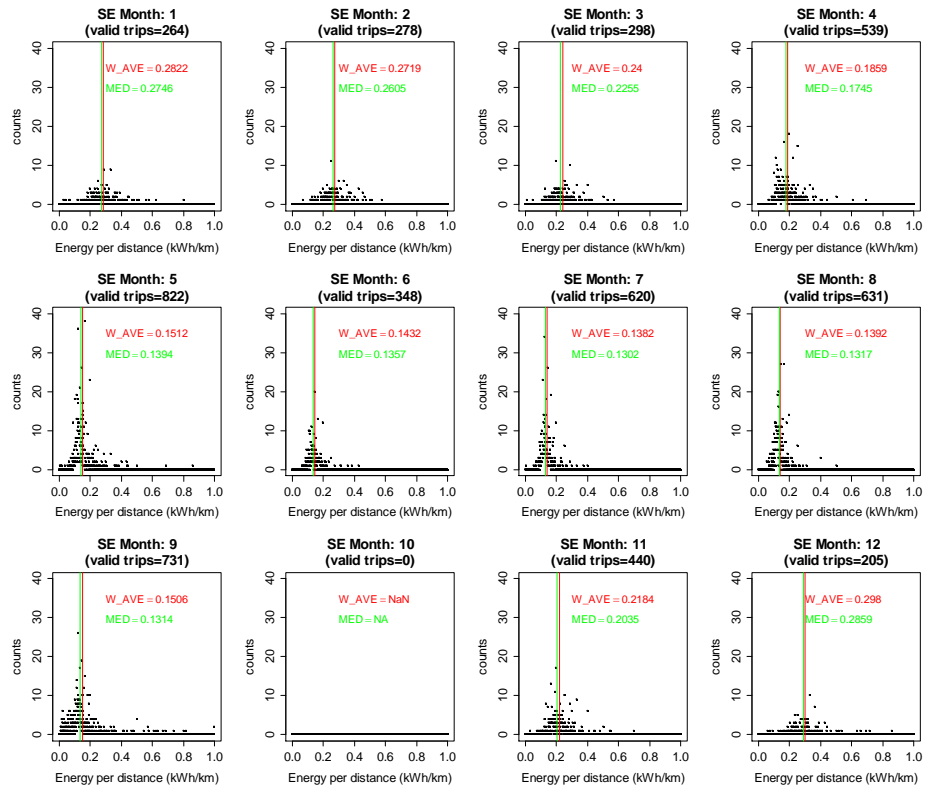**Figure A16. Electric energy consumption per km (Ireland) during the year: 1=Jan to 12=Dec.**
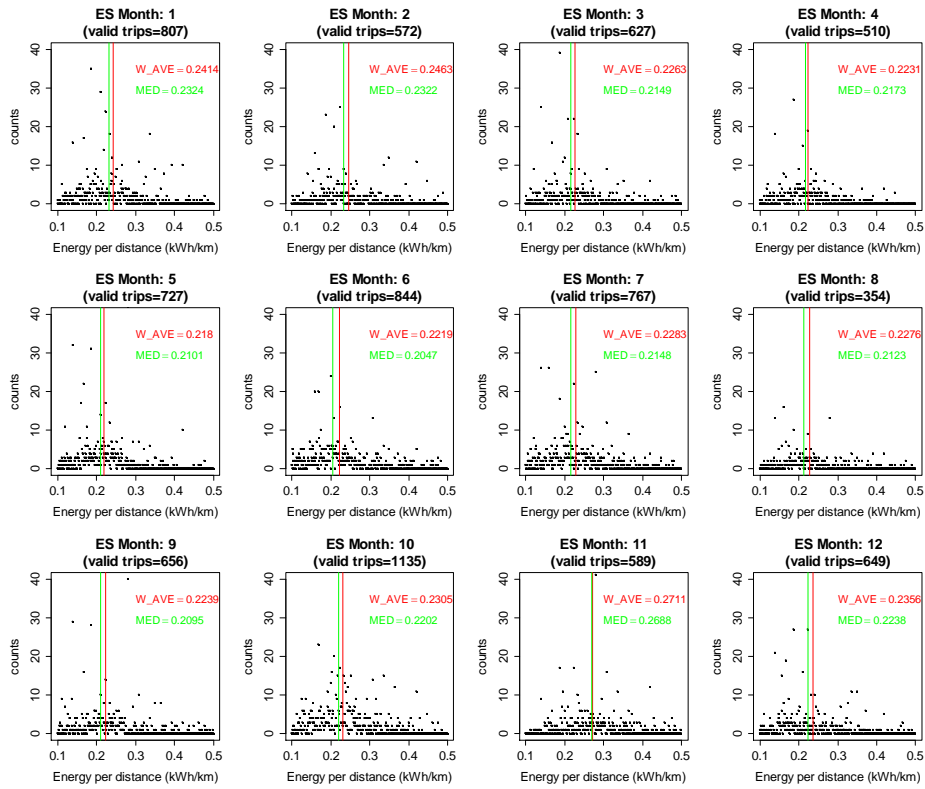
Figure A17. Electric energy consumption per km (Spain) during the year: 1=Jan to 12=Dec.

Figure A18. Electric energy consumption per km (Sweden) during the year: 1=Jan to 12=Dec.

61

Appendix B

The output of the Java processing code is:

1. Motion state versus GPS signal quality (SG= "Signal Goodness") table for Modena (top) and Florence (bottom);

Modena	MS=0 (engine on)	MS=1 (motion)	MS=2 (engine off)
SG=1 (no signal)	260,416	0	240,158
SG=2 (weak signal)	26,776	124,314	30,189
SG=3 (good signal)	1,810,912	11,135,176	1,826,986
Anomalous events with full trip removal: 7.24%			

Florence	MS=0 (engine on)	MS=1 (motion)	MS=2 (engine off)
SG=1 (no signal)	166,414	0	141,168
SG=2 (weak signal)	23,011	636,764	26,562
SG=3 (good signal)	1,289,409	28,493,205	1,310,194
Anomalous events with full trip removal: 4.95%			

2. Cleaned version of the original dataset, after removal of the inconsistent (anomalous) events/trips, as defined above;
3. Detailed information on the anomalous trips and stops filtered out;
4. Summary statistics, like the one presented in Table 1;
5. Distributions and statistics files, log/control files, for a total of approximately 95 output files;
6. A file with stop times not aggregated into a histogram (used for some MATLAB calculations).

Europe Direct is a service to help you find answers to your questions about the European Union
Freephone number (*): 00 800 6 7 8 9 10 11

(*) Certain mobile telephone operators do not allow access to 00 800 numbers or these calls may be billed.

A great deal of additional information on the European Union is available on the Internet.
It can be accessed through the Europa server *http://europa.eu*.

How to obtain EU publications

Our publications are available from EU Bookshop *(http://bookshop.europa.eu)*,
where you can place an order with the sales agent of your choice.

The Publications Office has a worldwide network of sales agents.
You can obtain their contact details by sending a fax to (352) 29 29-42758.

JRC Mission

As the Commission's in-house science service, the Joint Research Centre's mission is to provide EU policies with independent, evidence-based scientific and technical support throughout the whole policy cycle.

Working in close cooperation with policy Directorates-General, the JRC addresses key societal challenges while stimulating innovation through developing new methods, tools and standards, and sharing its know-how with the Member States, the scientific community and international partners.

Serving society
Stimulating innovation
Supporting legislation